



# Water masers accompanying OH and methanol masers in star formation regions

S. L. Breen,<sup>1,2</sup>★ J. L. Caswell,<sup>2</sup> S. P. Ellingsen<sup>1</sup> and C. J. Phillips<sup>2</sup>

<sup>1</sup>School of Mathematics and Physics, University of Tasmania, Private Bag 37, Hobart, Tasmania 7001, Australia

<sup>2</sup>Australia Telescope National Facility, CSIRO, PO Box 76, Epping, NSW 1710, Australia

Accepted 2010 April 2. Received 2010 March 30; in original form 2010 February 17

## ABSTRACT

The Australia Telescope Compact Array has been used to measure positions with arcsecond accuracy for 379 masers at the 22-GHz transition of water. The principal observation targets were 202 OH masers of the variety associated with star formation regions (SFRs) in the Southern Galactic plane. At a second epoch, most of these targets were observed again, and new targets of methanol masers were added. Many of the water masers reported here are new discoveries and others had been reported, with position uncertainties exceeding 10 arcsec, from Parkes telescope single-dish observations many years ago.

Variability in the masers is often acute, with very few features directly corresponding to those discovered two decades ago. Within our current observations, less than a year apart, spectra are often dissimilar, but positions at the later epoch, even when measured for slightly different features, mostly correspond to the detected maser site measured earlier, to within the typical extent of the whole site, of a few arcseconds.

The precise water positions show that approximately 79 per cent (160 of 202) of the OH maser sites show coincident water maser emission, the best estimate yet obtained for this statistic; however, there are many instances where additional water sites are present offset from the OH target, and consequently less than half of the water masers coincide with a 1665-MHz ground-state OH maser counterpart. Our less uniform sample of methanol targets is not suitable for a full investigation of their association with water masers, but we are able to explore differences between the velocities of peak emission from the three species and quantify the typically larger deviations shown by water maser peaks from systemic velocities.

Clusters of two or three distinct but nearby sites, each showing one or several of the principal molecular maser transitions, are found to be common. We also report the detection of ultracompact H II regions towards some of the sites. In combination with an investigation of correlations with IR sources from the *Spitzer* Galactic Legacy Infrared Mid-Plane Survey Extraordinaire (GLIMPSE) catalogue, these comparative studies allow further progress in the use of the maser properties to assign relative evolutionary stages in star formation to individual sites.

**Key words:** masers – stars: formation – H II regions – ISM: molecules – radio lines: ISM.

## 1 INTRODUCTION

Masers of hydroxyl (OH), water and methanol are key tools for investigating the formation of massive stars. The masers reside in the dusty molecular envelope or torus of a massive star in its earliest stage of formation, and the masers are a sensitive probe for discovering stars in this embryonic state when the star is not visible because of obscuration from the dust.

Detailed studies of selected maser sites have been made comparing OH with water and OH with methanol (Forster & Caswell 1989,

1999, hereafter FC89, FC99, respectively; Caswell et al. 1995b, hereafter CVF95; Caswell 1997, hereafter C97). These suggest that the maser spots of all species are usually contained inside a region of diameter less than 30 mpc ( $= 0.93 \times 10^{15} \text{ m} = 0.93 \times 10^{17} \text{ cm} \approx 6200 \text{ au} \approx 0.1 \text{ light-year}$ ), corresponding to an angular diameter of about 1 arcsec at a typical distance of 6 kpc. A positional precision of about 1 arcsec is therefore desirable to establish whether masers of different species originate from the same site.

Within many star formation regions (SFRs), on a larger scale of 100 mpc or more, the FC89 and C97 studies revealed many instances where a number of maser sites are present in a small cluster, often with different combinations of maser species present. There has

★E-mail: Shari.Breen@utas.edu.au

been considerable speculation that the various combinations are indicative of massive young stars at a different evolutionary stage or in a different mass range (e.g. Ellingsen et al. 2007; Breen et al. 2010). Water maser emission is especially puzzling. It has commonly been thought to be most prolific at an early stage of stellar evolution, but isolated water masers are only partly accounted for by very young sites preceding OH maser excitation. Other offset positions indicate the additional occurrence of water masers towards lower mass stars or in high-velocity fragments that have travelled far from the initial site. In the latter case, maser spots from individual fragments are sometimes ephemeral and disappear on a time-scale as short as months, but are often replaced by generally similar emission in the same region, although at a slightly different position and velocity.

To date, the most extensive unbiased survey for masers of the SFR variety completed in the Galactic plane is at the 1665-MHz transition of OH, presented as a catalogue reporting positions of arc-second accuracy for more than 200 masers (Caswell 1998, hereafter C98). Sensitive observations of 6.6-GHz methanol at these positions have already been made, with a detection rate of 80 per cent after high precision positions are compared (C98; Caswell 2009). Early 22-GHz water maser surveys with the Parkes radio telescope towards southern SFRs have been reported by Caswell et al. (1989) and references therein, with positions measured to about 10-arcsec accuracy. Until recent years, follow-up observations to arcsecond accuracy were restricted to northerly objects accessible to the Very Large Array (VLA; FC89; FC99). The availability of the 22-GHz frequency band at the Australia Telescope Compact Array (ATCA) has allowed us to search with high sensitivity and high positional precision for water masers towards the full sample of OH masers as well as  $\sim 100$  methanol maser sites.

## 2 OBSERVATIONS AND DATA REDUCTION

Water maser observations were made with the ATCA on two separate occasions. During the first epoch of observations (2003 October 4 and 5) OH maser sites from C98 were targeted (see also Section 5.3), and during the second epoch (2004 July 25, 26 and 30) many water maser detections towards the OH masers were re-observed and a selected set of methanol masers (chiefly from Caswell 2009) were observed for the first time. OH maser sources that were targeted in the first epoch but showed no detectable water maser emission were not observed at the second epoch, and only a few of the water maser sources that had previously been observed by FC89 with the VLA, and successfully confirmed during the first epoch, were re-observed.

Our first observations were made with an east-west array yielding 10 baselines between 30 and 352 m (project c1190). The correlator sampled a single linear polarization, processed to give a 512-channel spectrum across a 32-MHz bandwidth. The observing strategy was to observe approximately 100 targets over each 12-h session. After initial calibration, the first 10 targets were observed for 1.5 min each, followed by a calibrator, and similarly for the remaining 90 targets. Then the cycle was repeated two more times so as to provide for each source adequate *uv* coverage, combined with a total integration time of 4.5 min. Primary flux calibration is relative to PKS B1934–638 and in general is expected to be accurate to  $\sim 20$  per cent. PKS B1921–293 was used for bandpass calibration.

The AIPS reduction package was used for processing of the data collected in this first epoch, following the general procedure described in C97. In the realignment of channels using the CVEL task, the adopted rest frequency was 22 235.08 MHz and the velocity scale was with respect to the local standard of rest (lsr). The channel

separation was  $0.84 \text{ km s}^{-1}$  which, with uniform weighting of the correlation function, yields a final velocity resolution of  $1.0 \text{ km s}^{-1}$ . The quite coarse resolution was a compromise chosen in order to allow a large velocity coverage of more than  $400 \text{ km s}^{-1}$ . With this coverage, it was possible to recognize any high-velocity features indicative of close association with outflows (for which the water masers are renowned).

Total intensity maps were then produced of the channels with maser emission apparent in the scalar averaged spectrum or in a vector averaged spectrum shifted to the location of the target OH or methanol maser emission. The rms noise in an individual channel image was typically 150 mJy. The synthesized beam has a half-power width of approximately 8 arcsec in right ascension, but is larger in declination by a factor cosec(declination) as expected for an array aligned east–west with a maximum baseline of 352 m.

Our second series of observations (project c1330) were made in similar fashion but with a different array configuration, H168. The correlator configuration, and therefore the spectral resolution and velocity coverage, was identical to that used in the 2003 observations. A few sample observations from this epoch were reduced, first with AIPS (as for the 2003 data) and secondly with MIRIAD software package (Sault, Teuben & Wright 1995). There was excellent agreement between data reduced in the respective data reduction packages. The full data set from this epoch was reduced using MIRIAD, applying the standard techniques for ATCA spectral line and continuum observations. Image cubes of the entire primary beam and velocity ranges were produced for each source. The flux densities of sources that were located away from the centre of the primary beam have been corrected to account for beam attenuation. Spectra for each source detected at this epoch were produced by integrating the emission in the ATCA image cubes for each source. The typical resultant rms noise in each spectrum was 40–50 mJy. For the H168 array used in 2004, the synthesized beam was typically  $13 \times 9$  arcsec $^2$ . The ATCA observations are most sensitive at the targeted positions, but provide useful measurements, albeit at lower sensitivity, of any other sources that happen to lie within the field of view of the primary beam; the full width to the first null is nearly 5 arcmin and the half power beam width (HPBW) is 2.29 arcmin = 137 arcsec.

## 3 RESULTS

The search for 22-GHz water masers carried out with the ATCA in 2003 October and 2004 July towards 202 OH maser sites and 104 methanol maser sites (with no reported OH maser emission) resulted in the detection of 379 distinct water maser sites (Table 1). Spectra of all detected sources are shown in Fig. 1. For the majority of sources, the spectra are taken from the 2004 data, except where sources were either not observed or not detected at this epoch. For these latter cases, we show the 2003 spectra and distinguish them from the 2004 spectra with ‘2003’ marked in the top left-hand corner of each spectrum. The 2003 spectra were obtained directly from the *uv* data with a phase shift to the source position and amplitude correction for offset from the field centre. For eight sources we show a spectrum from each epoch to either highlight that a weak source is a genuine detection ( $333.387+0.032$  and  $336.983-0.183$ ) or give an indication of the level of variability seen over the 10-month time-scale ( $284.350-0.418$ ,  $321.148-0.529$ ,  $327.291-0.578$ ,  $345.004-0.224$ ,  $15.026-0.654$  and  $15.028-0.673$ ). A velocity range of  $200 \text{ km s}^{-1}$  is shown for the majority of sources, but there are several instances where we either decreased this value to clearly show individual features in

**Table 1.** 22-GHz water masers detected towards sites of OH and methanol masers.

Water maser ( <i>l, b</i> ) (deg)	RA (J2000) (h m s)	Dec. (J2000) ( $^{\circ}$ $'$ $''$ )	V peak 2003	V range 2003	S peak 2003	V peak 2004	V range 2004	S peak 2004	Associations
G 240.316+0.071	07 44 51.94	-24 07 41.9	89	58, 100	10			-	o $\gamma$
G 263.250+0.514	08 48 47.91	-42 54 27.1	19	17, 21	3.0	20	17, 21	0.7	om $\gamma$
G 284.350-0.418	10 24 10.60	-57 52 33.0	-4	-42, 72	60	7	-78, 71	102	o $\gamma$
G 285.260-0.067	10 31 24.57	-58 03 03.7	-28	-95, 20	22	-92	-96, 20	30	$\gamma$
G 285.263-0.050	10 31 29.64	-58 02 18.9	2	-59, 50	1100	3	-36, 63	1651	o $\gamma$
G 287.371+0.644	10 48 04.25	-58 27 00.7	1	-14, 6	3.5	-1	-13, 1	4.9	om $\gamma$
G 290.374+1.661	11 12 17.98	-58 46 21.6	-12	-20, -10	3.5	-47	-47, -33	0.26	om $\gamma$
G 290.384+1.663	11 12 22.53	-58 46 29.0	-38	-50, -35	6	-37	-41, -35	4.5	$\gamma$
G 291.270-0.719	11 11 49.67	-61 18 53.8	-102	-110, -23	65	-102	-109, -17	53	m $\gamma$
G 291.274-0.709	11 11 53.28	-61 18 24.1	-32	-51, 14	60	-32	-59, -14	64	om $\gamma$
G 291.284-0.716	11 11 56.58	-61 19 01.1	-133	-142, -120	930	-133	-139, -120	701	$\gamma$
G 291.578-0.434	11 15 04.91	-61 09 50.7		<0.2	18	17, 27	16	$\gamma$	
G 291.579-0.431	11 15 05.67	-61 09 41.0	12	-29, 41	215	13	-31, 22	608	om $\gamma$
G 291.581-0.435	11 15 06.17	-61 09 56.1	26	25, 27	4.0		<0.2	$\gamma$	
G 291.610-0.529	11 15 02.58	-61 15 48.8	13	-66, 20	18	12	-66, 28	39	oc $\gamma$
G 291.627-0.529	11 15 10.18	-61 16 12.7	22	8, 23	12	22	20, 25	31	$\gamma$
G 291.629-0.541	11 15 08.88	-61 16 54.8	11	8, 16	70	10	-2, 21	46	$\gamma$
G 294.511-1.622	11 35 32.04	-63 14 44.3	-12	-20, -6	250	-12	-20, -4	112	om $\gamma$
G 294.976-1.733	11 39 13.77	-63 29 03.3		-	1	-17, 5	2.2	$\gamma$	
G 294.989-1.719	11 39 22.56	-63 28 25.1		-	-17	-18, -10	0.6	m $\gamma$	
G 297.660-0.974	12 04 08.76	-63 21 37.3	29	-80, 38	90	26	-79, 82	75	o
G 299.012+0.125	12 17 24.05	-62 29 13.6		<0.2	-26	-27, -24	0.44		
G 299.013+0.128	12 17 24.58	-62 29 04.8	19	18, 30	100	19	-1, 50	83	omcg
G 300.491-0.190	12 29 55.99	-62 57 33.8	24	23, 25	2.3	25	22, 25	1.6	
G 300.504-0.176	12 30 03.42	-62 56 50.2	11	-37, 14	180	11	-26, 14	94	omg
G 300.968+1.143	12 34 52.51	-61 39 57.9	-61	-86, -42	70	-58	-86, -3	26	$\gamma$
G 300.971+1.143	12 34 54.34	-61 39 57.1		<3	-43	-46, -42	3.0	$\gamma$	
G 301.136-0.225	12 35 34.76	-63 02 28.5		t	-47	-48, -41	17		
G 301.136-0.226a	12 35 34.93	-63 02 34.5	-29	-56, -18	80	-29	-31, -28	78	g
G 301.136-0.226b	12 35 34.84	-63 02 31.1		t	-45	-63, -43	92	(omc)	
G 301.137-0.225	12 35 35.21	-63 02 30.6		t	-36	-40, -33	39	omc	
G 305.191-0.006	13 11 12.95	-62 47 27.7	31	28, 36	25	32	29, 35	4.8	g
G 305.198+0.007	13 11 16.38	-62 46 37.4	-39	-42, -27	8	-35	-41, -24	3.5	
G 305.208+0.207	13 11 13.37	-62 34 40.0	-39	-43, -37	300	-39	-44, -38	235	om
G 305.361+0.150	13 12 35.61	-62 37 18.9	-43	-45, -28	250	-36	-44, -29	126	omg
G 305.799-0.245	13 16 42.92	-62 58 31.7	-26	-45, 35	400	-34	-119, 37	266	omg
G 306.318-0.331	13 21 20.87	-63 00 22.7	-19	-24, -14	2.1	-18	-23, -15	0.7	
G 307.805-0.456	13 34 27.32	-62 55 12.4	-13	-15, -7	1.4	-7	-11, -7	0.6	og
G 308.754+0.549	13 40 57.47	-61 45 42.4	-49	-50, -48	3.4	-49	-50, -48	0.7	omg
G 308.918+0.124	13 43 01.64	-62 08 48.9	-56	-66, -45	0.7	-61	-62, -49	1.5	om $\#$
G 309.384-0.135	13 47 24.01	-62 18 11.4	-50	-57, -41	3.5	-50	-51, -48	2.2	omg
G 310.144+0.760	13 51 58.53	-61 15 40.6	-58	-60, -55	2.5	-58	-59, -57	1.6	omg
G 310.146+0.760	13 51 59.61	-61 15 39.7	-63	-64, -62	8		<0.2		
G 311.643-0.380	14 06 38.77	-61 58 22.7	35	18, 50	320	36	8, 56	167	omcg
G 312.106+0.278	14 08 46.06	-61 12 30.1		-	-54	-55, -53	0.6	g	
G 312.109+0.262	14 08 49.45	-61 13 23.4		-	-48	-48, -47	0.43	mg	
G 312.596+0.045	14 13 14.13	-61 16 57.6	-61	-62, -58	0.6	-59	-64, -56	1.5	m
G 312.599+0.046	14 13 15.19	-61 16 51.9	-75	-102, -58	2.7	-79	-96, -56	9	om
G 313.457+0.193	14 19 35.05	-60 51 54.2	-1	-2, 0	1.9	45	-1, 46	1.0	c
G 313.470+0.191	14 19 40.97	-60 51 46.2	-5	-10, -2	6	-6	-10, -1	4.5	omg
G 313.578+0.325	14 20 08.63	-60 41 59.0	-46	-58, -32	55	-47	-54, -32	46	omg
G 313.767-0.862	14 25 01.71	-61 44 57.2	-54	-56, -48	160	-54	-57, -36	162	omg
G 314.320+0.112	14 26 26.37	-60 38 29.4	-44	-70, -40	34	-45	-70, -40	16	om
G 316.360-0.361	14 43 11.07	-60 17 10.3	3	-4, 21	30	3	-7, 20	16	
G 316.361-0.363	14 43 12.22	-60 17 16.6	-3	-4, -1	6	-3	-7, -1	2.6	
G 316.412-0.308	14 43 23.22	-60 12 58.8	-22	-30, 6	6	-20	-24, 5	15	omcg
G 316.640-0.087	14 44 18.39	-59 55 10.7	-19	-104, -2	12	-15	-40, 92	12	omg
G 316.763-0.011	14 44 56.32	-59 47 59.8	-47	-51, -33	60	-48	-49, -33	4.1	og
G 316.812-0.057	14 45 26.58	-59 49 14.1	-46	-47, -36	500	-46	-56, -11	408	om
G 317.429-0.561	14 51 37.72	-60 00 18.2	16	12, 25	0.5	25	24, 25	0.27	oc

**Table 1** – *continued*

Water maser ( <i>l, b</i> ) (deg)	RA (J2000) (h m s)	Dec. (J2000) (° ' '')	V peak 2003 (km s <sup>-1</sup> )	V range 2003 (km s <sup>-1</sup> )	S peak 2003 (Jy)	V peak 2004 (km s <sup>-1</sup> )	V range 2004 (km s <sup>-1</sup> )	S peak 2004 (Jy)	Associations
G 317.429–0.556	14 51 36.75	−60 00 03.4	26	25,36	0.5	28	27,29	0.6	
G 318.044–1.404	14 59 08.61	−60 28 23.9	42	31,44	3.5	42	32,42	3.5	omγ
G 318.050+0.087	14 53 42.62	−59 08 52.3	−55	−61,−39	470	−48	−69,−38	50	omg
G 318.948−0.196a	15 00 55.18	−58 58 51.6	−41	−44,−28	5	−36	−44,−27	9	g
G 318.948−0.196b	15 00 55.33	−58 58 53.6			t	−38	−39,−21	7	omg
G 319.399−0.012	15 03 17.50	−58 36 11.4	−4.5	−20,1	10	−5	−7,2	3.8	oc
G 319.836−0.196	15 06 54.54	−58 32 58.6	−13	−23,0	9	−11	−19,0	2.8	omg
G 320.120−0.440	15 09 43.83	−58 37 06.3	−46	−70,−40	1.2	−46	−158,30	0.9	o
G 320.221−0.281	15 09 47.00	−58 25 47.6			<0.4	−73	−75,−72	0.7	
G 320.232−0.284	15 09 51.92	−58 25 38.0	−63	−70,−61	9	−67	−81,−72	2	om
G 320.233−0.284	15 09 52.50	−58 25 35.7	−60	−61,−58	3.5	−60	−61,−54	3.4	c
G 320.255−0.305	15 10 06.14	−58 26 00.8			−	−126	−144,−111	45	
G 320.285−0.308	15 10 18.88	−58 25 16.5			−	−69	−81,−56	15	g
G 321.028−0.484	15 15 50.90	−58 11 19.7	−60	−70,−55	2.5	−58	−70,−52	5	
G 321.033−0.483	15 15 52.60	−58 11 07.2	−60	−68,−58	3.6	−61	−64,−49	0.25	m
G 321.148−0.529	15 16 48.25	−58 09 50.1	−64	−66,−62	0.8	−97	−98,−61	1.6	omg
G 322.158+0.636	15 18 34.52	−56 38 24.7	−73	−81,−61	5	−76	−86,−65	2.7	om
G 322.165+0.625	15 18 39.74	−56 38 46.7	−40	−67,−36	9	−39	−67,−36	2.8	g
G 323.740−0.263	15 31 45.48	−56 30 49.6	−50	−72,−46	140	−50	−88,−42	70	omg
G 324.201+0.122	15 32 52.76	−55 56 04.9	−87	−100,−47	50	−87	−100,−48	14	o
G 324.716+0.342	15 34 57.41	−55 27 22.3	−55	−72,−47	10	−58	−81,−30	26	omg
G 326.662+0.521	15 45 02.73	−54 09 03.3	−39	−50,−34	256			−	m
G 326.665+0.553	15 44 55.82	−54 07 25.6			t	−42	−127,−39	16	g
G 326.670+0.554	15 44 57.03	−54 07 10.6	−42	−44,−40	26	−40	−48,8	101	o
G 326.780−0.241	15 48 55.10	−54 40 38.6	−64	−66,−60	36	−66	−92,−52	18	og
G 326.859−0.676	15 51 13.82	−54 58 03.6			−	−103	−104,−103	0.42	mg
G 327.119+0.511	15 47 32.56	−53 52 39.3	−87	−90,−80	25	−88	−89,−57	19	omg
G 327.291−0.578	15 53 07.65	−54 37 07.2	−56	−80,−39	400	−63	−84,−36	668	omg
G 327.391+0.200	15 50 18.31	−53 57 06.1			−	−86	−92,−86	0.40	mg
G 327.402+0.445	15 49 19.32	−53 45 13.8	−80	−83,−68	230	−81	−84,−69	195	o <sup>#</sup> mcg
G 327.581−0.077	15 52 29.50	−54 02 51.6			−	−101	−102,−95	1.0	
G 327.594−0.095	15 52 38.19	−54 03 11.5			−	−99	−102,−91	0.8	g
G 327.619−0.111	15 52 50.31	−54 03 00.0			−	−85	−85,−84	0.20	mg
G 327.935−0.123	15 54 33.09	−53 51 29.1			−	−98	−100,−76	2.1	
G 328.236−0.548	15 57 58.21	−53 59 25.4	−38	−39,−37	30	−38	−40,10	20	omcg
G 328.254−0.532	15 57 59.69	−53 58 00.7	−50	−53,−48	200	−50	−51,−48	155	omg
G 328.306+0.432	15 54 05.91	−53 11 37.4	−96	−97,−87	40	−93	−96,−87	141	c
G 328.808+0.633	15 55 48.23	−52 43 05.2	−46	−47,−44	10	−46	−48,−44	4.4	omcg
G 329.021−0.186	16 00 24.32	−53 12 16.9	−42	−43,−41	2.4	−44	−44,−43	0.34	g
G 329.029−0.199	16 00 30.22	−53 12 34.3	−38	−40,−37	1.6			<0.2	og
G 329.030−0.205	16 00 31.90	−53 12 48.7	−39	−54,−34	8	−46	−52,−35	6	om
G 329.031−0.198	16 00 30.34	−53 12 26.5	−39	−54,33	5	−52	−65,33	1.2	omg
G 329.066−0.307	16 01 09.89	−53 16 01.5	−48	−50,−47	1.4	−45	−46,−45	0.6	omg
G 329.183−0.313	16 01 46.90	−53 11 41.7	−51	−66,−36	24	−50	−60,−39	34	omg
G 329.342+0.130	16 00 38.87	−52 45 22.9	−112	−115,−95	1.1	−112	−114,−100	2.2	
G 329.404−0.459	16 03 31.81	−53 09 30.8	−113	−117,−106	3.1	−113	−116,−111	2.4	
G 329.405−0.459	16 03 32.15	−53 09 29.0	−78	−80,−60	15	−77	−79,−44	10	om
G 329.407−0.459	16 03 32.77	−53 09 25.0	−74	−76,−72	80			<0.2	mg
G 329.421−0.167	16 02 19.85	−52 55 41.8			<0.8	−77	−78,−75	2.4	
G 329.424−0.164	16 02 20.03	−52 55 25.9	−78	−83,−60	0.8			<0.2	g
G 329.426−0.161	16 02 19.71	−52 55 12.8	−73	−78,−71	8	−73	−74,−72	10	
G 329.457+0.503	15 59 36.93	−52 23 53.6			−	−66	−68,−65	4.3	
G 329.622+0.138	16 02 00.28	−52 33 57.7			−	−82	−110,−66	30	mg
G 330.070+1.064	16 00 15.56	−51 34 25.7			−	−50	−75,−45	11	mγ
G 330.879−0.367	16 10 20.04	−52 06 06.8	−64	−72,−28	90	−60	−72,−25	95	omc
G 330.954−0.182	16 09 52.65	−51 54 54.6	−80	−150,70	240	−91	−191,56	323	ocg
G 331.132−0.244	16 10 59.73	−51 50 22.5	−99	−102,−73	280	−99	−118,−55	47	omg
G 331.278−0.188	16 11 26.51	−51 41 55.8	−86	−104,−79	55	−90	−118,−64	42	omg
G 331.342−0.346	16 12 26.49	−51 46 14.9	−60	−62,−59	1.8	−62	−64,−60	11	omg
G 331.418+0.252	16 10 10.56	−51 16 52.2			−	−71	−71,−70	0.6	g
G 331.442−0.187	16 12 12.46	−51 35 09.3	−88	−93,−72	70	−88	−113,−80	212	omcg

**Table 1 – continued**

Water maser ( <i>l, b</i> ) (deg)	RA (J2000) (h m s)	Dec. (J2000) (° ''')	V peak (km s <sup>-1</sup> ) 2003	V range (km s <sup>-1</sup> ) 2003	S peak (Jy) 2003	V peak (km s <sup>-1</sup> ) 2004	V range (km s <sup>-1</sup> ) 2004	S peak (Jy) 2004	Associations
G 331.512–0.103	16 12 10.01	−51 28 36.7	−89	−162,−33	700	−90	−159,−32	534	ocg
G 331.555–0.122	16 12 27.20	−51 27 42.6	−99	−170,−96	20	−99	−166,−86	9	
G 332.094–0.421	16 16 16.68	−51 18 26.2			−	−59	−59,−58	0.29	m
G 332.296–0.094	16 15 45.84	−50 55 52.7			−	−50	−71,−43	6	m
G 332.349–0.433	16 17 30.03	−51 08 16.6			−	−67	−68,−67	2.9	
G 332.352–0.117	16 16 07.10	−50 54 31.0	−45	−48,−41	2.0	−60	−61,−60	0.5	om
G 332.604–0.167	16 17 29.45	−50 46 11.7			−	−46	−48,−45	2.4	mg
G 332.725–0.621	16 20 02.91	−51 00 33.1	−42	−43,−41	0.6	−58	−59,−56	5	omg
G 332.826–0.549	16 20 11.17	−50 53 14.6	−56	−72,−30	45	−59	−71,−35	70	mc
G 332.964–0.679	16 21 23.03	−50 52 57.3			−	−52	−52,−50	2.9	mg
G 333.030–0.063	16 18 56.86	−50 23 53.6			−	−40	−153,−40	3.4	mc
G 333.055–0.436	16 20 42.47	−50 38 46.4			−	−47	−57,−48	0.39	
G 333.114–0.439	16 20 59.30	−50 36 21.9	−62	−63,−60	4.6	−62	−62,−53	2.0	
G 333.121–0.434	16 20 59.70	−50 35 50.8	−57	−59,12	38	−47	−91,−33	21	m
G 333.126–0.440	16 21 02.69	−50 35 54.1	−50	−70,−48	19	−52	−72,−47	12	m
G 333.128–0.440	16 21 03.18	−50 35 51.8			<0.2	−124	−125,−124	0.79	m
G 333.130–0.425	16 20 59.75	−50 35 05.1	−39	−67,−38	23	−64	−65,−31	1.9	
G 333.132–0.560	16 21 36.46	−50 40 45.4			−	−53	−67,−46	1.9	
G 333.219–0.062	16 19 47.40	−50 15 53.8			<0.3	−13	−14,84	0.5	g
G 333.234–0.060	16 19 50.85	−50 15 09.7	−88	−102,−83	140	−88	−102,82	117	og
G 333.315+0.106	16 19 28.75	−50 04 39.7	−48	−68,−41	2.2	−48	−60,−48	6	omg
G 333.387+0.032	16 20 07.52	−50 04 47.4	−61	−63,−60	0.4	−61	−61,−60	0.14	omg
G 333.467–0.164	16 21 20.20	−50 09 46.1	−44	−46,−40	3.5	−42	−47,−40	3.2	om
G 333.608–0.215	16 22 11.08	−50 05 56.3	−51	−76,−45	50	−49	−83,−41	24	o
G 333.646+0.058	16 21 09.12	−49 52 45.1			−	−89	−90,−84	3.3	m
G 333.682–0.436	16 23 29.67	−50 12 07.4			−	−3	−3,−2	0.24	mg
G 333.930–0.134	16 23 14.68	−49 48 48.8			−	−46	−50,−45	0.18	m
G 334.635–0.015	16 25 45.83	−49 13 37.0			−	−26	−29,−15	49	mg
G 334.935–0.098	16 27 24.22	−49 04 11.0			−	−17	−18,−14	1.0	mg
G 334.951–0.092	16 27 26.96	−49 03 14.7			−	−21	−25,−20	1.3	
G 335.059–0.428	16 29 23.20	−49 12 31.3			t	−38	−39,−37	1.7	
G 335.060–0.428	16 29 23.24	−49 12 28.0	−46	−50,−37	12	−37	−44,15	3.0	omg
G 335.070–0.423	16 29 24.72	−49 11 47.7	−88	−109,−84	1.0	−90	−105,−84	5	g
G 335.585–0.285	16 30 57.34	−48 43 39.4	−45	−50,−40	30	−42	−49,−32	25	omg
G 335.586–0.290	16 30 58.73	−48 43 51.2	−48	−61,−33	5	−56	−57,−42	20	omg
G 335.588–0.264	16 30 52.52	−48 42 39.5	−51	−56,−48	16			<0.2	g
G 335.727+0.191	16 29 27.52	−48 17 51.9			−	−51	−51,−42	13	m
G 335.787+0.177	16 29 46.18	−48 15 49.1	−55	−56,−48	3.0	−49	−59,−45	10	
G 335.789+0.174	16 29 47.33	−48 15 50.8	−46	−51,−45	3.0			<0.2	omg
G 335.789+0.183	16 29 45.10	−48 15 30.4	−91	−112,−89	4.2			<0.2	
G 336.018–0.827	16 35 09.35	−48 46 47.7	−54	−59,−36	120	−54	−59,−36	82	omc
G 336.352–0.149	16 33 30.73	−48 04 27.6	−79	−81,−78	0.4	−79	−81,−78	0.43	
G 336.359–0.137	16 33 29.37	−48 03 41.5	−67	−67,−66	0.5			<0.2	omc
G 336.433–0.262	16 34 20.31	−48 05 30.5			−	−89	−90,−88	0.6	mg
G 336.496–0.258	16 34 34.52	−48 02 34.3			−	−25	−38,−14	8	
G 336.830–0.375	16 36 26.19	−47 52 29.5			−	−20	−45,−19	0.28	mg
G 336.864+0.005	16 34 54.50	−47 35 37.7	−78	−80,−64	3.0	−66	−79,−65	2.2	om
G 336.864–0.002	16 34 56.02	−47 35 55.3	−73	−76,−71	4.5	−73	−77,−71	1.5	
G 336.870–0.003	16 34 57.91	−47 35 42.7	−77	−78,−55	2.0	−77	−78,−71	3.7	
G 336.983–0.183	16 36 12.38	−47 37 59.1	−76	−77,−74	0.4	45	−78,45	0.18	o <sup>#</sup> mc
G 336.991–0.024	16 35 32.53	−47 31 12.4	−48	−61,−44	4	−49	−54,−44	1.0	c
G 336.994–0.027	16 35 34.01	−47 31 12.2	−121	−137,−80	160	−120	−177,−47	158	omg
G 336.995–0.024	16 35 33.53	−47 31 00.6			<0.2	−54	−54,−48	1.1	g
G 337.258–0.101	16 36 56.36	−47 22 27.5	−69	−71,−52	1.6	−69	−69,−68	0.33	omg
G 337.404–0.402	16 38 50.57	−47 28 00.8	−40	−53,−37	140	−40	−49,−35	137	omcg
G 337.612–0.060	16 38 09.46	−47 05 00.3	−52	−101,−47	38	−51	−99,−46	17	omg
G 337.687+0.137	16 37 35.60	−46 53 46.3			−	−74	−151,−73	0.6	mg
G 337.705–0.053	16 38 29.72	−47 00 35.7	−48	−147,5	54	−49	−159,−31	39	omcg
G 337.916–0.477	16 41 10.49	−47 08 02.9	−46	−80,−28	400	−33	−65,−27	321	o
G 337.920–0.456	16 41 06.14	−47 07 02.3	−40	−42,−39	50	−40	−69,−27	22	om
G 337.994+0.133	16 38 48.63	−46 40 15.7	−114	−117,−110	4.5	−113	−116,−111	4.5	

**Table 1** – *continued*

Water maser ( <i>l, b</i> ) (deg)	RA (J2000) (h m s)	Dec. (J2000) (° ' '')	V peak (km s <sup>-1</sup> ) 2003	V range (km s <sup>-1</sup> ) 2003	S peak (Jy) 2003	V peak (km s <sup>-1</sup> ) 2004	V range (km s <sup>-1</sup> ) 2004	S peak (Jy) 2004	Associations
G 337.998+0.137	16 38 48.53	-46 39 56.4	-39	-50,-32	30	-38	-47,-30	27	omg
G 338.069+0.011	16 39 37.98	-46 41 44.9	-37	-40,-21	1.3	-28	-46,-22	3.9	g
G 338.075+0.012	16 39 38.88	-46 41 26.8	-50	-51,-50	0.5			<0.2	omc
G 338.075+0.010	16 39 39.78	-46 41 31.8	-132	-139,-21	1.2	-48	-51,-28	1.2	m
G 338.077+0.019	16 39 37.69	-46 41 05.6	-40	-41,-38	1.0	-40	-40,-39	1.3	g
G 338.281+0.542	16 38 09.16	-46 11 02.6	-61	-68,-59	12	-64	-67,-58	4.6	omg
G 338.427+0.051	16 40 50.25	-46 24 05.5			-	-30	-46,-29	0.48	
G 338.430+0.053	16 40 50.50	-46 23 53.0			-	-44	-51,-29	3.2	g
G 338.433+0.057	16 40 50.08	-46 23 33.8			-	-29	-30,-29	0.19	m
G 338.435+0.055	16 40 51.23	-46 23 34.5			-	-31	-31,-30	0.58	
G 338.436+0.057	16 40 51.05	-46 23 26.8			-	-35	-56,-34	0.30	
G 338.440+0.064	16 40 49.87	-46 22 59.5			-	-81	-81,-80	0.6	g
G 338.461-0.245	16 42 15.57	-46 34 18.6	-53	-119,-51	9	-52	-114,-49	8	omg
G 338.462-0.259	16 42 19.49	-46 34 48.3			<0.2	-54	-55,-53	0.35	
G 338.472+0.289	16 39 58.99	-46 12 36.2	-54	-62,-22	25	-29	-62,-25	10	omg
G 338.562+0.217	16 40 38.12	-46 11 24.8			-	-39	-40,-39	0.22	mg
G 338.567+0.110	16 41 07.16	-46 15 28.1			-	-76	-92,-74	3.2	m
G 338.682-0.084	16 42 24.12	-46 17 59.1	-6	-18,-5	2.2	-16	-18,-6	0.7	ocg
G 338.920+0.550	16 40 34.02	-45 42 07.9	-110	-125,-65	17	-68	-127,-64	5.3	mg
G 338.925+0.556	16 40 33.63	-45 41 37.9	-63	-85,-61	160	-62	-86,-6	116	om
G 338.924-0.060	16 43 13.25	-46 06 04.2			-	-64	-69,-63	2.3	
G 339.582-0.127	16 45 58.88	-45 38 47.4			-	-28	-32,-26	0.27	mg
G 339.584-0.128	16 45 59.63	-45 38 44.3			-	-40	-41,-26	1.8	o
G 339.585-0.126	16 45 59.18	-45 38 36.7			-	-41	-75,-39	0.40	o
G 339.586-0.128	16 45 59.92	-45 38 39.7			-	-106	-112,-105	0.5	o
G 339.609-0.115	16 46 01.57	-45 37 07.3			<0.2	-71	-82,-67	3.0	
G 339.622-0.121	16 46 06.03	-45 36 44.5	-34	-38,-32	90	-33	-36,-32	43	om
G 339.762+0.055	16 45 51.56	-45 23 31.0			-	-57	-58,-57	0.25	mg
G 339.884-1.259	16 52 04.71	-46 08 33.6	-32	-50,-28	50	-51	-52,-24	4.3	omγ
G 340.054-0.243	16 48 13.82	-45 21 43.9	-54	-58,-44	35			-	omg
G 340.785-0.096	16 50 14.84	-44 42 24.7	-120	-121,-111	1.0			<0.2	omg
G 341.218-0.212	16 52 17.92	-44 26 51.6	-43	-47,-38	120	-39	-49,-23	33	omg
G 341.276+0.062	16 51 19.50	-44 13 44.0	-77	-80,-58	5	-64	-83,-62	10	omg
G 342.484+0.183	16 55 02.39	-43 12 59.3			-	-43	-44,-36	0.6	mg
G 343.126-0.065	16 58 17.54	-42 52 15.8	-16	-17,-15	2.5	-21	-23,-20	8	
G 343.127-0.063	16 58 17.29	-42 52 06.6	-35	-45,-20	250	-30	-46,-16	208	o
G 344.226-0.576	17 04 09.36	-42 18 58.0			<0.2	-19	-19,-18	0.33	
G 344.228-0.569	17 04 07.85	-42 18 38.9	-24	-28,31	8	-25	-52,-9	1.4	omg
G 344.421+0.046	17 02 08.53	-41 46 56.4	-27	-32,-18	1.8	-26	-31,-24	0.9	
G 344.582-0.024	17 02 57.94	-41 41 54.1	-4	-20,5	250	-4	-52,6	127	omcg
G 345.004-0.224	17 05 11.12	-41 29 04.1	-23	-46,16	3.0	15	-89,15	3.7	om <sup>#</sup> cg
G 345.010+1.793	16 56 47.51	-40 14 23.9	-17	-19,10	2.0			<0.2	omcγ
G 345.010+1.802	16 56 45.41	-40 14 04.2	-28	-33,-26	7	-25	-31,-18	23	γ
G 345.012+1.797	16 56 47.01	-40 14 08.5	-12	-13,7	50	-12	-12,7	29	mγ
G 345.397-0.950	17 09 33.08	-41 36 20.4	-21	-22,-20	3.1	-21	-27,-20	6	
G 345.402-0.948	17 09 33.62	-41 36 02.9	-26	-32,-21	8	-23	-32,-21	2.9	
G 345.405-0.947	17 09 33.83	-41 35 50.8			<0.5	-28	-28,-23	0.5	
G 345.406-0.942	17 09 32.71	-41 35 37.6	-15	-19,-12	3.0	-18	-20,-17	1.9	
G 345.408-0.953	17 09 35.85	-41 35 56.5			<0.5	-15	-16,36	0.5	o <sup>#</sup> m <sup>#</sup> c
G 345.412-0.955	17 09 37.08	-41 35 48.9			<0.2	-55	-55,-54	1.6	
G 345.425-0.951	17 09 38.64	-41 35 03.3	-13	-15,-12	1.5	-13	-16,-13	1.1	m
G 345.438-0.074	17 05 56.75	-41 02 54.9	-11	-32,-9	40	-12	-37,-8	15	o
G 345.482+0.309	17 04 28.41	-40 46 52.1	-52	-80,-24	15	-55	-82,-51	1.8	
G 345.487+0.314	17 04 28.19	-40 46 28.6	-16	-24,2	6	-13	-39,-12	0.7	m
G 345.493+1.469	16 59 41.47	-40 03 46.2	5	3,6	6			<0.2	oγ
G 345.494+1.470	16 59 41.15	-40 03 39.9	1	-16,2	1.0	0	-18,-4	1.8	γ
G 345.495+1.473	16 59 40.78	-40 03 28.9	-60	-62,-16	4.0	-9	-10,-8	1.5	γ
G 345.505+0.348	17 04 23.02	-40 44 23.5	-3	-43,1	22	-4	-42,4	4.5	om
G 345.505+0.343	17 04 24.35	-40 44 32.1			<0.2	-68	-70,-67	0.8	
G 345.699-0.090	17 06 50.72	-40 50 58.9	-10	-87,102	200	-5	-92,141	216	og

**Table 1 – continued**

Water maser ( <i>l, b</i> ) (deg)	RA (J2000) (h m s)	Dec. (J2000) (° ''')	V peak (km s <sup>-1</sup> ) 2003	V range (km s <sup>-1</sup> ) 2003	S peak (Jy) 2003	V peak (km s <sup>-1</sup> ) 2004	V range (km s <sup>-1</sup> ) 2004	S peak (Jy) 2004	Associations
G 346.480+0.132	17 08 22.67	-40 05 26.9	-10	-12,-8	1.2			<0.2	omg
G 346.522+0.085	17 08 42.35	-40 05 08.1			-	4	-2,14	2.9	m
G 346.529+0.106	17 08 38.12	-40 04 03.9			-	4	-1,5	1.6	
G 347.588+0.213	17 11 27.61	-39 09 08.1			-	-93	-94,-93	0.7	
G 347.623+0.148	17 11 50.09	-39 09 45.8	-118	-120,-117	0.5	-118	-122,-116	1.0	
G 347.628+0.149	17 11 50.85	-39 09 29.6	-125	-133,-122	0.5			<0.2	omg
G 347.632+0.210	17 11 36.30	-39 07 06.5			-	-88	-95,-24	6	mc
G 348.533-0.974	17 19 16.20	-39 04 30.6	-56	-59,-10	3.2	-31	-93,24	1.8	
G 348.534-0.983	17 19 18.64	-39 04 47.3	-21	-30,-11	2.2	-14	-109,-12	0.9	
G 348.551-0.979	17 19 20.61	-39 03 49.2	-30	-32,-15	1.4	-18	-18,-17	0.28	mg
G 348.726-1.038	17 20 06.42	-38 57 13.2	-11	-64,42	115	-10	-77,61	162	$\gamma$
G 348.885+0.096	17 15 50.25	-38 10 12.3	-81	-84,-77	8	-80	-87,-77	8	omg
G 348.892-0.180	17 17 00.26	-38 19 27.9	7	6,12	2.0			-	omg
G 349.052+0.002	17 16 43.25	-38 05 18.2	15	14,17	3.0			<0.2	
G 349.067-0.018	17 16 50.82	-38 05 13.8	5	3,7	1.6	13	-14,19	1.0	omg
G 349.074-0.015	17 16 51.23	-38 04 49.3	-27	-32,-20	1.6	-26	-32,-24	1.2	g
G 349.068+0.110	17 16 19.24	-38 00 48.3	-25	-32,-22	3.0	-21	-22,-20	1.4	
G 349.092+0.105	17 16 24.66	-37 59 45.4	-80	-84,-74	43	-80	-84,-72	154	omg
G 350.015+0.433	17 17 45.43	-37 03 12.9	-35	-50,-26	4.7			-	omg
G 350.098+0.080	17 19 26.67	-37 11 20.8	-66	-68,-65	6	-67	-69,-67	2.6	g
G 350.100+0.081	17 19 26.74	-37 11 09.8	-68	-69,-67	4.0	-68	-69,-63	5	
G 350.105+0.084	17 19 26.78	-37 10 51.5	-71	-102,-38	6	-71	-74,-29	14	m
G 350.110+0.087	17 19 26.96	-37 10 29.0	-72	-74,-71	8	-72	-73,-70	14	g
G 350.112+0.089	17 19 26.96	-37 10 19.9	-172	-175,-110	2.0	-128	-164,-106	2.9	
G 350.113+0.095	17 19 25.69	-37 10 04.8	-66	-70,-64	2.5	-64	-79,-63	1.4	og
G 350.274+0.120	17 19 47.07	-37 01 16.6			-	-63	-63,-61	2.9	
G 350.299+0.122	17 19 50.89	-37 00 00.6			-	-68	-68,-67	0.17	m
G 350.330+0.100	17 20 01.79	-36 59 14.3	-68	-69,-60	1.0	-62	-68,-48	1.9	o
G 350.341+0.140	17 19 53.60	-36 57 19.0			-	-105	-105,-58	3.2	g
G 350.686-0.491	17 23 28.71	-37 01 47.9	-23	-22,-24	0.6	-14	-14,-13	1.0	omg
G 350.690-0.490	17 23 29.19	-37 01 35.6			<0.6	-22	-24,-21	3.4	
G 351.160+0.696	17 19 57.50	-35 57 54.1	-3	-11.5,-0.5	9	-3	-10,2	18	omc
G 351.163+0.696	17 19 58.13	-35 57 48.9			t	-10	-13,-9	10	
G 351.240+0.668	17 20 17.98	-35 54 57.6			-	-24	-38,31	21	
G 351.243+0.671	17 20 17.76	-35 54 42.8			-	-77	-108,84	453	m
G 351.246+0.668	17 20 19.01	-35 54 38.2			-	21	19,22	1.3	c
G 351.417+0.646	17 20 53.29	-35 46 58.3	-10	-58,50	1400			-	om
G 351.582-0.353	17 25 25.35	-36 12 44.0	-89	-120,-87	1600			-	omg
G 351.775-0.536	17 26 42.50	-36 09 15.9	-2	-32,21	85			-	om
G 352.098+0.160	17 24 45.25	-35 29 48.8			-	-75	-75,-73	2.5	g
G 352.111+0.176	17 24 43.79	-35 28 37.7			-	-60	-61,-60	1.3	mg
G 352.133-0.944	17 29 22.46	-36 04 59.9			-	-11	-17,-6	27	mg
G 352.162+0.199	17 24 46.36	-35 25 19.9	-45	-46,-44	1	-45	-119,-43	0.28	og
G 352.517-0.155	17 27 11.34	-35 19 32.0	-49	-53,-46	12			-	om
G 352.525-0.158	17 27 13.44	-35 19 15.7	-51	-53,-49	3.6			-	mg
G 352.623-1.076	17 31 14.93	-35 44 47.5	2	0,2	28	2	-7,3	8	$\gamma$
G 352.630-1.067	17 31 13.94	-35 44 08.8	-2	-10,20	35	0	-13,18	700	omg
G 353.273+0.641	17 26 01.57	-34 15 14.7			-	-49	-110,-5	366	m
G 353.408-0.350	17 30 23.38	-34 41 29.8			<0.2	-14	-15,-13	0.6	g
G 353.411-0.356	17 30 25.31	-34 41 35.0			<0.2	-20	-21,-17	6.4	
G 353.411-0.362	17 30 26.78	-34 41 46.6			<0.2	-7	-7,-5	1.8	c
G 353.413-0.367	17 30 28.47	-34 41 49.1	-17	-29,-8	2.0	-20	-26,-9	7	g
G 353.413-0.365	17 30 27.84	-34 41 44.6	-20	-24,-18	4.5	-19	-25,-18	2.2	
G 353.414-0.363	17 30 27.56	-34 41 38.9	-10	-11,-9	2	1	-22,7	1.7	
G 353.463+0.563	17 26 51.25	-34 08 25.3	-47	-52,-46	1			-	g
G 353.464+0.562	17 26 51.61	-34 08 24.1	-60	-61,-59	0.7			-	omg
G 354.594+0.469	17 30 14.47	-33 15 03.2	-22	-25,-20	9			<0.2	
G 354.615+0.472	17 30 17.22	-33 13 54.4	-38	-40,-12	1.6			<0.2	om
G 354.703+0.297	17 31 12.96	-33 15 17.6			<0.4	105	104,112	1.6	
G 354.712+0.293	17 31 15.38	-33 14 57.8	96	95,105	1.1			<0.2	g
G 354.722+0.302	17 31 14.87	-33 14 08.3			<0.2	99	96,101	0.38	

**Table 1** – *continued*

Water maser ( <i>l, b</i> ) (deg)	RA (J2000) (h m s)	Dec. (J2000) (° ' '')	V peak 2003 (km s <sup>-1</sup> )	V range 2003 (km s <sup>-1</sup> )	S peak 2003 (Jy)	V peak 2004 (km s <sup>-1</sup> )	V range 2004 (km s <sup>-1</sup> )	S peak 2004 (Jy)	Associations
G 355.343+0.147	17 33 29.00	−32 48 00.1	17	9.35	34			–	om
G 355.345+0.149	17 33 28.83	−32 47 49.9	72	8,109	2.2			–	m
G 357.965−0.164	17 41 20.12	−30 45 15.9	−4	−5,−3	53	−19	−20,−19	0.9	mg
G 357.967−0.163	17 41 20.30	−30 45 07.0	0	−80,100	40	−65	−81,87	57	om
G 358.371−0.468	17 43 32.01	−30 34 11.4	10	−5,12	2.7	2	2,31	1.4	mg
G 358.386−0.483	17 43 37.72	−30 33 50.6	−1	−4,1	4.5	0	−3,1	3.6	omcg
G 359.137+0.032	17 43 25.61	−29 39 18.6	−1	−117,26	300			–	omg
G 359.419−0.104	17 44 38.27	−29 29 12.0		<0.2	−26	−59,2	1.0		
G 359.436−0.102	17 44 40.23	−29 28 12.2	−59	−61,−50	15	−59	−61,−54	9	mg
G 359.436−0.104	17 44 40.66	−29 28 16.1	−56	−57,−55	1.5	−47	−48,−47	0.37	om
G 359.441−0.111	17 44 42.87	−29 28 15.4	−65	−66,−64	1.8		<0.2		
G 359.442−0.106	17 44 42.00	−29 28 00.6	−53	−54,−52	9	−53	−56,−52	0.28	g
G 359.442−0.104	17 44 41.47	−29 27 58.8		t	−60	−62,−58	0.8		
G 359.443−0.104	17 44 41.82	−29 27 56.5		t	−49	−52,−48	0.6	g	
G 359.615−0.243	17 45 39.12	−29 23 29.6	22	−16,73	7	64	−15,68	14	omg
G 359.969−0.457	17 47 20.08	−29 11 59.0	11	10,16	27			–	om
G 0.209−0.002	17 46 07.44	−28 45 32.1		–	39	18,42	2.2	c	
G 0.212−0.002	17 46 07.86	−28 45 23.0		–	56	55,65	0.9	m	
G 0.216−0.023	17 46 13.20	−28 45 49.8		–	−11	−16,8	1.7	g	
G 0.308−0.177	17 47 02.38	−28 45 55.2		–	−26	−27,−26	1.8	g	
G 0.316−0.201	17 47 09.29	−28 46 15.5		–	23	14,31	22	mg	
G 0.376+0.040	17 46 21.29	−28 35 39.7	40	5,58	55			–	omg
G 0.497+0.188	17 46 03.96	−28 24 50.7	−8	−72,25	7	26	−50,34	2.5	omg
G 0.547−0.851	17 50 14.52	−28 54 28.8	20	−60,110	200			–	omg
G 0.655−0.045	17 47 20.88	−28 23 59.9	−52	−55,−50	4.0			–	og
G 0.657−0.042	17 47 20.44	−28 23 46.4	62	60,64	70			–	og
G 0.665−0.032	17 47 19.07	−28 23 03.5	4	0,7	4.3			–	o <sub>g</sub>
G 0.668−0.035	17 47 20.26	−28 23 02.6	59	50,90	408			–	og
G 0.677−0.028	17 47 19.64	−28 22 18.9	36	14,132	330			–	o <sub>g</sub>
G 2.143+0.009	17 50 36.13	−27 05 46.4	37	35,70	0.6			–	omg
G 2.536+0.198	17 50 46.66	−26 39 44.9		–	25	−1,63	30	m	
G 5.886−0.392	18 00 30.52	−24 03 58.2	11	−10,23	40			–	o <sup>#</sup> m <sup>#</sup>
G 5.897−0.445	18 00 43.90	−24 04 58.1		–	19	19,20	0.9		
G 5.901−0.430	18 00 40.95	−24 04 19.6		–	14	−40,30	3.9	m	
G 5.913−0.388	18 00 33.12	−24 02 28.4	−50	−65,−47	9.2			–	g
G 6.049−1.447	18 04 53.19	−24 26 40.3	20	18,22	1.0			–	o <sup>γ</sup>
G 6.534−0.105	18 00 49.44	−23 21 40.2		–	22	6,23	0.5	g	
G 6.611−0.082	18 00 54.15	−23 17 00.8		–	6	−34,11	7	mg	
G 6.796−0.257	18 01 57.71	−23 12 32.5	14	10,20	10	1	−1,24	5	omg
G 8.139+0.226	18 03 00.83	−21 48 09.5		–	16	1,24	18	mg	
G 8.670−0.356	18 06 19.17	−21 37 31.0	34	30,44	10	36	−9,43	3.4	omc
G 8.673−0.354	18 06 18.98	−21 37 17.9	−4	−23,−3	0.5	−8	−20,4	0.36	
G 9.620+0.194	18 06 14.97	−20 31 37.5	5	−30,50	25	6	−19,11	12	o
G 9.622+0.195	18 06 14.88	−20 31 31.0	21	0,22	1.4	22	0,23	1.3	om <sup>#</sup>
G 9.986−0.028	18 07 50.20	−20 18 55.9		–	49	44,60	4.0	mg	
G 10.288−0.125	18 08 49.44	−20 05 57.4		–	9	9,11	0.5	m	
G 10.307−0.270	18 09 24.29	−20 09 08.8		–	33	32,33	0.8		
G 10.323−0.160	18 09 01.57	−20 05 07.6		–	−3	−6,62	3.2	m	
G 10.331−0.159	18 09 02.30	−20 04 40.2		–	11	7,22	1.0		
G 10.342−0.143	18 09 00.11	−20 03 35.8		–	8	−40,61	4.8	mg	
G 10.445−0.018	18 08 45.01	−19 54 35.1	71	58,85	6	70	69,81	2.7	
G 10.473+0.027	18 08 38.30	−19 51 48.8	60	30,93	45	62	28,129	169	omcg
G 10.480+0.034	18 08 37.69	−19 51 12.4	64	63,65	12			<0.2	om
G 10.623−0.383	18 10 28.57	−19 55 49.4	2	−11,5	350			–	og
G 10.625−0.335	18 10 18.07	−19 54 20.5		–	−5	−6,−5	0.40		
G 10.959+0.022	18 09 39.38	−19 26 27.0		–	25	7,26	2.9	mcg	
G 11.034+0.062	18 09 39.75	−19 21 21.1	18	16,19	0.6			–	om
G 11.498−1.486	18 16 22.32	−19 41 26.1		–	17	−3,21	112	m <sup>γ</sup>	
G 11.903−0.142	18 12 11.41	−18 41 33.0	36	35,38	0.3			<0.2	om
G 12.203−0.107	18 12 40.25	−18 24 47.4	33	32,35	6	35	32,37	8	m
G 12.209−0.102	18 12 39.88	−18 24 17.1	21	−12,42	141	22	−15,50	51	mcg

**Table 1 – continued**

Water maser ( $l, b$ ) (deg)	RA (J2000) (h m s)	Dec. (J2000) ( $^{\circ} \text{ } '$ '')	V peak (km s $^{-1}$ ) 2003	V range (km s $^{-1}$ ) 2003	S peak (Jy) 2003	V peak (km s $^{-1}$ ) 2004	V range (km s $^{-1}$ ) 2004	S peak (Jy) 2004	Associations
G 12.216–0.119	18 12 44.55	–18 24 25.2	26	25.42	6	26	0.38	10	og
G 12.681–0.183	18 13 54.82	–18 01 47.0	61	55.63	1200	61	17.62	445	omg
G 12.884+0.502	18 11 47.92	–17 31 21.3	42	41.43	1.3	40	34.41	1.1	
G 12.889+0.489	18 11 51.54	–17 31 27.9	30	28.32	45	30	28.39	59	omg
G 12.901–0.242	18 14 34.50	–17 51 51.6	35	23.37	8	36	23.37	12	g
G 12.908–0.260	18 14 39.45	–17 52 01.4	37	21.39	0.8		<0.2		om
G 15.016–0.679	18 20 23.11	–16 12 38.8		t	19	14.21	11		
G 15.025–0.658	18 20 19.50	–16 11 31.9		t	25	14.31	4.2		
G 15.026–0.654	18 20 18.72	–16 11 23.3	27	27.31	29	28	26.31	16	
G 15.028–0.673	18 20 23.04	–16 11 48.4	19	17.28	197	20	14.31	67	
G 15.032–0.667	18 20 22.35	–16 11 27.2	45	44.46	1.8	40	–8.41	1.1	g
G 15.032–0.670	18 20 23.01	–16 11 30.1		t	26	14.28	12		
G 15.034–0.667	18 20 22.58	–16 11 18.4		t	17	17.21	3.8		
G 17.638+0.156	18 22 26.45	–13 30 12.4	27	15.29	230	27	17.35	245	om

Note. Column 1 shows the source name in Galactic coordinates, Columns 2 and 3 give the right ascension and declination, Column 4–6 give the velocity of the water maser peak, velocity range and peak flux density in the 2003 observations, while Columns 7–9 give the velocity of the water maser peak, velocity range and peak flux density in the 2004 observations. A ‘–’ in either Column 6 or 9 indicates that no observations were made of the given source during the 2003 or the 2004 epoch, respectively, while the presence of a number preceded by a ‘<’ indicates that there was no emission detected above the quoted threshold. For some complicated sources, a ‘t’ is present in either Column 6 or 9 and this indicates that the exact nature of the detection is discussed in Section 4. Associations are given in Column 10, where the presence of an ‘o’ denotes an OH maser, an ‘m’ denotes a methanol maser, a ‘c’ denotes the presence of a 22-GHz radio continuum source, a ‘g’ the presence of a GLIMPSE point source and the presence of a ‘γ’ indicates that the water maser source is outside the range of the GLIMPSE survey region. A ‘#’ indicates that the proceeding associated source is strictly outside our association threshold but has been added through special circumstances. See Section 3 for a more extensive description.

spectra that are complex (or include multiple nearby sources) or increased it in order to display extremely high-velocity features. A decreased velocity range of 100 km s $^{-1}$  is shown for the following sources: 301.136–0.225, 301.136–0.226a, 301.136–0.226b, 301.137–0.225, 335.060–0.428/335.059–0.428, 336.991–0.024, 336.995–0.024, 359.441–0.111, 359.442–0.106, 359.442–0.104, 359.443–0.104. An increased range of 300 km s $^{-1}$  was used for 320.120–0.440, 330.954–0.182, 333.219–0.062, 333.234–0.060, 345.699–0.090, 357.965–0.164, 357.967–0.163, 0.547–0.851, 0.668–0.035, 0.665–0.032, 0.655–0.045, 0.657–0.042 and 0.677–0.028.

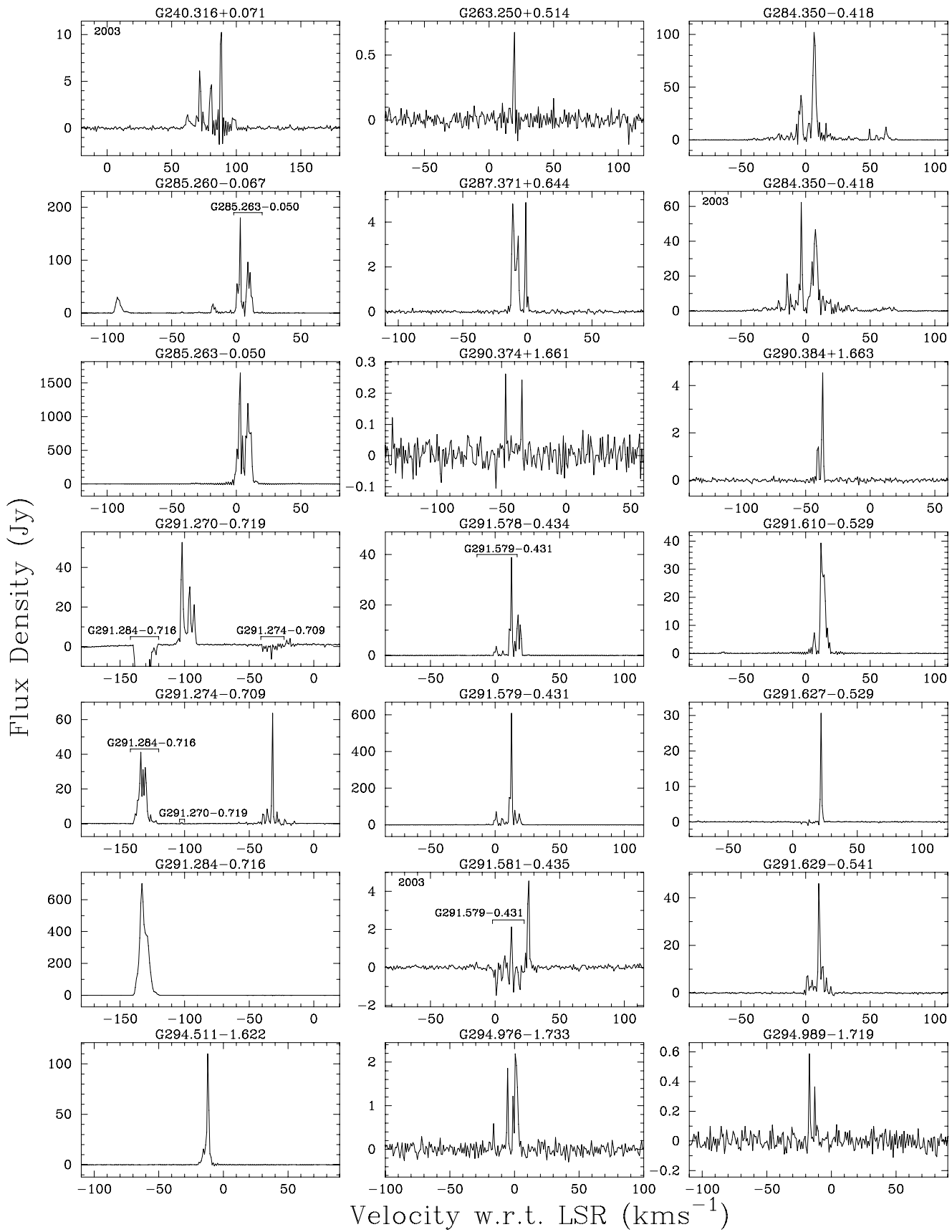
A number of the sources that we detect have been observed previously and have been presented in the literature (e.g. Johnston et al. 1972; Caswell et al. 1974; Kaufmann et al. 1976; Genzel & Downes 1977; Batchelor et al. 1980; Braz & Scalise 1982; Braz & Epcstein 1983; Caswell et al. 1989, and references therein), but the majority of these earlier observations (performed up to 20 yr ago) were made with relatively poor positional accuracy. Due to the intrinsically variable nature of water masers, many sources exhibit levels of variability so extreme that they display no common spectral features at epochs separated by many years. This, combined with the tendency of water masers to form in clusters, and the previously poor positional information mean that it is almost impossible to accurately match up sources from the literature with our present data. We have therefore limited our references (in Section 4) to previous detections of sources that were observed with high positional precision (e.g. FC89; Breen et al. 2007; Caswell & Phillips 2008) or where there was little doubt that the sources were the same.

The majority of OH maser targets were observed in both 2003 and 2004, whereas the methanol maser targets were observed in 2004 only. Where appropriate data were available for both epochs, reported positions are the average of the two since, in general, it provides the most accurate positions for the sources. For sources north of declination  $-20^{\circ}$ , we have used a weighting of 2:1 for the

declinations in favour of the 2004 data to account for the three times more elongated beam of the 2003 observations (a consequence of the different array configurations). Sources that were observed at both epochs allowed a direct comparison of the positions for each of the sources and therefore afford verification of the positional uncertainties.

Additional to direct comparison of 2003 with 2004 data, an overall assessment of data quality and reliability was made in several other ways. FC89 and FC99 used their VLA observations of a sample of more than 70 SFR targets with OH and water masers, to show that more than half were a simple association of water and OH masers coincident to within their combined relative errors (of typically 1 arcsec). Subsequent observation of the more southerly OH masers in that sample with the ATCA (C98) showed that the most southerly ones (observed by the VLA inevitably at low elevation) had significantly larger position uncertainties, and corrections to the positions resulted in an increased number of close OH/water maser associations. Thus we may expect the majority of our sample to show a water maser position coincident with OH, and thus the OH position is an indirect check on the accuracy of the newly derived water positions.

A further assessment was made using the 35 masers north of declination  $-47^{\circ}$  which are present in the FC89 target list. The FC89 absolute positions for the more southerly targets, although of variable quality for the OH masers (where ionospheric effects at low elevation can be significant), appear to remain excellent for the water masers. Thus we can directly compare our positions to those of FC89, to assess the errors in our current data. Furthermore, in some fields there is a strong ultracompact H II (UCHII) region that has been measured to subarcsecond accuracy, such as in the 6-GHz observations of C97 and C2001; where these are detectable in the current 22-GHz observations, they allow a further check on the positions, without the need for any assumptions concerning the true relative positions of the masers.

**Figure 1.** Spectra of the 22-GHz water masers detected in 2004 towards sites of OH and methanol masers.

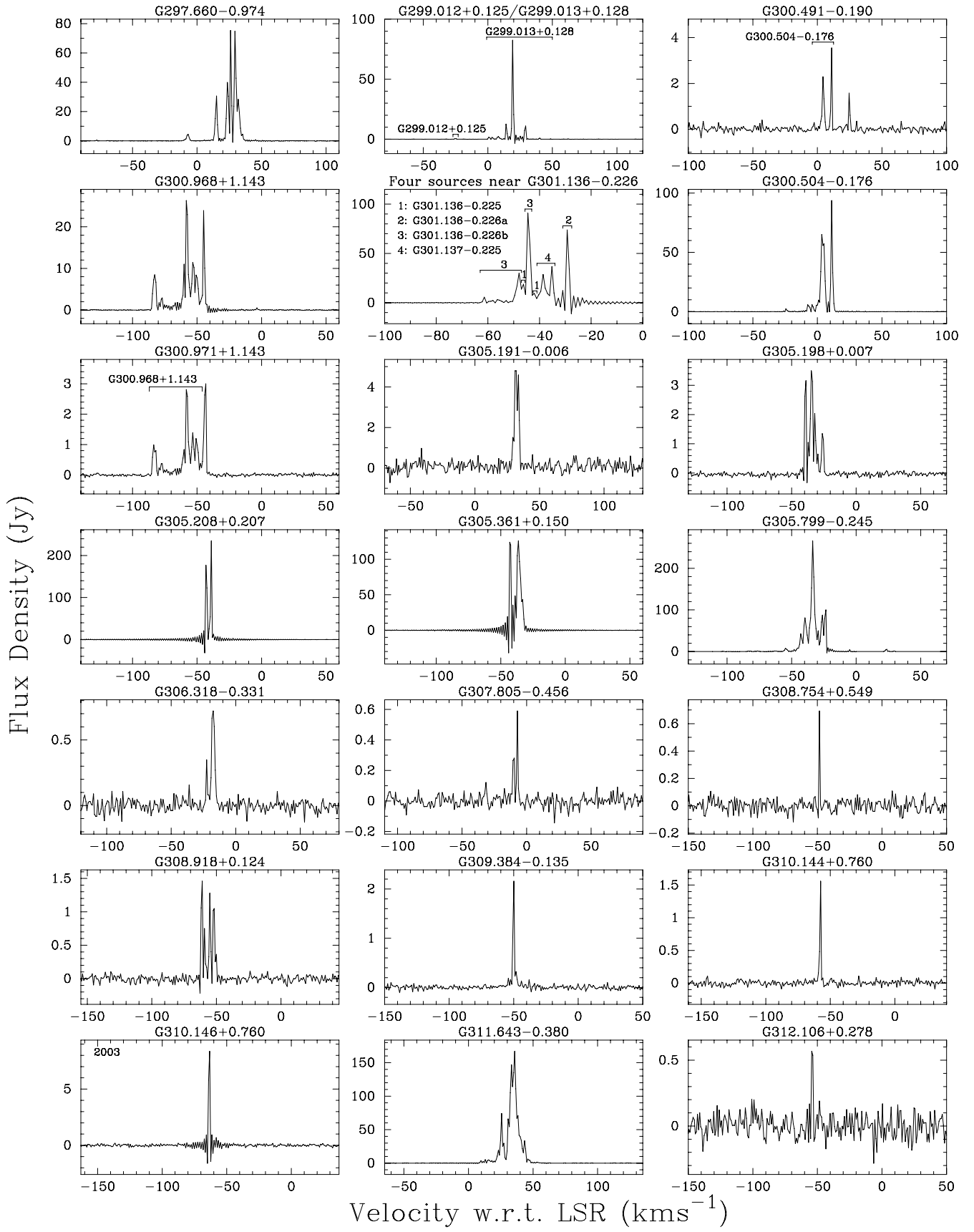
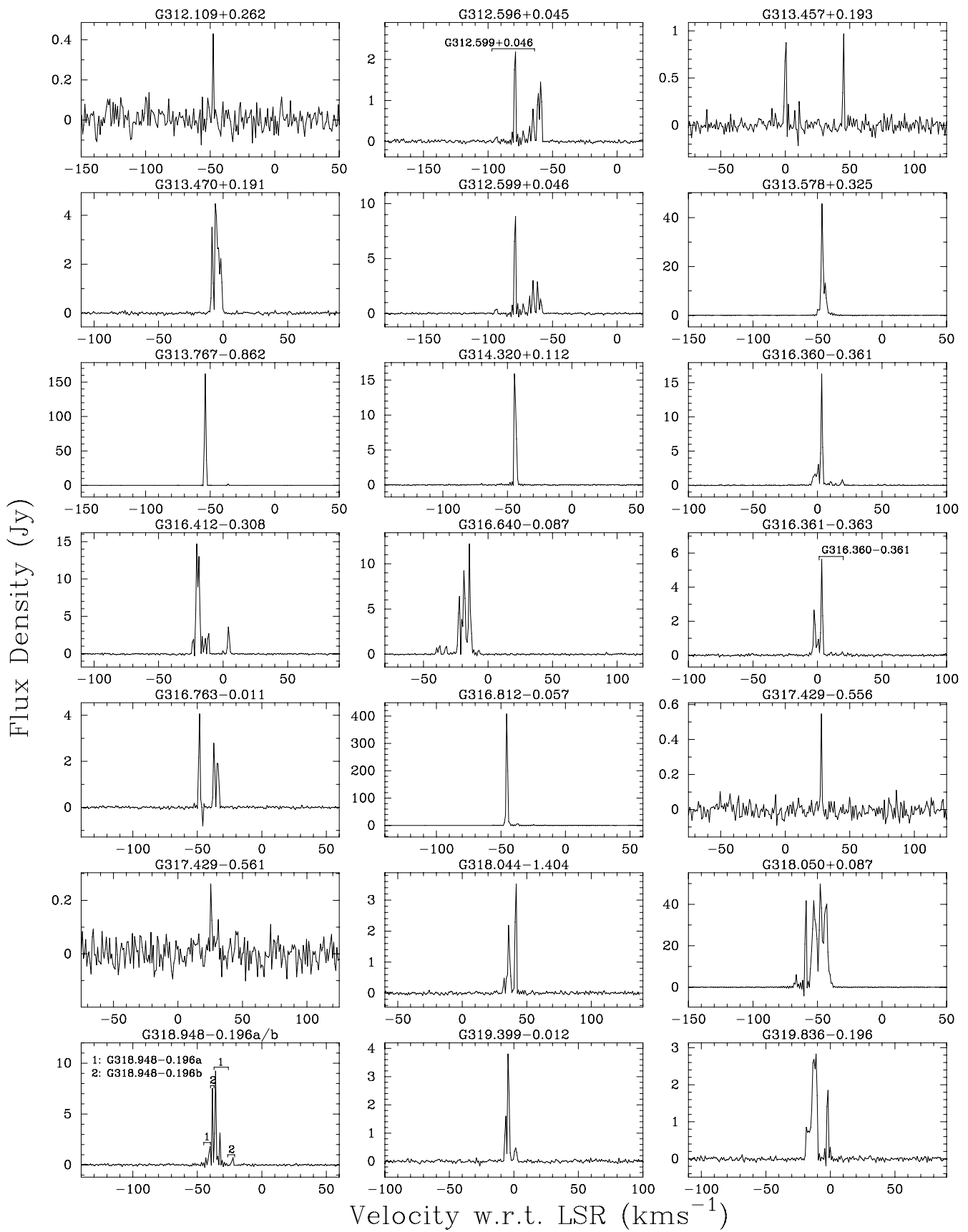
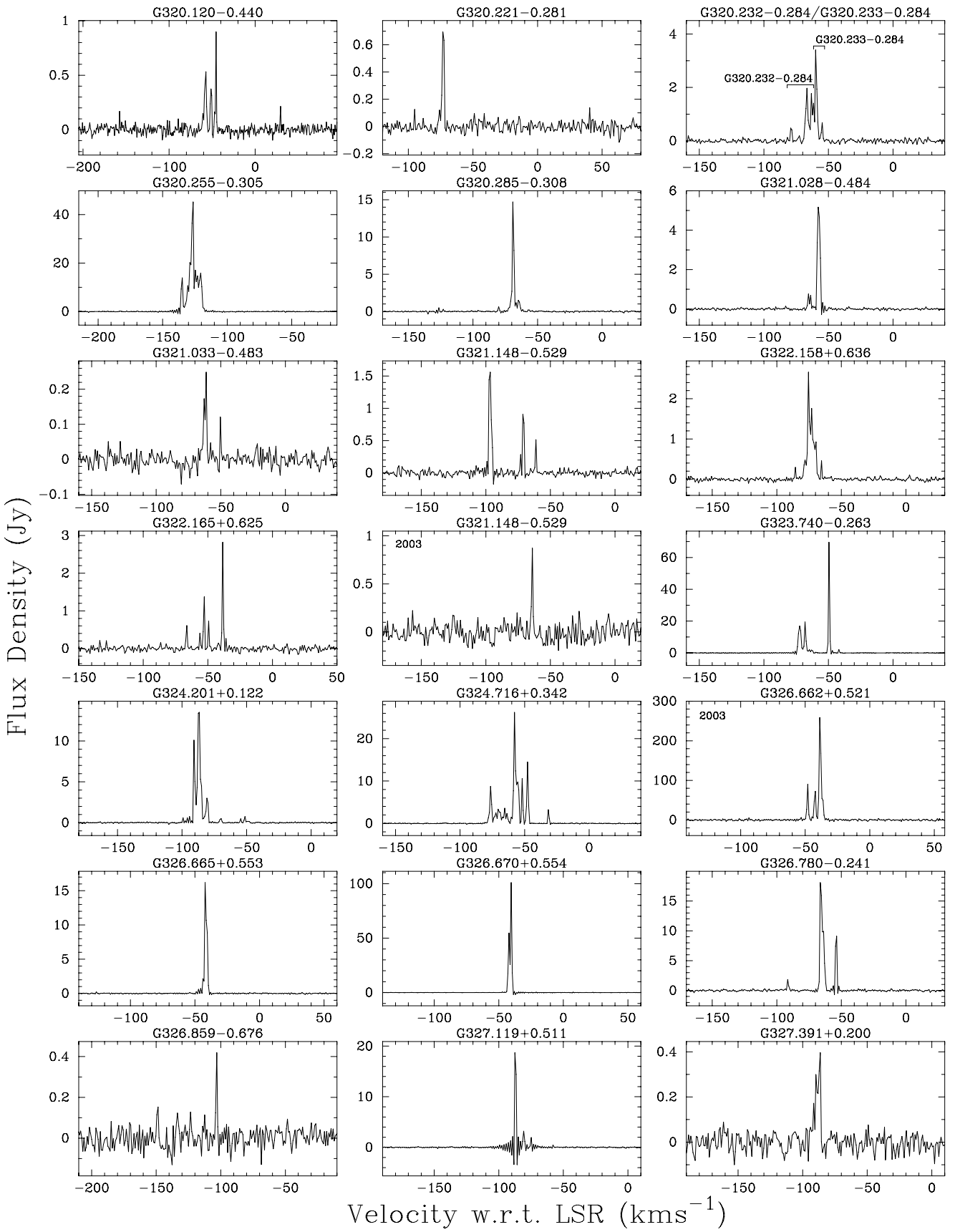
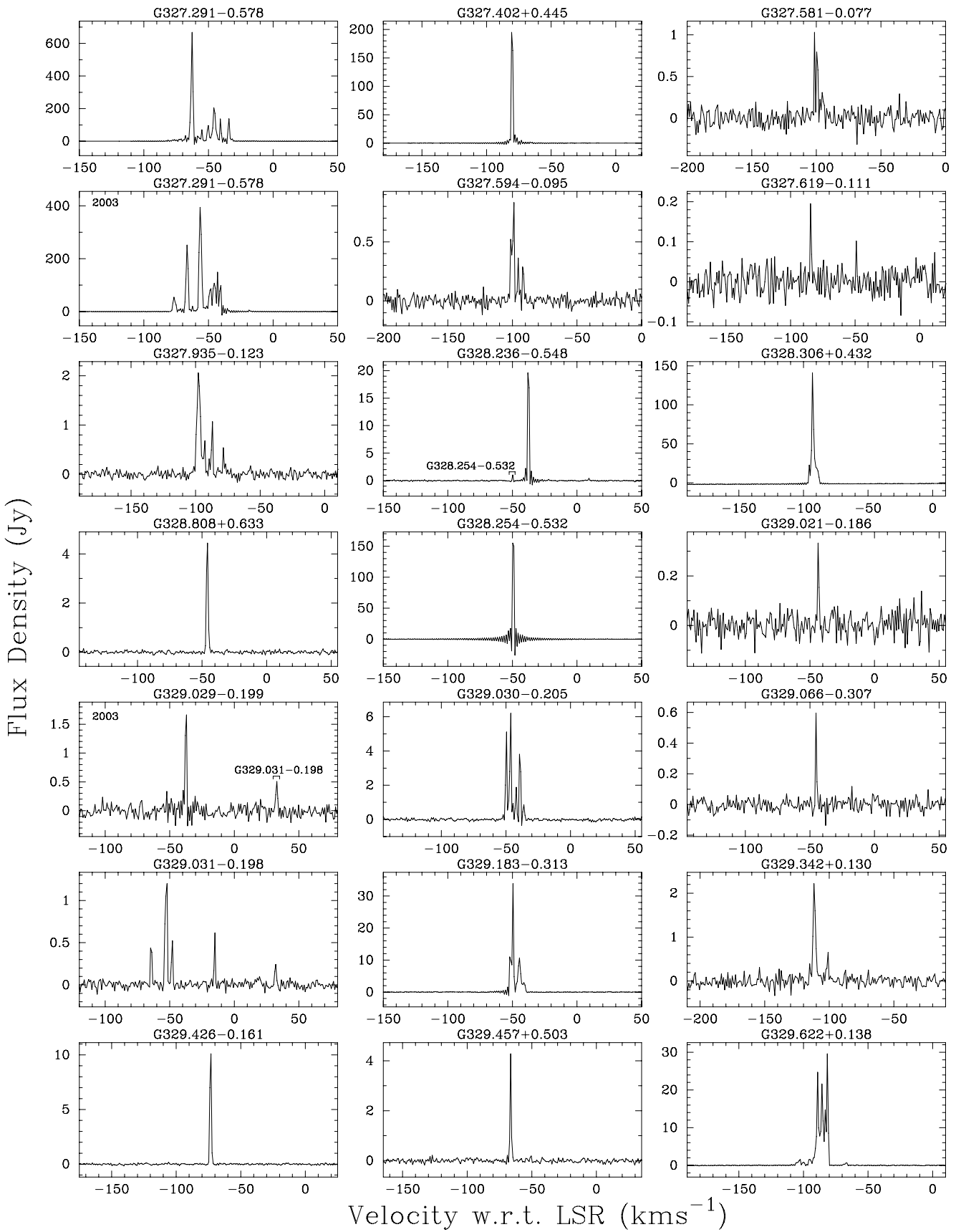


Figure 1 – continued

**Figure 1 – continued**

**Figure 1 – continued**

**Figure 1 – continued**

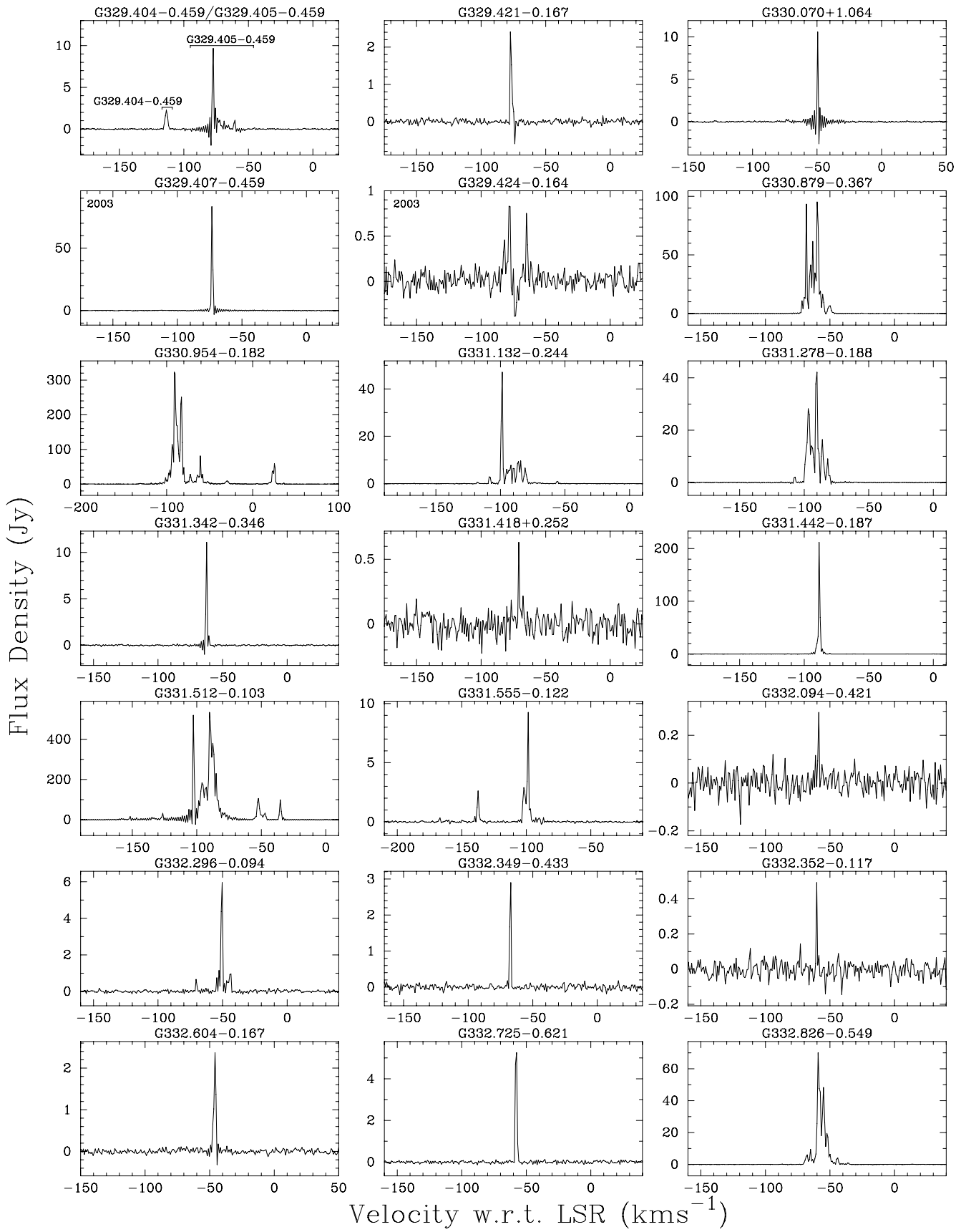


Figure 1 – continued

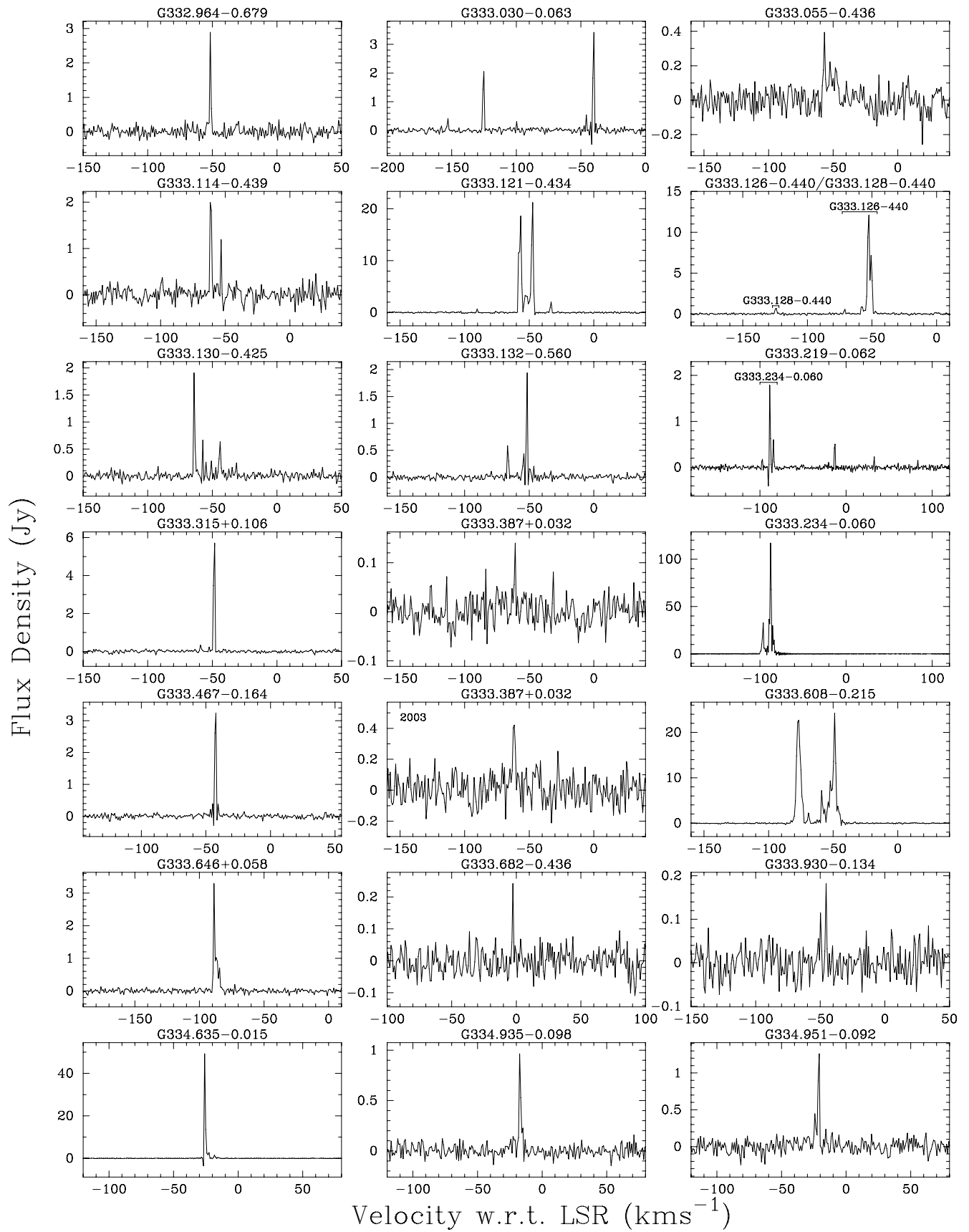
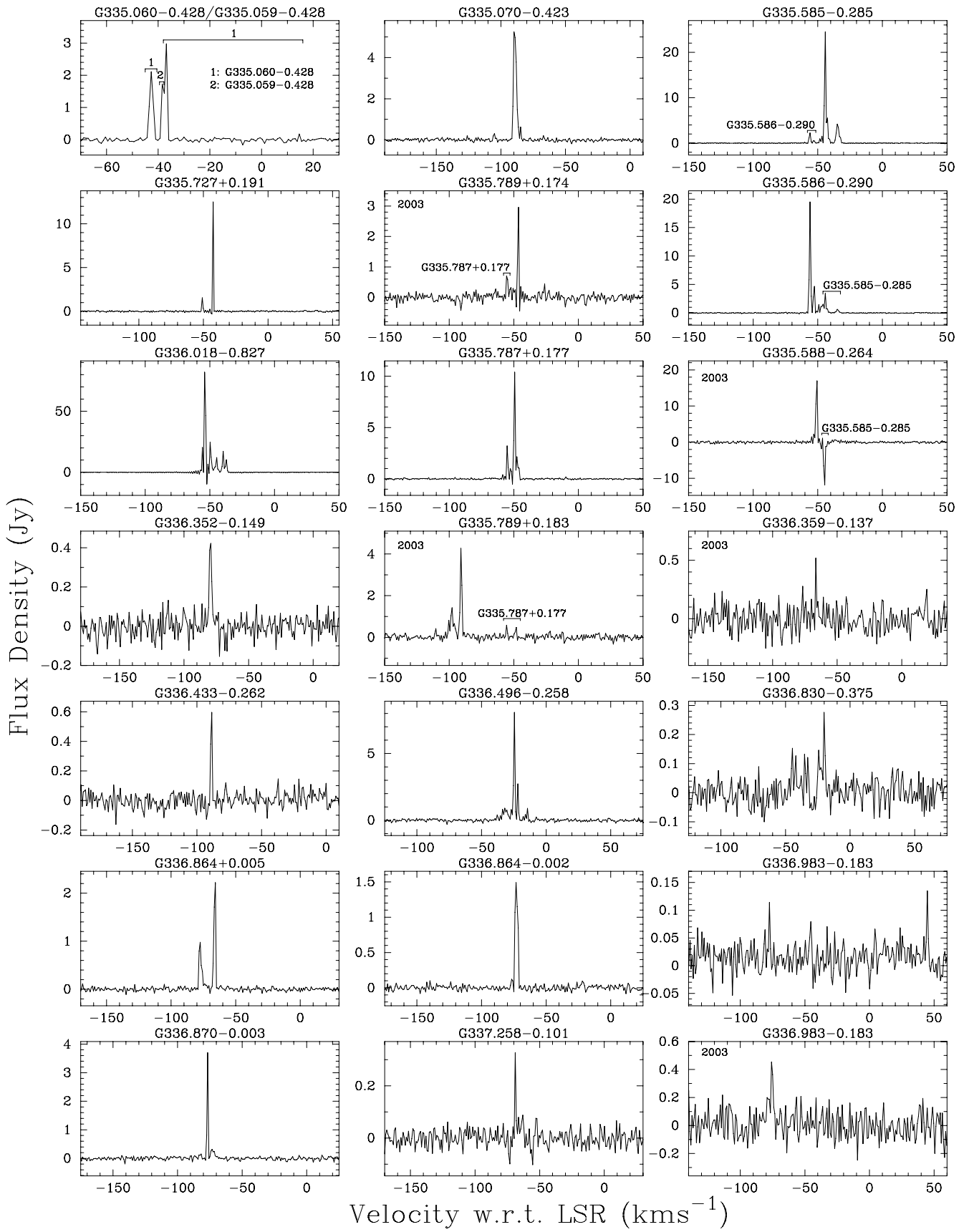


Figure 1 – continued

**Figure 1 – continued**

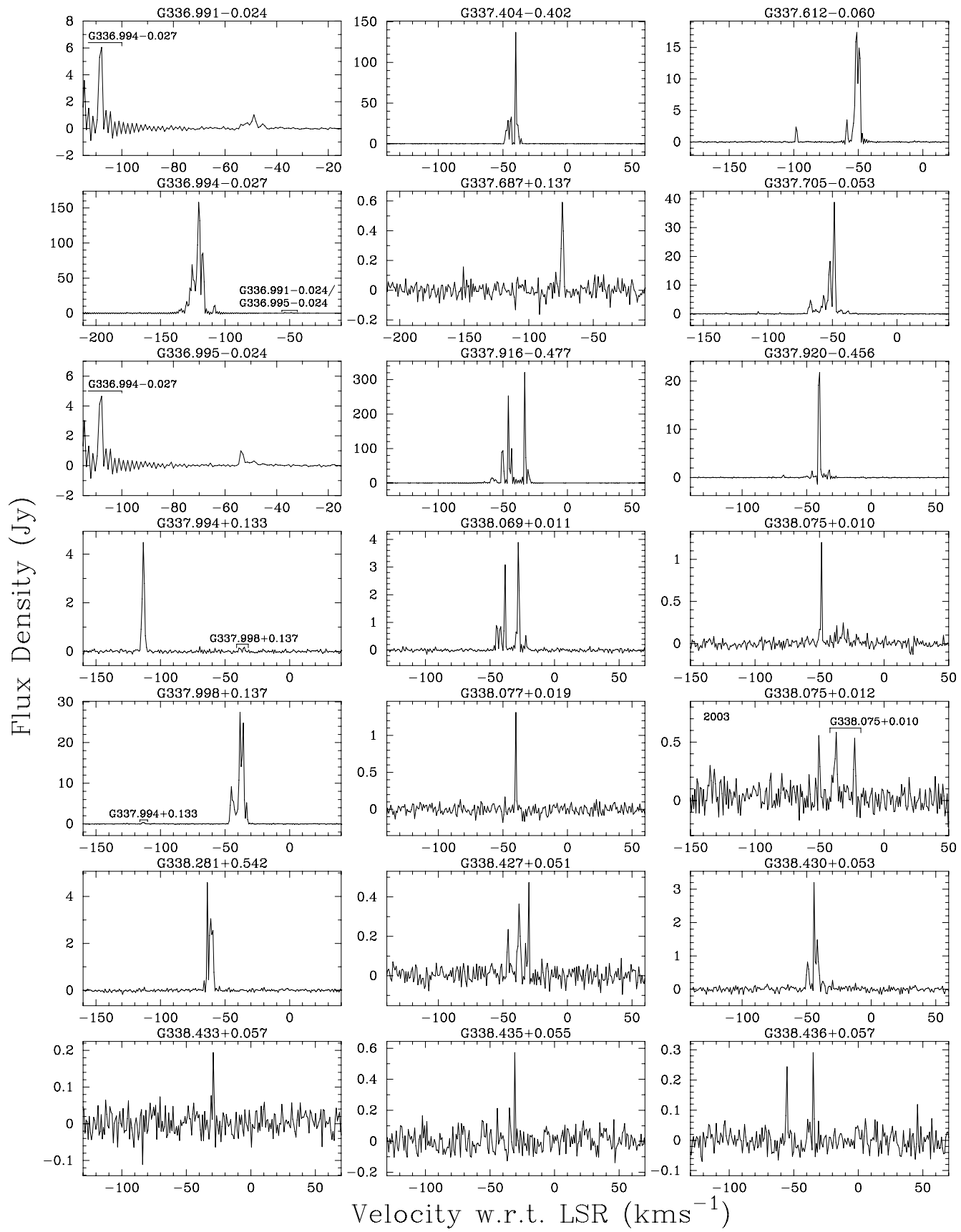
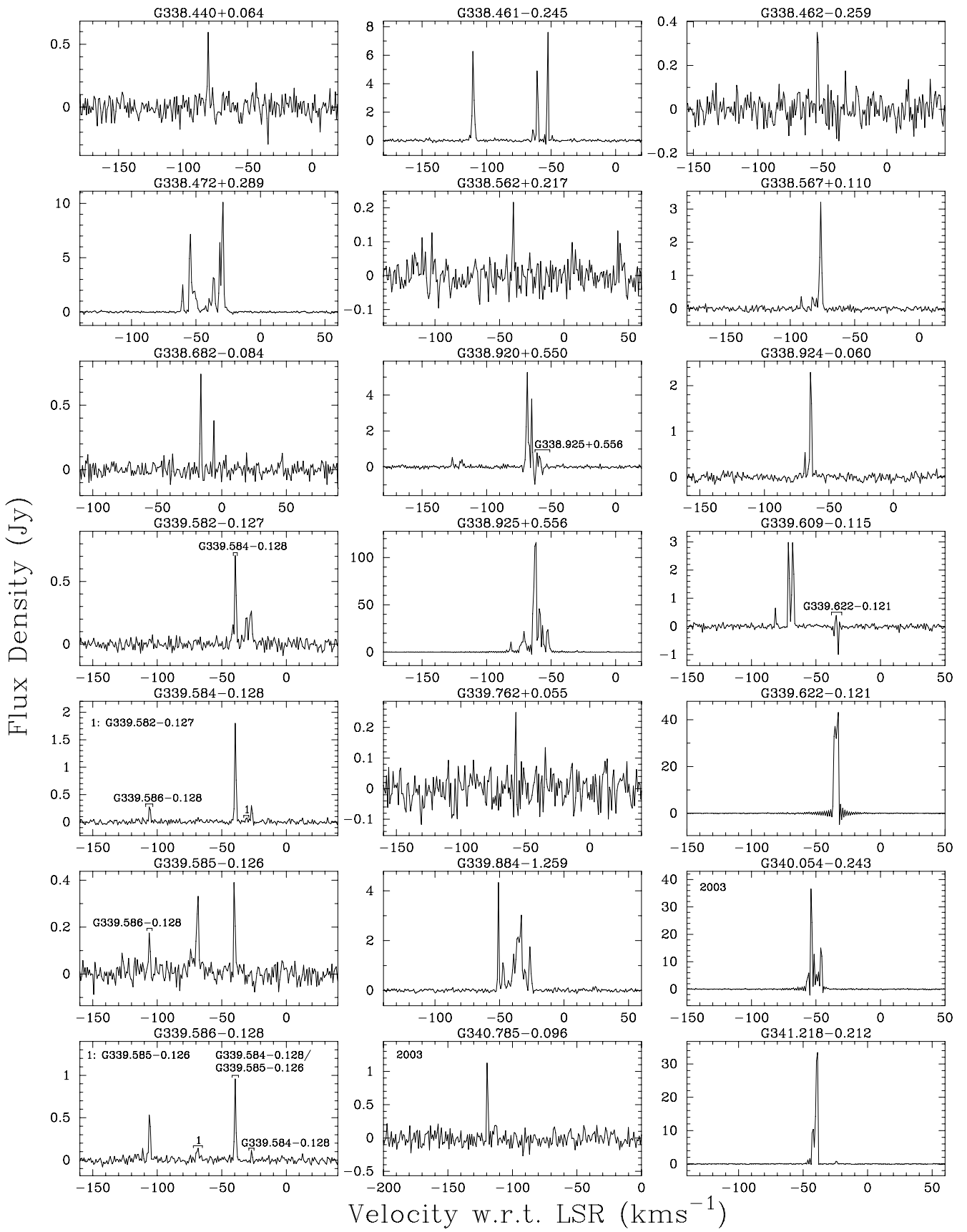
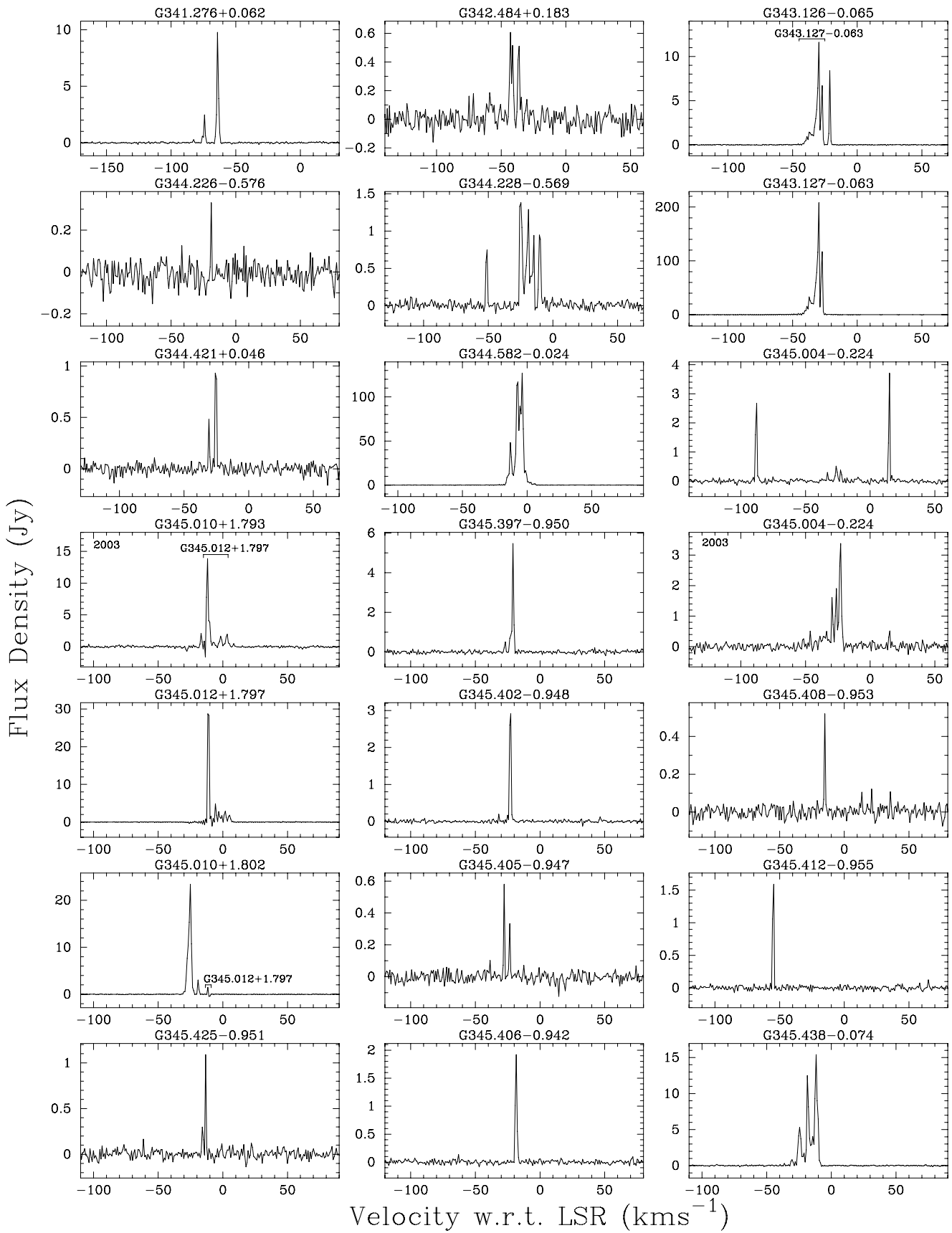
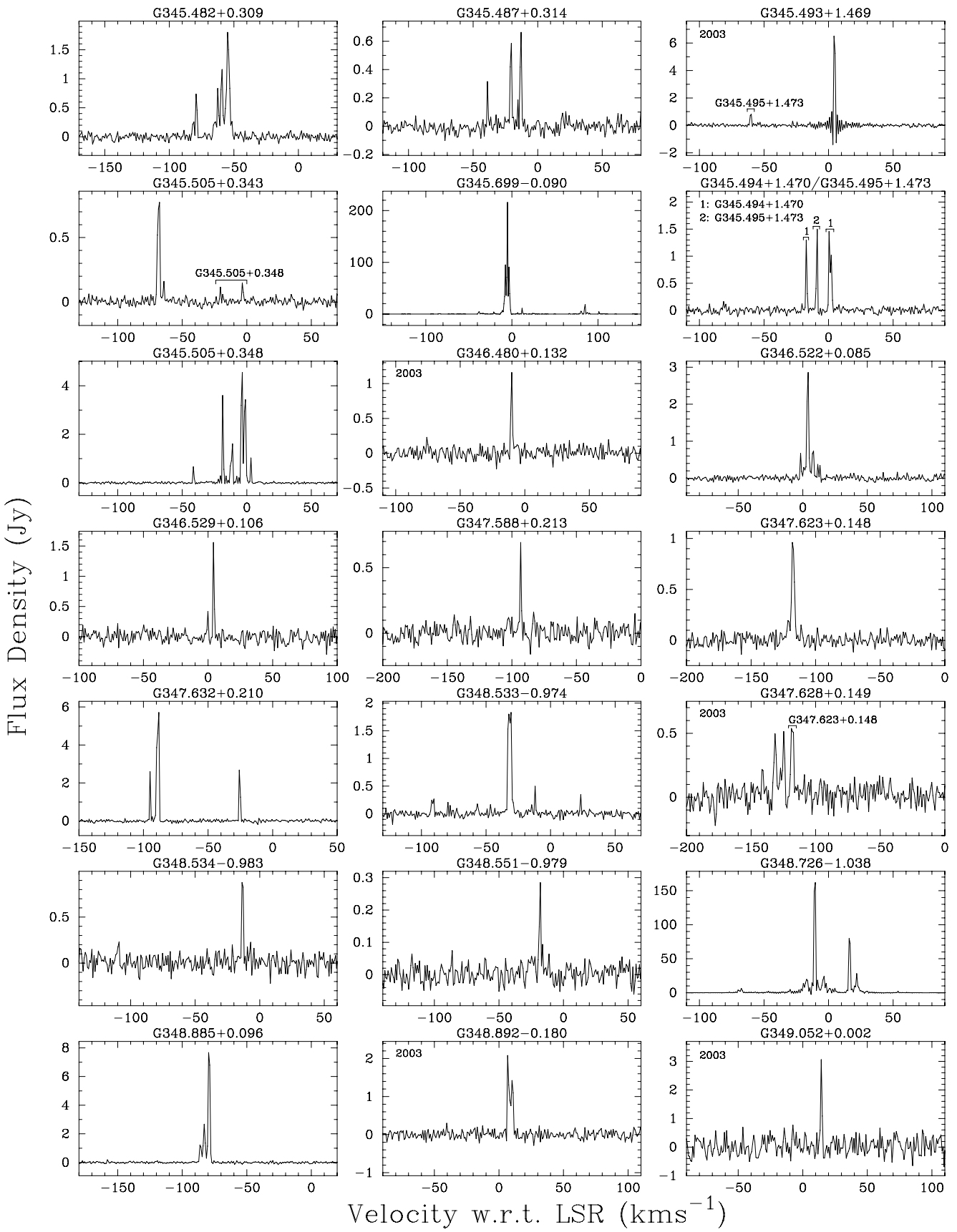


Figure 1 – continued

**Figure 1 – continued**

**Figure 1 – continued**

**Figure 1 – continued**

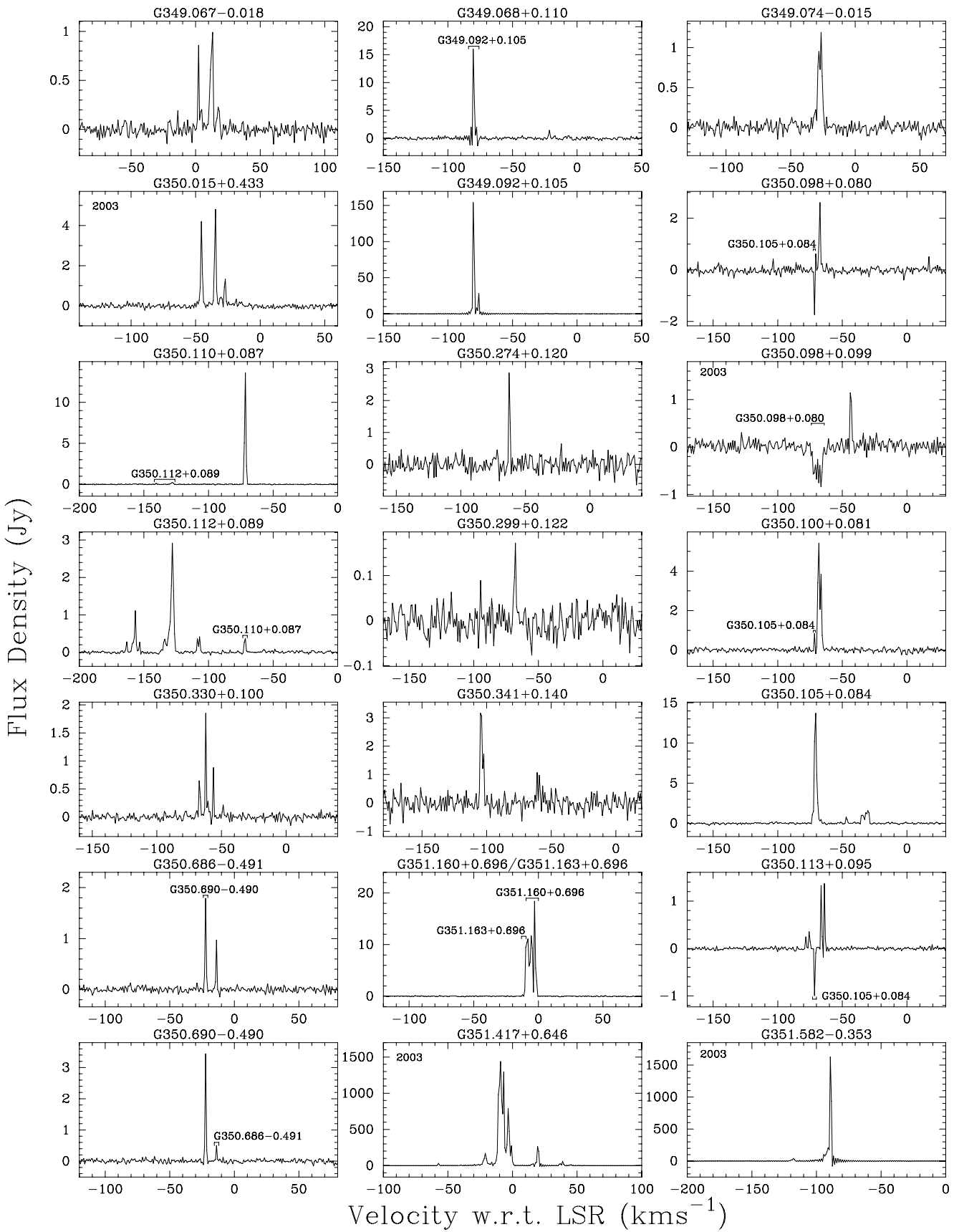
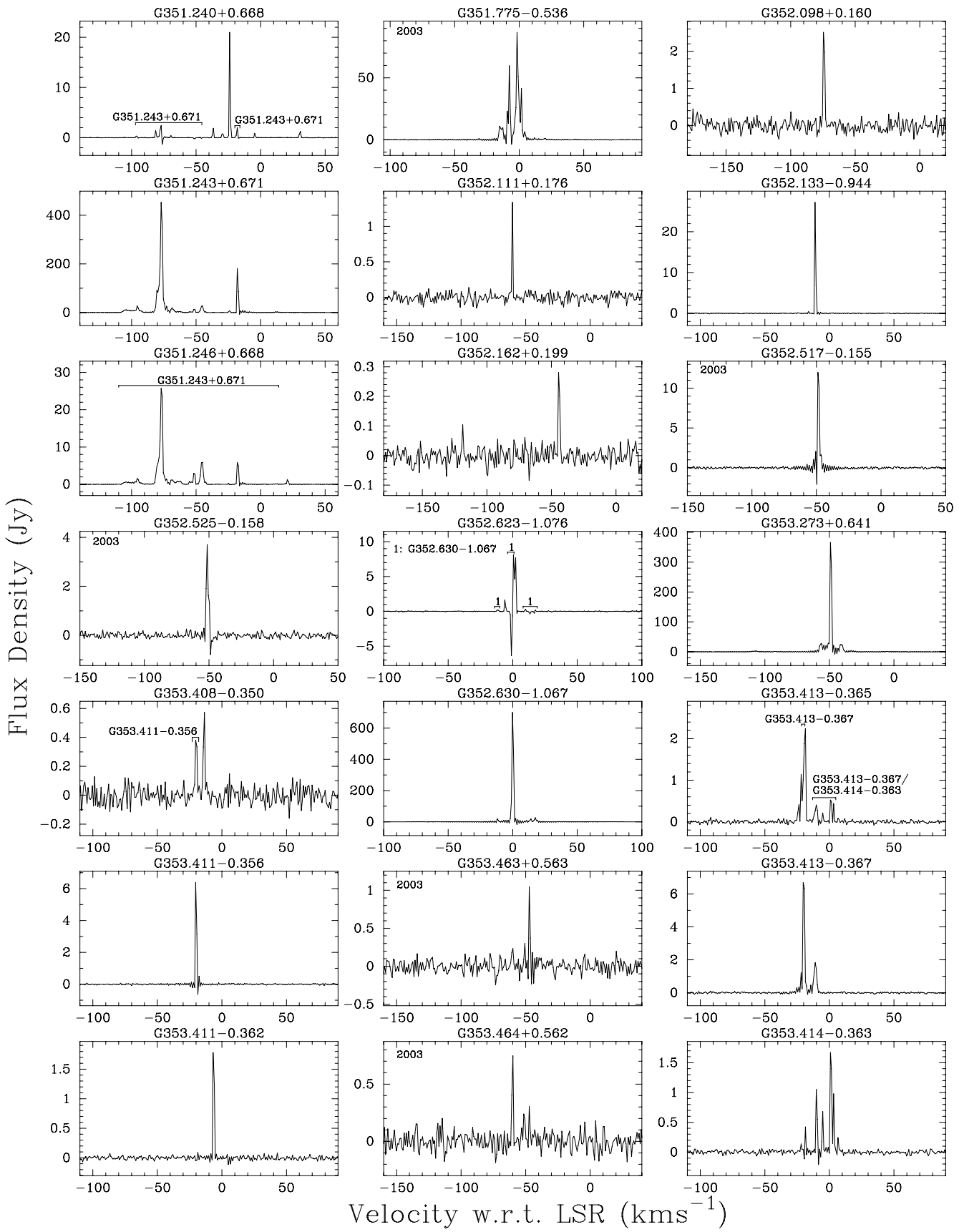


Figure 1 – continued

**Figure 1 – continued**

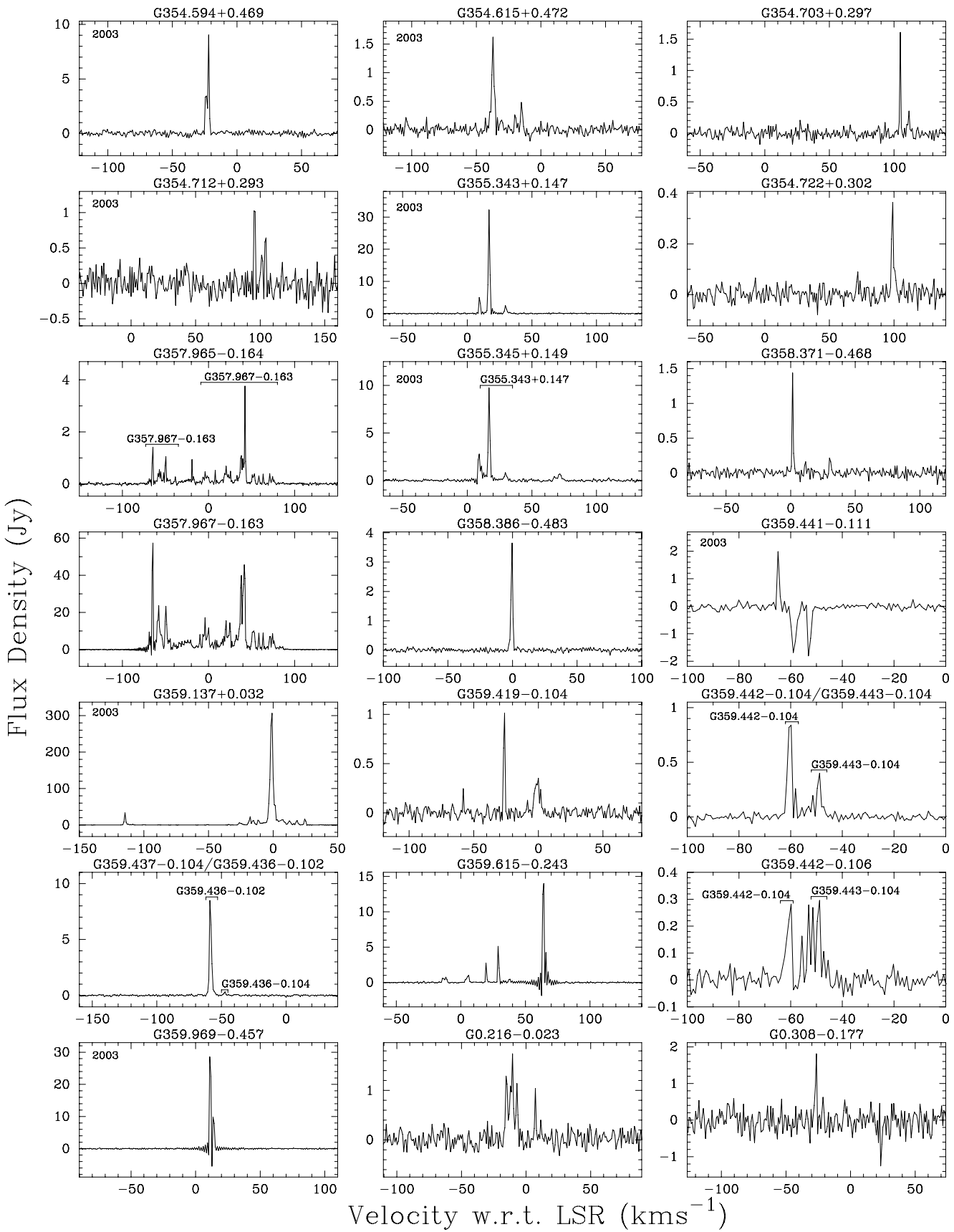
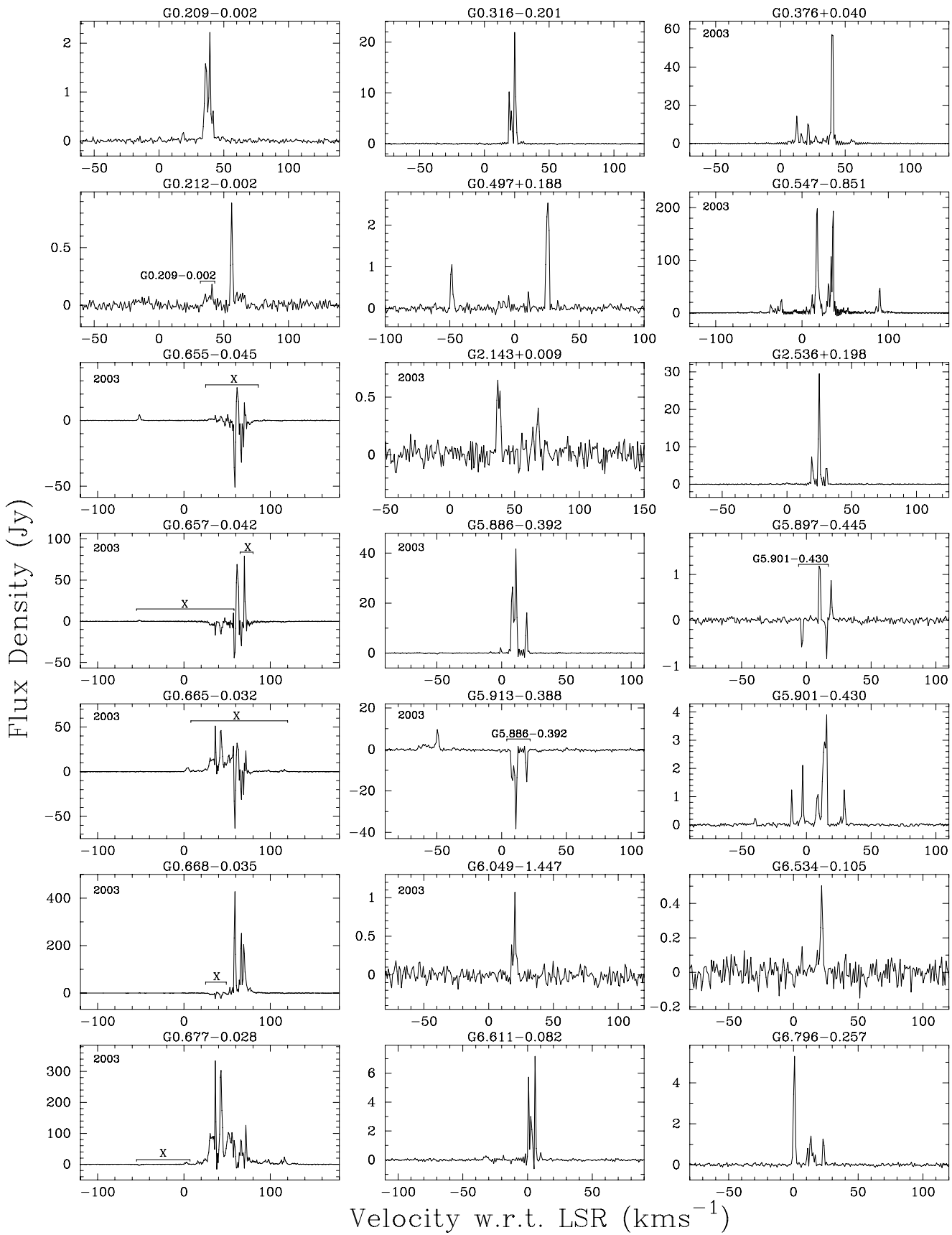


Figure 1 – continued

**Figure 1 – continued**

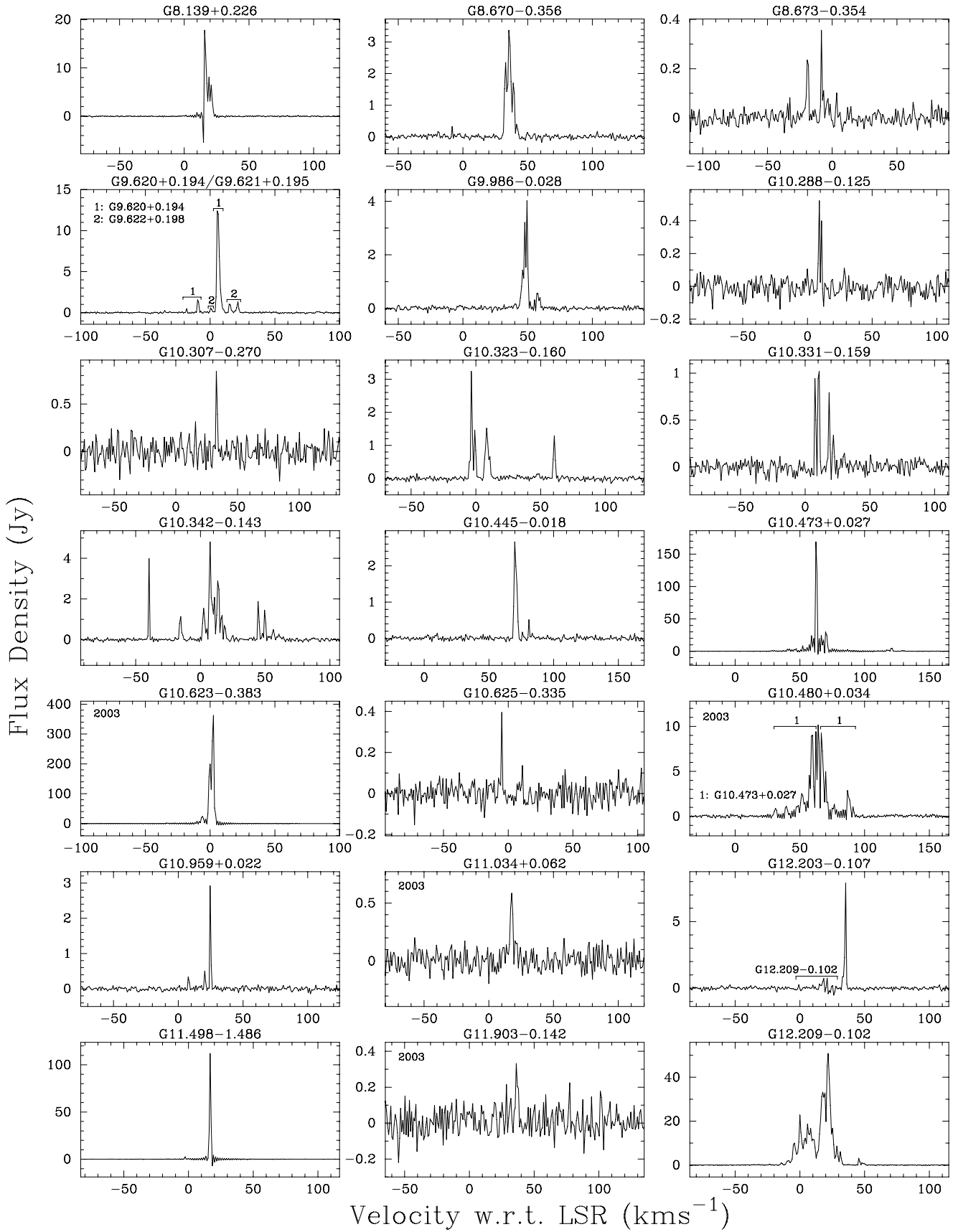
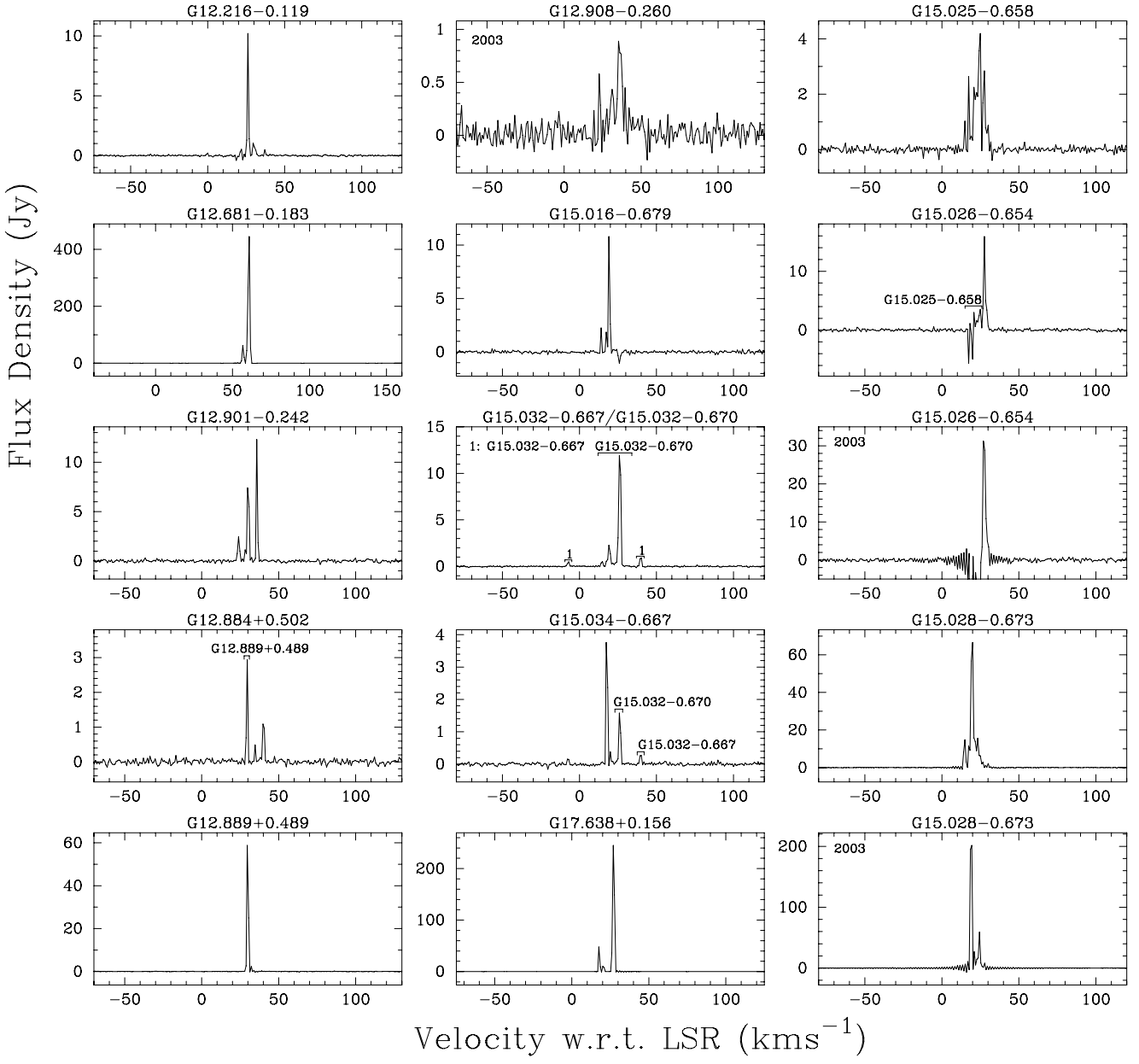


Figure 1 – continued

**Figure 1 – continued**

From these many comparisons, we are able to estimate our rms positional uncertainty as 2 arcsec. The target OH and methanol masers have rms position uncertainties of 0.4 arcsec (C98; Caswell 2009). An additional positional uncertainty in characterizing any water maser site by a single position arises because a single site sometimes consists of many separate spots with angular separations as extensive as 4 arcsec (e.g. Reid et al. 1988), explicable by an outflow (e.g. Caswell & Phillips 2008). We therefore regard our water maser sources to be associated with OH or methanol masers when they are separated by less than 3 arcsec, a threshold which captures most associations without diluting them with too many false, chance, coincidences; see also further discussion in Section 5.2. Where the water maser positions are derived from a single epoch, we relax this threshold to 4.5 arcsec. As the positions of the 22-GHz radio continuum have also been determined from a single epoch, a threshold of 4.5 arcsec is similarly adopted for con-

tinuum associations. Most of our proposed associations correspond to a much better accuracy (see Table 3) than our thresholds. There are, however, some more complex cases that have been judged on individual merit as discussed in detailed considerations summarized in Section 4. For example, the required precision of agreement was relaxed for sources believed to be nearby, at a distance of less than 2 kpc. Comparison of our 379 water maser positions with the positions of OH and methanol masers shows that 128 are coincident with both species, 33 are coincident with OH only and 70 are coincident with the location of methanol masers (see Section 5.3 for more extensive discussion). Surprisingly, 148 sources have no association with other maser species and we describe these as ‘solitary’.

Details for the 379 sources that we detect are presented in Table 1 and, following the usual practice, the Galactic longitude and latitude of each source, listed in the first column, are used as an identifying source name for each water maser. These Galactic coordinates are

derived from the more precise measurements of equatorial coordinates given in Columns 2 and 3. The peak velocity and velocity range (w.r.t.  $\text{lsr}$ ), followed by the peak flux density, are given in Columns 4–6 for the 2003 epoch and in Columns 7–9 for the 2004 epoch. The presence of a ‘–’ in either Column 6 or 9 indicates that no observations were made for that source during the 2003 or 2004 observations, respectively, and a ‘t’ in either column indicates that there is a comment in the text of Section 4 explaining the nature of the detection status at the indicated epoch. The presence of a number preceded by a ‘<’ in either Column 6 or 9 indicates that no emission above the quoted flux density was detected at that epoch. Column 10 gives a list of associations for each water maser source; here, the presence of an ‘o’ denotes the presence of an associated OH maser, ‘m’ the presence of an associated methanol maser, ‘c’ the presence of associated 22-GHz continuum emission (in our observations) and ‘g’ the presence of an associated GLIMPSE point source. A ‘γ’ in this column indicates that the source is outside the GLIMPSE survey region. A ‘#’ following an ‘o’ indicates that the OH maser is strictly outside our association threshold but is associated with the methanol maser that falls within our threshold for a given source, meaning that either all three sources are coincident, or the water maser is offset; this is similar for the case where a ‘#’, follows an ‘m’. In some cases we have the situation that both the OH and the methanol masers are strictly located outside the association threshold but we regard them as associated through special circumstances, in which case we have used the ‘#’ after both the ‘o’ and the ‘m’. In the case of 301.136–0.226 a second water maser site lies within the association threshold for the same methanol and OH masers, and the association is shown in parentheses.

OH masers that were searched and resulted in no water maser detection are listed in Table 2. The first column gives the name of the OH maser followed by its right ascension and declination. Column 4 gives the angular separation between the OH maser and the nearest methanol maser (Caswell 2009) within 2.5 arcsec, and when a ‘–’ is present, this signifies that there is no methanol maser within 2.5 arcsec of the OH maser.

An extensive list of the OH and methanol masers associated with our water maser sources, as well as water maser associations with 22-GHz continuum sources, is given in Table 3. All OH and methanol masers as well as 22-GHz radio continuum that fall within 5 arcsec of the water masers are presented. Column 1 in Table 3 gives the water maser source name, and the names of the nearby OH and methanol masers are given in Columns 2 and 4, respectively. The source names, based on the precise positions of individual species, inevitably differ slightly in a few cases due to different small position errors. The angular separations between the water masers and OH masers are given in Column 3 and between water and methanol masers in Column 5. Columns 6–8 give the peak velocity of the water (2004 values are given unless not available, in which case the 2003 value is used) and the coincident OH and methanol maser sources. Column 9 gives the Galactic coordinates of 22-GHz continuum sources that we detect, followed by the angular separation between the continuum source and the water maser in Column 10. The discussion of individual sources in Section 4 includes some comparisons between the positions of water maser sources and other masers, continuum and GLIMPSE sources.

A complete list of the continuum sources detected towards water maser sources in the 2004 observations is given in Table 4. Associations between the 29 water maser sources observed only during the 2003 observations and possibly associated 22-GHz continuum sources (see Section 5.6) have not been determined.

**Table 2.** OH masers with no associated water maser emission.

OH maser ( $l, b$ ) (deg)	RA (J2000) (h m s)	Dec. (J2000) ( $^{\circ} \text{ } '$ )	Methanol maser sep. (arcsec)
G 232.621+0.996	07 32 09.82	−16 58 13.0	0.7
G 300.969+1.147	12 34 53.24	−61 39 40.3	0.5
G 305.200+0.019	13 11 16.90	−62 45 54.7	0.5
G 305.202+0.208	13 11 10.61	−62 34 37.8	1.3
G 306.322−0.334	13 21 23.00	−63 00 30.4	0.9
G 309.921+0.479	13 50 41.73	−61 35 09.8	0.9
G 313.705−0.190	14 22 34.72	−61 08 27.4	0.8
G 316.359−0.362	14 43 11.00	−60 17 15.3	2.5
G 321.030−0.485	15 15 51.67	−58 11 18.0	0.9
G 323.459−0.079	15 29 19.36	−56 31 21.4	1.4
G 328.307+0.430	15 54 06.48	−53 11 40.3	–
G 329.339+0.148	16 00 33.15	−52 44 39.8	0.2
G 331.542−0.066	16 12 09.05	−51 25 47.2	0.5
G 331.543−0.066	16 12 09.16	−51 25 45.3	0.2
G 331.556−0.121	16 12 27.19	−51 27 38.1	0.2
G 332.295+2.280	16 05 41.72	−49 11 30.5	0.2
G 332.824−0.548	16 20 10.23	−50 53 18.1	–
G 333.135−0.431	16 21 02.97	−50 35 10.1	2.4
G 335.556−0.307	16 30 56.00	−48 45 51.0	0.8
G 336.822+0.028	16 34 38.26	−47 36 33.0	0.8
G 336.941−0.156	16 35 55.22	−47 38 45.7	0.4
G 338.875−0.084	16 43 08.23	−46 09 12.8	0.2
G 339.053−0.315	16 44 49.16	−46 10 14.4	2.2
G 339.282+0.136	16 43 43.12	−45 42 08.4	0.4
G 339.682−1.207	16 51 06.21	−46 15 57.8	0.4
G 343.930+0.125	17 00 10.92	−42 07 18.7	0.6
G 344.419+0.044	17 02 08.67	−41 47 08.6	1.8
G 345.498+1.467	16 59 42.81	−40 03 36.2	0.4
G 347.870+0.014	17 13 08.80	−39 02 29.5	–
G 348.550−0.979	17 19 20.39	−39 03 51.8	0.3
G 348.579−0.920	17 19 10.56	−39 00 24.5	0.6
G 348.698−1.027	17 19 58.91	−38 58 14.1	–
G 348.703−1.043	17 20 03.96	−38 58 31.3	1.2
G 348.727−1.037	17 20 06.55	−38 57 08.2	0.9
G 350.011−1.342	17 25 06.50	−38 04 00.7	0.5
G 353.410−0.360	17 30 26.20	−34 41 45.5	0.3
G 354.724+0.300	17 31 15.52	−33 14 05.3	0.5
G 356.662−0.264	17 38 29.22	−31 54 40.6	2.0
G 3.910+0.001	17 54 38.77	−25 34 45.2	0.5
G 8.683−0.368	18 06 23.46	−21 37 10.2	0.4
G 12.025−0.031	18 12 01.88	−18 31 55.6	0.3
G 15.034−0.677	18 20 24.75	−16 11 34.9	0.6

*Note.* Listed in Column 1 is the OH maser source name followed in Columns 2 and 3 by the right ascension and declination, respectively. Column 4 shows the angular separation between the listed OH maser and a nearby methanol maser; a – in this column indicates that there are no known methanol maser sources within 2.5 arcsec.

#### 4 INDIVIDUAL SOURCES

Here we draw attention to information on the sources that cannot be adequately conveyed in the tables and spectra. We discuss some entries in Table 1 where close companions may be either discrete extra maser sites or merely multiple features in an unusually extended site. Our interpretation of the likely systemic velocity, based on association with methanol or OH maser emission, is given in some cases where water shows high-velocity features that dominate the spectrum. Extreme variability is sometimes evident from Table 1, and a few examples of this variability are demonstrated by spectra shown from both 2003 and 2004. The absence of an entry

**Table 3.** Water maser sources with associated OH and methanol masers as well as 22-GHz continuum emission.

Water ( <i>l, b</i> ) (deg)	OH ( <i>l, b</i> ) (deg)	Sep. (arcsec)	Methanol ( <i>l, b</i> ) (deg)	Sep. (arcsec)	Water V peak (km s <sup>-1</sup> )	OH V peak (km s <sup>-1</sup> )	Methanol V peak (km s <sup>-1</sup> )	Continuum ( <i>l, b</i> ) (deg)	Sep. (arcsec)
G 240.316+0.071	G 240.316+0.071	0.7	–	89	63	–	–	–	–
G 263.250+0.514	G 263.250+0.514	2.1	G 263.250+0.514	1.5	20	15.3	12.3	–	–
G 284.350–0.418	G 284.351–0.418	1.1	–	7	6	–	–	–	–
G 285.263–0.050	G 285.263–0.050	2.0	–	3	6	–	–	–	–
G 287.371+0.644	G 287.371+0.644	1.6	G 287.371+0.644	1.5	–11	–4	–1.8	–	–
G 290.374+1.661	G 290.374+1.661	1.6	G 290.374+1.661	1.0	–12	–23.3	–24.2	–	–
G 291.270–0.719	–	–	G 291.270–0.719	2.5	–102	–	–26.5	–	–
G 291.274–0.709	G 291.274–0.709	1.3	G 291.274–0.709	0.7	–32	–24.5	–29.6	–	–
G 291.579–0.431	G 291.579–0.431	0.6	G 291.579–0.431	0.7	13	13	14.5	–	–
G 291.581–0.435	–	–	G 291.582–0.435	3.8	26	–	10.5	–	–
G 291.610–0.529	G 291.610–0.529	0.7	–	12	18	–	–	G 291.611–0.529	2.6
G 291.627–0.529	–	–	–	–	–	–	–	G 291.626–0.531	4.8
G 294.511–1.622	G 294.511–1.621	2.1	G 294.511–1.621	1.8	–12	–12.7	–12.3	–	–
G 294.989–1.719	–	–	G 294.990–1.719	2.5	–17	–	–12.3	–	–
G 297.660–0.974	G 297.660–0.973	2.0	–	26	27.6	–	–	–	–
G 299.013+0.128	G 299.013+0.128	1.2	G 299.013+0.128	1.1	19	20.3	18.4	G 299.012+0.128	3.3
G 300.504–0.176	G 300.504–0.176	0.6	G 300.504–0.176	1.8	11	22.4	7.5	–	–
G 301.136–0.226b	G 301.136–0.226	2.0	G 301.136–0.226	2.5	–44	–40.2	–39.8	G 301.136–0.226	1.0
G 301.137–0.225	G 301.136–0.226	2.0	G 301.136–0.226	2.0	–35	–40.2	–39.8	–	–
G 305.208+0.207	G 305.208+0.206	3.0	G 305.208+0.206	2.7	–42	–38	–38.3	–	–
G 305.361+0.150	G 305.362+0.150	2.1	G 305.362+0.150	2.0	–36	–39.5	–36.5	–	–
G 305.799–0.245	G 305.799–0.245	3.0	G 305.799–0.245	2.5	–34	–36.7	–39.5	–	–
G 307.805–0.456	G 307.805–0.456	1.5	–	–7	–	–14.5	–	–	–
G 308.754+0.549	G 308.754+0.549	0.8	G 308.754+0.549	1.4	–48	–43.5	–51.0	–	–
G 308.918+0.124	G 308.918+0.123	3.0	G 308.918+0.123	3.6	–61	–54	–54.7	–	–
G 309.384–0.135	G 309.384–0.135	1.3	G 309.384–0.135	0.6	–50	–52	–49.6	–	–
G 310.144+0.760	G 310.144+0.760	2.2	G 310.144+0.760	1.0	–63	–57	–55.6	–	–
G 311.643–0.380	G 311.643–0.380	1.3	G 311.643–0.380	0.4	36	38	32.5	G 311.643–0.380	1.3
G 312.109+0.262	–	–	G 312.108+0.262	1.9	–48	–	–50.0	–	–
G 312.596+0.045	–	–	G 312.597+0.045	1.6	–59	–	–60.0	–	–
G 312.599+0.046	G 312.598+0.045	2.1	G 312.598+0.045	2.1	–79	–65.2	–67.9	–	–
G 313.457+0.193	–	–	–	–	–	–	–	G 313.458+0.193	2.1
G 313.470+0.191	G 313.469+0.190	0.9	G 313.469+0.190	1.1	–15	–10	–9.4	–	–
G 313.578+0.325	G 313.577+0.325	1.0	G 313.577+0.325	1.9	–47	–47	–47.9	–	–
G 313.767–0.862	G 313.767–0.863	1.1	G 313.767–0.863	0.9	–54	–53.5	–54.6	–	–
G 314.320+0.112	G 314.320+0.112	2.2	G 314.320+0.112	2.3	–45	–45	–43.7	–	–
G 316.361–0.363	–	–	G 316.359–0.362	3.2	–3	–	3.5	–	–
G 316.412–0.308	G 316.412–0.308	1.5	G 316.412–0.308	2.3	–20	–2	–5.7	G 316.412–0.308	0.7
G 316.640–0.087	G 316.640–0.087	0.7	G 316.640–0.087	0.9	–15	–22	–19.8	–	–
G 316.763–0.011	G 316.763–0.012	1.0	–	–48	–	–40	–	–	–
G 316.812–0.057	G 316.811–0.057	2.2	G 316.811–0.057	2.5	–46	–43.5	–46.3	–	–
G 317.429–0.561	G 317.429–0.561	2.1	–	25	25.5	–	–	G 317.430–0.561	2.6
G 318.044–1.404	G 318.044–1.405	2.0	G 318.043–1.404	1.6	42	45	46.2	–	–
G 318.050+0.087	G 318.050+0.087	0.6	G 318.050+0.087	0.4	–48	–53	–46.5	–	–
G 318.948–0.196b	G 318.948–0.196	0.8	G 318.948–0.196	0.9	–38	–35.5	–34.7	–	–
G 319.399–0.012	G 319.398–0.012	1.1	–	–5	–1	–	–	G 319.399–0.012	0.8
G 319.836–0.196	G 319.836–0.196	1.5	G 319.836–0.197	1.6	–11	–10.5	–9.1	–	–
G 320.120–0.440	G 320.120–0.440	0.5	–	–46	–	–55.5	–	–	–
G 320.232–0.284	G 320.232–0.284	0.4	G 320.231–0.284	0.6	–67	–64	–66.5	–	–
G 320.233–0.284	–	–	–	–	–	–	–	G 320.234–0.283	3.5
G 321.033–0.483	–	–	G 321.033–0.483	0.5	–61	–	–61.6	–	–
G 321.148–0.529	G 321.148–0.529	1.1	G 321.148–0.529	1.1	–97	–63	–66.1	–	–
G 322.158+0.636	G 322.158+0.636	1.2	G 322.158+0.636	1.2	–76	–61	–63.3	–	–
G 323.740–0.263	G 323.740–0.263	1.1	G 323.740–0.263	0.6	–50	–39	–51.1	–	–
G 324.201+0.122	G 324.200+0.121	2.9	–	–87	–91.5	–	–	–	–
G 324.716+0.342	G 324.716+0.342	1.7	G 324.716+0.342	1.5	–58	–50	–46	–	–
G 326.662+0.521	–	–	G 326.662+0.521	2.0	–39	–	–38.6	–	–
G 326.670+0.554	G 326.670+0.554	2.6	–	–40	–40.8	–	–	–	–
G 326.780–0.241	G 326.780–0.241	0.9	–	–66	–65	–	–	–	–
G 326.859–0.676	–	–	G 326.859–0.677	3.4	–103	–	–58.0	–	–
G 327.119+0.511	G 327.120+0.511	2.3	G 327.120+0.511	1.8	–88	–80.5	–87.0	–	–

**Table 3** – *continued*

Water ( <i>l, b</i> ) (deg)	OH ( <i>l, b</i> ) (deg)	Sep. (arcsec)	Methanol ( <i>l, b</i> ) (deg)	Sep. (arcsec)	Water V peak (km s <sup>-1</sup> )	OH V peak (km s <sup>-1</sup> )	Methanol V peak (km s <sup>-1</sup> )	Continuum ( <i>l, b</i> ) (deg)	Sep. (arcsec)
G 327.291–0.578	G 327.291–0.578	1.2	G 327.291–0.578	0.8	−63	−50.5	−36.8	—	
G 327.391+0.200	—		G 327.392+0.199	1.5	−86		−84.6	—	
G 327.402+0.445	G 327.402+0.444	3.2	G 327.402+0.444	1.6	−81	−77	−82.6	G 327.402+0.445	0.6
G 327.619−0.111	—		G 327.618−0.111	0.9	−85		−97.6	—	
G 328.236−0.548	G 328.237−0.547	2.9	G 328.237−0.547	2.6	−38	−41	−44.5	G 328.236−0.547	2.1
G 328.254−0.532	G 328.254−0.532	1.5	G 328.254−0.532	0.8	−50	−37	−37.5	—	
G 328.306+0.432	—		—					G 328.307+0.431	3.3
G 328.808+0.633	G 328.809+0.633	2.9	G 328.808+0.633	2.4	−46	−43.5	−43.8	G 328.808+0.633	2.0
G 329.029−0.199	G 329.029−0.200	1.9	—		−38	−38.5		—	
G 329.030−0.205	G 329.029−0.205	1.5	G 329.029−0.205	1.3	−46	−38.5	−37.4	—	
G 329.031−0.198	G 329.031−0.198	1.3	G 329.031−0.198	0.8	−52	−45.5	−45.5	—	
G 329.066−0.307	G 329.066−0.308	1.5	G 329.066−0.308	1.2	−45	−43.5	−43.8	—	
G 329.183−0.313	G 329.183−0.314	2.3	G 329.183−0.314	1.9	−50	−53	−55.7	—	
G 329.405−0.459	G 329.405−0.459	2.0	G 329.405−0.459	1.5	−77	−69.5	−70.5	—	
G 329.407−0.459	—		G 329.407−0.459	2.1	−74		−66.7	—	
G 329.622+0.138	—		G 329.622+0.138	1.7	−82		−84.8	—	
G 330.070+1.064	—		G 330.070+1.064	1.2	−50		−38.8	—	
G 330.879−0.367	G 330.878−0.367a	0.9	G 330.878−0.367	2.6	−60	−61.8	−59.3	G 330.879−0.367	1.7
	G 330.878−0.367b	1.2	—			−65.6			
G 330.954−0.182	G 330.954−0.182	1.3	G 330.953−0.182	3.9	−91	−85.5	−87.6	G 330.954−0.182	1.6
G 331.132−0.244	G 331.132−0.244	0.2	G 331.132−0.244	0.3	−99	−88.5	−84.3	—	
G 331.278−0.188	G 331.278−0.188	0.9	G 331.278−0.188	1.1	−90	−89.5	−78.2	—	
G 331.342−0.346	G 331.342−0.346	1.4	G 331.342−0.346	1.6	−62	−67	−67.4	—	
G 331.442−0.187	G 331.442−0.186	0.5	G 331.442−0.187	0.9	−88	−83	−88.4	G 331.443−0.187	3.5
G 331.512−0.103	G 331.512−0.103	1.4	—		−90	−88.2		G 331.512−0.103	1.0
G 331.555−0.122	G 331.556−0.121	4.5	G 331.556−0.121	4.4	−99	−100	−103.4	—	
G 332.094−0.421	—		G 332.094−0.421	2.2	−59		−58.6	—	
G 332.296−0.094	—		G 332.295−0.094	4.4	−50		−47.0	—	
G 332.352−0.117	G 332.352−0.117	0.8	G 332.352−0.117	0.2	−60	−44	−41.8	—	
G 332.604−0.167	—		G 332.604−0.167	1.6	−46		−50.9	—	
G 332.725−0.621	G 332.726−0.621	1.4	G 332.726−0.621	1.0	−58	−48	−49.6	—	
G 332.826−0.549	—		G 332.826−0.549	3.0	−59		−61.7	G 332.826−0.549	1.1
G 332.964−0.679	—		G 332.963−0.679	1.6	−52		−45.8	—	
G 333.030−0.063	—		G 333.029−0.063	1.3	−40		−55.2	G 333.030−0.063	0.7
G 333.121−0.434	—		G 333.121−0.434	1.2	−47		−49.3	—	
G 333.126−0.440	—		G 333.126−0.440	1.0	−52		−43.9	—	
G 333.128−0.440	—		G 333.128−0.440	2.5	−124		−44.6	—	
G 333.234−0.060	G 333.234−0.060	0.6	—		−88	−84		—	
G 333.315+0.106	G 333.315+0.105	2.8	G 333.315+0.105	3.0	−48	−47	−45	—	
G 333.387+0.032	G 333.387+0.032	0.6	G 333.387+0.032	1.1	−61	−74	−73.9	—	
G 333.467−0.164	G 333.466−0.164	2.1	G 333.466−0.164	2.5	−42	−43.5	−42.5	G 333.466−0.163	4.7
G 333.608−0.215	G 333.608−0.215	0.2	—		−49	−51		—	
G 333.646+0.058	—		G 333.646+0.058	0.9	−89		−87.3	—	
G 333.682−0.436	—		G 333.683−0.437	1.6	−3		−5.3	—	
G 333.930−0.134	—		G 333.931−0.135	1.5	−46		−36.7	—	
G 334.635−0.015	—		G 334.635−0.015	1.0	−26		−30	—	
G 334.935−0.098	—		G 334.935−0.098	0.4	−17		−19.5	—	
G 335.060−0.428	G 335.060−0.427	1.5	G 335.060−0.427	1.3	−37	−36	−47.0	—	
G 335.585−0.285	G 335.585−0.285	0.5	G 335.585−0.285	0.7	−42	−48	−49.3	—	
G 335.586−0.290	G 335.585−0.289	1.1	G 335.585−0.289	0.8	−56	−53.5	−51.4	—	
			G 335.585−0.290	2.3			−47.3		
G 335.727+0.191	—		G 335.726+0.191	2.0	−51		−44.4	—	
G 335.789+0.174	G 335.789+0.174	0.5	G 335.789+0.174	0.9	−46	−51.5	−47.6	—	
G 336.018−0.827	G 336.018−0.827	0.6	G 336.018−0.827	0.9	−54	−41.5	−53.4	G 336.018−0.828	0.5
G 336.359−0.137	G 336.358−0.137	3.0	G 336.358−0.137	3.1	−67	−82	−73.6	G 336.360−0.137	3.8
G 336.433−0.262	—		G 336.433−0.262	1.9	−89		−93.3	—	
G 336.830−0.375	—		G 336.830−0.375	1.6	−20		−22.7	—	
G 336.864+0.005	G 336.864+0.005	1.2	G 336.864+0.005	0.7	−66	−89	−76.1	—	
G 336.983−0.183	G 336.984−0.183	4.2	G 336.983−0.183	3.0	45	−80.5	−80.8	G 336.984−0.184	2.5
G 336.991−0.024	—		—					G 336.990−0.025	2.3
G 336.994−0.027	G 336.994−0.027	1.0	G 336.994−0.027	0.6	−120	−123	−125.8	—	

**Table 3 – continued**

Water ( <i>l, b</i> ) (deg)	OH ( <i>l, b</i> ) (deg)	Sep. (arcsec)	Methanol ( <i>l, b</i> ) (deg)	Sep. (arcsec)	Water V peak (km s <sup>-1</sup> )	OH V peak (km s <sup>-1</sup> )	Methanol V peak (km s <sup>-1</sup> )	Continuum ( <i>l, b</i> ) (deg)	Sep. (arcsec)
G 337.258–0.101	G 337.258–0.101	0.7	G 337.258–0.101	1.2	–69	–70	–69.3	–	
G 337.404–0.402	G 337.405–0.402	1.5	G 337.404–0.402	0.7	–40	–38	–39.7	G 337.404–0.403	2.0
G 337.612–0.060	G 337.613–0.060	0.6	G 337.613–0.060	0.9	–51	–42	–42	–	
G 337.687+0.137	–		G 337.686+0.137	2.3	–74		–74.9	–	
G 337.705–0.053	G 337.705–0.053	0.6	G 337.705–0.053	0.9	–49	–49	–54.6	G 337.706–0.054	1.1
G 337.916–0.477	G 337.916–0.477	0.6	–	–33	–51			–	
G 337.920–0.456	G 337.920–0.456	0.7	G 337.920–0.456	0.9	–40	–39.5	–38.8	–	
G 337.998+0.137	G 337.997+0.136	1.3	G 337.997+0.136	1.1	–38	–35.5	–32.3	–	
G 338.075+0.012	G 338.075+0.012	2.1	G 338.075+0.012	2.3	–50	–47	–53.0	G 338.075+0.012	2.9
G 338.075+0.010	–		G 338.075+0.009	1.3	–48		–38.2	–	
G 338.281+0.542	G 338.280+0.542	1.2	G 338.280+0.542	1.1	–64	–61	–56.8	–	
G 338.433+0.057	–		G 338.432+0.058	4.4	–29		–30.2	–	
G 338.461–0.245	G 338.461–0.245	0.4	G 338.461–0.245	0.8	–52	–56	–50.4	–	
G 338.472+0.289	G 338.472+0.289	1.2	G 338.472+0.289	1.1	–29	–32	–30.5	–	
G 338.562+0.217	–		G 338.561+0.218	2.0	–39		–40.8	–	
G 338.567+0.110	–		G 338.566+0.110	1.4	–76		–75	–	
G 338.682–0.084	G 338.681–0.084	1.4	–	–16	–22			G 338.681–0.085	1.5
G 338.920+0.550	–		G 338.920+0.550	0.8	–68		–61.4	–	
G 338.925+0.556	G 338.925+0.557	0.9	G 338.925+0.557	1.3	–62	–61	–62.3	–	
G 339.582–0.127	–		G 339.582–0.127	0.6	–28		–31.3	–	
G 339.622–0.121	G 339.622–0.121	0.8	G 339.622–0.121	1.3	–33	–37.3	–32.8	–	
G 339.762+0.055	–		G 339.762+0.054	1.6	–57		–51	–	
G 339.884–1.259	G 339.884–1.259b	0.7	G 339.884–1.259	0.8	–51	–36	–38.7	–	
	G 339.884–1.259a	1.2	–			–29			
G 340.054–0.243	G 340.054–0.244	1.4	G 340.054–0.244	0.8	–54	–53.6	–59.7	–	
G 340.785–0.096	G 340.785–0.096	2.2	G 340.785–0.096	1.6	–120	–102	–105.1	–	
G 341.218–0.212	G 341.218–0.212	1.2	G 341.218–0.212	1.0	–39	–37.3	–37.9	–	
G 341.276+0.062	G 341.276+0.062	0.9	G 341.276+0.062	1.1	–64	–73	–73.8	–	
G 342.484+0.183	–		G 342.484+0.183	1.1	–43		–41.8	–	
G 343.127–0.063	G 343.127–0.063	2.1	–	–30	–31.5			–	
G 344.228–0.569	G 344.227–0.569	1.4	G 344.227–0.569	1.0	–25	–30.5	–19.8	–	
G 344.421+0.046	–		G 344.421+0.045	3.4	–26		–71.5	–	
G 344.582–0.024	G 344.582–0.024	2.2	G 344.581–0.024	2.5	–4	–2.3	1.4	G 344.582–0.024	1.7
G 345.004–0.224	G 345.003–0.224	3.0	G 345.003–0.224	3.1			–26.2	G 345.004–0.225	3.6
			G 345.003–0.223	3.3	15	–27	–22.5		
G 345.010+1.793	G 345.010+1.793	1.5	G 345.010+1.792	2.1	–17	–22.5	–18	G 345.010+1.792	4.3
G 345.012+1.797	–		G 345.012+1.797	2.2	–12		–12.7	–	
G 345.408–0.953	G 345.407–0.952	4.6	G 345.407–0.952	4.9	–15	–17.6	–14.4	G 345.408–0.952	3.2
G 345.425–0.951	–		G 345.424–0.951	1.6	–13		–13.5	–	
G 345.438–0.074	G 345.437–0.074	1.9	–	–12	–24.3			–	
G 345.487+0.314	–		G 345.487+0.314	0.6	–13		–22.6	–	
G 345.493+1.469	G 345.494+1.469	3.3	–	5	–12.7			–	
G 345.505+0.348	G 345.504+0.348	1.8	G 345.505+0.348	2.2	–4	–19.5	–17.7	–	
G 345.699–0.090	G 345.698–0.090	1.2	–	–5	–6			–	
G 346.480+0.132	G 346.481+0.132	1.5	G 346.481+0.132	1.4	–10	–8	–5.5	–	
G 346.522+0.085	–		G 346.522+0.085	0.7	4		5.5	–	
G 347.628+0.149	G 347.628+0.148	2.0	G 347.628+0.149	0.9	–125	–94.3	–96.6	–	
G 347.632+0.210	–		G 347.631+0.211	2.9	–88		–91.9	G 347.632+0.210	0.9
G 348.551–0.979	G 348.550–0.979	3.7	G 348.550–0.979n	1.9	–18	–19.7	–20.0	–	
			G 348.550–0.979	3.4			–10		
G 348.726–1.038	–		G 348.727–1.037	4.4	–10		–7.6	–	
G 348.885+0.096	G 348.884+0.096	1.2	G 348.884+0.096	1.4	–80	–73.2	–76.2	–	
G 348.892–0.180	G 348.892–0.180	0.6	G 348.892–0.180	1.0	7	9.5	1.4	–	
G 349.067–0.018	G 349.067–0.017	1.1	G 349.067–0.017	1.1	13	15	6.9	–	
G 349.092+0.105	G 349.092+0.106	0.8	G 349.092+0.106	0.9	–80	–80	–80.4	–	
			G 349.092+0.105	2.0			–76.5		
G 350.015+0.433	G 350.015+0.433	0.1	G 350.015+0.433	1.0	–35	–33	–31.7	–	
G 350.113+0.095	G 350.113+0.095	1.3	–	–64	–71			–	
G 350.105+0.084	–		G 350.104+0.084	2.0	–71		–68.4	–	
			G 350.105+0.083	3.3			–74.0		
G 350.299+0.122	–		G 350.299+0.122	0.7	–68		–62.1	–	

**Table 3** – *continued*

Water ( <i>l, b</i> ) (deg)	OH ( <i>l, b</i> ) (deg)	Sep. (arcsec)	Methanol ( <i>l, b</i> ) (deg)	Sep. (arcsec)	Water V peak (km s <sup>-1</sup> )	OH V peak (km s <sup>-1</sup> )	Methanol V peak (km s <sup>-1</sup> )	Continuum ( <i>l, b</i> ) (deg)	Sep. (arcsec)
G 350.330+0.100	G 350.329+0.100	2.5	–	–62	–64	–	–	G 350.331+0.099	3.9
G 350.686–0.491	G 350.686–0.491	0.4	G 350.686–0.491	1.3	–14	–14.5	–13.8	–	–
G 351.160+0.696	G 351.160+0.697	2.5	G 351.160+0.697	1.3	–3	–8.5	–5.2	G 351.161+0.696	3.0
G 351.243+0.671	–	–	G 351.243+0.671	3.4	–77	–	2.5	–	–
G 351.246+0.668	–	–	–	–	–	–	–	G 351.247+0.667	3.6
G 351.417+0.646	G 351.417+0.645	3.7	G 351.417+0.646	1.7	–10	–9.1	–11.2	–	–
–	–	–	G 351.417+0.645	3.1	–	–	–10.4	–	–
G 351.582–0.353	G 351.581–0.353	1.6	G 351.581–0.353n	2.1	–89	–97.6	–91.1	–	–
–	–	–	G 351.581–0.353	3.4	–	–	–94.4	–	–
G 351.775–0.536	G 351.775–0.536	1.8	G 351.775–0.536	1.9	–2	–2	1.3	–	–
G 352.111+0.176	–	–	G 352.111+0.176	2.8	–60	–	–54.8	–	–
G 352.133–0.944	–	–	G 352.133–0.944	2.8	–11	–	–16	–	–
G 352.162+0.199	G 352.161+0.200	1.0	–	–	–45	–42.2	–	–	–
G 352.517–0.155	G 352.517–0.155	0.2	G 352.517–0.155	0.3	–49	–50.6	–51.2	–	–
G 352.525–0.158	–	–	G 352.525–0.158	0.3	–51	–	–53	–	–
G 352.623–1.076	–	–	G 352.624–1.077	4.7	–6	–	5.8	–	–
G 352.630–1.067	G 352.630–1.067	0.5	G 352.630–1.067	0.4	0	0	–2.8	–	–
G 353.273+0.641	–	–	G 353.273+0.641	0.3	–49	–	–5.2	–	–
G 353.411–0.362	–	–	–	–	–	–	G 353.411–0.362	1.7	–
G 353.464+0.562	G 353.464+0.562	0.9	G 353.464+0.562	1.9	–60	–45	–50.7	–	–
G 354.615+0.472	G 354.615+0.472	1.9	G 354.615+0.472	1.8	–38	–15.4	–24.6	–	–
G 355.343+0.147	G 355.344+0.147	2.0	G 355.344+0.147	1.7	17	19	20	–	–
–	–	–	G 355.343+0.148	2.7	–	–	5.7	–	–
G 355.345+0.149	–	–	G 355.346+0.149	1.4	72	–	10	–	–
G 357.965–0.164	–	–	G 357.965–0.164	1.5	–19	–	–8.8	–	–
G 357.967–0.163	G 357.968–0.163	1.7	G 357.967–0.163	0.5	–65	–6.3	–3.2	–	–
G 358.371–0.468	–	–	G 358.371–0.468	1.0	1	–	1	–	–
G 358.386–0.483	G 358.387–0.482a	2.3	G 358.386–0.483	1.5	0	–6.3	–6.0	G 358.387–0.483	3.4
–	G 358.387–0.482b	3.3	–	–	–7.8	–	–	–	–
G 359.137+0.032	G 359.137+0.032	1.3	G 359.138+0.031	1.5	–1	–1	–3.9	–	–
G 359.436–0.102	–	–	G 359.436–0.102	0.4	–59	–	–53.6	–	–
G 359.436–0.104	G 359.436–0.103	1.9	G 359.436–0.104	0.7	–47	–52	–52	–	–
G 359.615–0.243	G 359.615–0.243	0.8	G 359.615–0.243	0.6	64	22.5	22.5	–	–
G 359.969–0.457	G 359.970–0.457	1.2	G 359.970–0.457	1.3	11	15.5	23.0	–	–
G 0.209–0.002	–	–	–	–	–	–	G 0.209–0.002	2.4	–
G 0.212–0.002	–	–	G 0.212–0.001	3.7	56	–	49.2	–	–
G 0.316–0.201	–	–	G 0.316–0.201	0.7	23	–	21	–	–
–	–	–	G 0.315–0.201	2.1	–	–	18	–	–
G 0.376+0.040	G 0.376+0.040	1.3	G 0.376+0.040	1.6	40	36	37.1	–	–
G 0.497+0.188	G 0.496+0.188	2.1	G 0.496+0.188	2.1	26	–5.5	0.8	–	–
G 0.547–0.851	G 0.546–0.852	2.7	G 0.546–0.852	3.2	20	13.5	13.8	–	–
G 0.657–0.042	G 0.658–0.042	0.4	G 0.657–0.041	4.8	62	52	–	–	–
G 0.668–0.035	G 0.666–0.035	4.0	–	–	59	61	–	–	–
G 2.143+0.009	G 2.143+0.009	0.8	G 2.143+0.009	0.1	37	59.8	62.7	–	–
G 2.536+0.198	–	–	G 2.536+0.198	2.5	25	–	3.2	–	–
G 5.886–0.392	G 5.885–0.392	6.3	G 5.885–0.392	5.5	11	13.9	6.7	–	–
G 5.901–0.430	–	–	G 5.900–0.430	1.7	14	–	10	–	–
G 6.049–1.447	G 6.048–1.447	2.0	–	–	20	11.2	–	–	–
G 6.611–0.082	–	–	G 6.610–0.082	2.1	6	–	0.7	–	–
G 6.796–0.257	G 6.795–0.257	2.1	G 6.795–0.257	2.4	1	16.1	26.6	–	–
G 8.139+0.226	–	–	G 8.139+0.226	1.2	16	–	20.0	–	–
G 8.670–0.356	G 8.669–0.356	2.9	G 8.669–0.356	2.7	36	39.2	39.3	G 8.670–0.356	1.1
G 9.620+0.194	G 9.620+0.194	1.6	–	–	6	22	–	–	–
G 9.622+0.195	G 9.621+0.196	2.9	G 9.621+0.196	3.3	22	1.4	1.3	–	–
G 9.986–0.028	–	–	G 9.986–0.028	1.3	49	–	47.1	–	–
G 10.288–0.125	–	–	G 10.287–0.125	1.9	9	–	5	–	–
G 10.323–0.160	–	–	G 10.323–0.160	1.5	–3	–	10	–	–
G 10.342–0.143	–	–	G 10.342–0.142	1.8	8	–	14.8	–	–
G 10.445–0.018	G 10.444–0.018	3.3	G 10.444–0.018	3.7	70	75.5	73.2	–	–
G 10.473+0.027	G 10.473+0.027	0.9	G 10.473+0.027	1.9	62	51.5	75	G 10.473+0.027	1.8
G 10.480+0.034	G 10.480+0.033	4.5	G 10.480+0.033	4.5	64	66	65	–	–

**Table 3 – continued**

Water ( <i>l, b</i> ) (deg)	OH ( <i>l, b</i> ) (deg)	Sep. (arcsec)	Methanol ( <i>l, b</i> ) (deg)	Sep. (arcsec)	Water V peak (km s <sup>-1</sup> )	OH V peak (km s <sup>-1</sup> )	Methanol V peak (km s <sup>-1</sup> )	Continuum ( <i>l, b</i> ) (deg)	Sep. (arcsec)
G 10.623–0.383	G 10.623–0.383	0.6	–		2	–2		–	
G 10.959+0.022	–		G 10.958+0.022	1.4	25		24.4	G 10.959+0.022	0.7
G 11.034+0.062	G 11.034+0.062	1.6	G 11.034+0.062	1.5	18	21.7	20.6	–	
G 11.498–1.486	–		G 11.497–1.485	2.9	17		6.7	–	
G 11.903–0.142	G 11.904–0.141	3.5	G 11.904–0.141	4.4	36	40.5	42.8	–	
G 12.203–0.107	–		G 12.203–0.107	0.2	35		20.5	–	
G 12.209–0.102	–		G 12.209–0.102	1.0	22		19.8	G 12.209–0.102	3.0
G 12.216–0.119	G 12.216–0.119	1.5	–		26	27.9		–	
G 12.681–0.183	G 12.680–0.183	1.0	G 12.681–0.182	1.1	61	64.5	57.6	–	
G 12.889+0.489	G 12.889+0.489	3.0	G 12.889+0.489	2.7	30	33	39.3	–	
G 12.908–0.260	G 12.908–0.260	1.2	G 12.909–0.260	1.8	37	38	39.9	–	
G 17.637+0.156	G 17.638+0.157	2.1	G 17.638+0.157	2.2	27	20	20.7	–	

Note. Column 1 shows the water maser source name; Column 2 gives the source name of the nearest OH maser within 5 arcsec (– if none) of the detected water maser; Column 3 gives the angular separation between the water and the OH masers; Column 4 gives the source name of the nearest methanol maser within 5 arcsec (– if none) of the detected water maser; Column 5 gives the angular separation between the water maser and the methanol maser; Columns 6–8 give the water maser, OH maser and methanol maser peak velocities, respectively; Column 9 gives detected UCH<sub>II</sub> regions with 5 arcsec of the detected water masers (– if none); and Column 10 gives the angular separation between the UCH<sub>II</sub> region and the detected water maser.

at one epoch is occasionally due to confusion from nearby features, as remarked in these notes. There are many instances where high-velocity emission is present (as indicated in Table 1), but is rather weak and barely visible on the spectrum, so we draw attention to it here.

284.350–0.418. This water maser is coincident with the main-line OH maser 284.351–0.418, with accompanying emission at 6035 MHz (C97), but clearly offset from the nearby methanol maser 284.352–0.419 by 6 arcsec. Spectra from epoch 2003 as well as 2004 are shown as an example of the typical variability seen between our observing epochs.

285.260–0.067 and 285.263–0.059. The latter is a very strong water maser associated with an OH maser and having similar velocity of its strongest emission. In the case of OH masers, the velocity of the strongest emission is a reliable indication of the systemic velocity. The first maser, offset by 1 arcmin, may be loosely associated, but it is difficult to recognize possible emission near the systemic velocity because of confusion with the stronger companion. Its spectrum varied markedly from 2003 to 2004, and highly blueshifted emission dominates the 2004 spectrum.

290.374+1.661 and 290.384+1.663. The first of these sources is coincident with both OH and methanol maser emission. The positions measured in 2003 and 2004 are coincident, but detected features do not overlap in velocity ranges. There has been a substantial decrease in the peak flux density from 3.5 to 0.26 Jy from the first to the second epoch.

The second source, 290.384+1.663, is offset from the OH and methanol targets and appears to be solitary, with no associated OH or methanol maser emission.

291.270–0.719, 291.274–0.709 and 291.284–0.716. The 2003 data for these sources are presented in Caswell (2004b), along with extensive discussion on associated sources. Note that the OH target 291.274–0.709 was a supplementary addition to the list of C98. The variability of the water masers between the two epochs is moderate, with minimal changes in the velocity ranges of the detected emission but many changes in the relative flux densities of individual features.

291.270–0.719 is associated with methanol maser emission and has weak emission near the systemic velocity but much stronger

emission blueshifted by almost 80 km s<sup>-1</sup>. 291.274–0.709, shows emission only near the systemic velocity and is coincident with both OH and methanol maser emission. The strongest source, 291.284–0.716, is associated with neither OH nor methanol maser emission and shows no detectable water maser emission at the systemic velocity but has strong blueshifted emission. Caswell & Phillips (2008) regard this source and 291.270–0.719 as members of a distinct class of water masers that are dominated by blueshifted outflows.

291.578–0.434, 291.579–0.431 and 291.581–0.435. The main strong source 291.579–0.431 is a persistent maser detected in both 2003 and 2004, and also in 1981 (Caswell et al. 1989), with intensity varying by a factor of 4. The other sources, detected at a single epoch, are even more variable. All are associated with NGC 3603 (Caswell 2004b).

291.610–0.529, 291.627–0.529 and 291.629–0.541. The three water masers of this cluster were all detected in both 2003 and 2004 and are associated with NGC 3603 (Caswell 2004b). Only G291.610–0.529 is coincident with an OH maser, and none of the sources is associated with any methanol maser emission.

297.660–0.974. The strongest water maser peaks, at 29 km s<sup>-1</sup> in 2003 and 26 km s<sup>-1</sup> in 2004, agree well with the associated OH maser peak at 27.6 km s<sup>-1</sup>, the probable systemic velocity for the region. There is a weak high-velocity water maser feature of 0.6 Jy at a velocity of –78 km s<sup>-1</sup>, slightly more than 100 km s<sup>-1</sup> from the systemic velocity.

299.012+0.125 and 299.013+0.128. 299.013+0.128, with the strongest peak at +19 km s<sup>-1</sup> in both 2003 and 2004, was first detected by Caswell et al. (1989) and is in good agreement with the position and velocity of methanol and OH masers. In 2004 we detected an additional weak source, 299.012+0.125, offset by ∼9 arcsec. We regard the latter as most likely a distinct source, probably in the same cluster but lacking emission at its systemic velocity.

300.968+1.143 and 300.971+1.143. 300.968+1.143 was first observed by Caswell et al. (1989), with high-velocity emission extending to –85 km s<sup>-1</sup>, remaining similar in our observations in both 2003 and 2004. This source is solitary, offset from the target OH maser by 18 arcsec. Observations in 2004 uncovered an additional source, 300.971+1.143, with a flux density of 3 Jy. As

**Table 4.** 22-GHz continuum sources detected towards water maser sources (i.e. continuum sources within 4.5 arcsec of detected water masers). See Tables 1 and 3 for details of the water maser sources that these continuum sources are associated with.

Continuum ( <i>l, b</i> ) (deg)	RA(2000) (h m s)	Dec.(2000) (° ' '')	<i>I</i> peak (mJy beam <sup>-1</sup> )	Total flux density (mJy)
G 291.611−0.529	11 15 02.62	−61 15 51.4	350	446
G 291.626−0.531 <sup>#</sup>	11 15 09.66	−61 16 15.7	137	357
G 299.012+0.128	12 17 24.12	−62 29 05.6	25	38
G 301.136−0.226	12 35 34.96	−63 02 31.6	1017	1116
G 311.643−0.380	14 06 38.73	−61 58 21.4	174	181
G 313.458+0.193	14 19 35.04	−60 51 52.1	205	272
G 316.412−0.308	14 43 23.25	−60 12 59.5	160	167
G 317.430−0.561	14 51 38.03	−60 00 19.5	32	35
G 319.399−0.012	15 03 17.60	−58 36 11.2	230	298
G 320.234−0.283	15 09 52.63	−58 25 32.4	282	293
G 327.402+0.445	15 49 19.35	−53 45 13.3	86	94
G 328.236−0.547	15 57 58.15	−53 59 23.4	26	36
G 328.307+0.431	15 54 06.24	−53 11 38.8	3361	3647
G 328.808+0.633	15 55 48.33	−52 43 07.0	1208	1357
G 330.879−0.367	16 10 19.95	−52 06 05.3	324	476
G 330.954−0.182	16 09 52.51	−51 54 54.1	2954	3151
G 331.443−0.187	16 12 12.83	−51 35 10.2	40	44
G 331.512−0.103	16 12 10.10	−51 28 37.2	109	113
G 332.826−0.549	16 20 11.12	−50 53 13.7	2510	2670
G 333.030−0.063	16 18 56.94	−50 23 53.5	27	25
G 333.466−0.163 <sup>#</sup>	16 21 19.71	−50 09 45.6	141	254
G 336.018−0.828	16 35 09.39	−48 46 47.6	85.1	80.8
G 336.360−0.137	16 33 29.64	−48 03 38.8	189	293
G 336.984−0.184	16 36 12.60	−47 37 57.8	51	56.8
G 336.990−0.025	16 35 32.48	−47 31 14.6	91	102
G 337.404−0.403	16 38 50.59	−47 28 02.8	117	121
G 337.706−0.054	16 38 29.83	−47 00 35.7	244	262
G 338.075+0.012	16 39 39.15	−46 41 26.2	818	1144
G 338.681−0.085	16 42 24.19	−46 18 00.4	74	74
G 344.582−0.024	17 02 58.03	−41 41 52.7	19	21
G 345.004−0.225	17 05 11.36	−41 29 06.5	353	355
G 345.010+1.792	16 56 47.85	−40 14 25.8	362	367
G 345.408−0.952	17 09 35.62	−41 35 54.6	493	608
G 347.632+0.210	17 11 36.22	−39 07 06.2	46	48
G 350.331+0.099	17 20 02.09	−36 59 12.8	55	65
G 351.161+0.696	17 19 57.65	−35 57 51.8	238	271
G 351.247+0.667	17 20 19.29	−35 54 39.4	1280	1567
G 353.411−0.362	17 30 26.66	−34 41 46.0	384	788
G 358.387−0.483	17 43 37.96	−30 33 49.2	109	113
G 0.209−0.002	17 46 07.57	−28 45 30.5	75	95
G 8.670−0.356	18 06 19.15	−21 37 32.1	677	689
G 10.473+0.027	18 08 38.41	−19 51 47.9	152	151
G 10.959+0.022	18 09 39.43	−19 26 27.0	150	153
G 12.209−0.102	18 12 39.85	−18 24 20.0	119	140

*Note.* Columns 1–5 show the name of the continuum source in Galactic coordinates, the source right ascension, declination, peak flux density (mJy beam<sup>-1</sup>) and integrated flux density (mJy). We present two additional continuum sources that fall just outside our association threshold and we distinguish these sources with a '#', following the source name in Column 1.

can be seen in Table 1, in 2003 we placed an upper limit on the flux density of this source of 3 Jy, quite crude because at this velocity there was confusion by strong emission from 300.968+1.143 at this epoch.

301.136−0.225, 301.136−0.226a, 301.136−0.226b and 301.137−0.225. Although we list four distinct water maser positions, they probably represent a single maser site, with the

last three locations all within 3 arcsec of OH and methanol maser emission. Confusion between features in 2003 prevented separate position measurement of any but the strongest feature.

305.191−0.006 and 305.198+0.007. 305.198+0.007 is probably the same source as 305.20+0.01 in Caswell et al. (1989). Both of these water masers are offset from the target OH maser, 305.200+0.019 (with the methanol maser, 305.199+0.005).

$305.208+0.207$ . Two strong peaks have positions separated by about 1 arcsec, with the weaker peak slightly closer to the associated OH and methanol emission.

$306.318-0.331$ . This is a new solitary water maser source found offset from target OH and methanol maser positions by  $\sim 15$  arcsec.

$308.754+0.549$ . The OH target is an addition to the C98 list. Details of methanol, OH and water are given by Caswell (2004b).

$308.918+0.124$ . The position of this water maser falls within our 3-arcsec association threshold of the OH maser G  $308.918+0.123$  but lies 3.6 arcsec from the methanol maser G  $308.918+0.123$ . The OH and methanol masers are almost certainly coincident, with a measured separation of 0.6 arcsec, and we treat all three species as coincident.

$309.921+0.479$ . Caswell et al. (1989) reported the detection of a 4.5-Jy water maser at  $-70 \text{ km s}^{-1}$  towards this OH and methanol site. We detect no emission ( $<0.3$  Jy) in either 2003 or 2004.

$310.144+0.760$  and  $G\,310.146+0.760$ . The first of this close pair of sources is located at the site of both OH and methanol maser emission and the second source is located at the site of an isolated 1720-MHz OH maser (Caswell 2004a) and is strongly variable.

$311.94-0.14$ . This is a methanol site from Caswell (2009) with position  $14^{\text{h}}07^{\text{m}}49\overset{\text{s}}{.}72$ ,  $-61^{\circ}23'08\overset{\text{s}}{.}3$  (uncertainty of 0.4 arcsec) from which there was no water detection in 2003 (this position was not observed in 2004). However, a water maser was reported by Caswell et al. (1989) with a peak flux density of 38 Jy from the position  $14^{\text{h}}07^{\text{m}}49\overset{\text{s}}{.}9$ ,  $-61^{\circ}23'20''$ , nominally offset from the methanol by 12 arcsec but with an rms position uncertainty of about 10 arcsec and thus possibly coincident with the methanol. An OH maser is listed by C98 at  $14^{\text{h}}07^{\text{m}}48\overset{\text{s}}{.}7$ ,  $-61^{\circ}23'22''$ , nominally offset from the methanol by 16 arcsec, but again, possibly coincident (to within the OH position uncertainty of more than 15 arcsec). Like the water maser, the OH has varied, and later observations to attempt an improved position determination failed to detect it. We have omitted this source from the statistics since for our position coincidence threshold of 3 arcsec, it may be an OH site accompanied by water, by methanol, by both or by neither, depending on the precise positions yet to be determined.

$312.106+0.278$  and  $312.109+0.262$ . The second source is located towards the targeted methanol maser and consists of a single feature, with velocity similar to the methanol. The first source is a slightly stronger single feature, offset from the second by nearly 1 arcmin and clearly offset in velocity by  $6 \text{ km s}^{-1}$ .

$312.596+0.045$  and  $312.599+0.046$ . These sources are a close pair, separated by  $\sim 10$  arcsec. The second of these sources was also detected by Caswell et al. (1989) and is coincident with both OH and methanol masers. The first source,  $312.596+0.045$ , is coincident with a methanol maser site.

$313.457+0.193$  and  $313.470+0.191$ . These sources have an angular separation of  $\sim 45$  arcsec.  $313.470+0.191$  was also detected in Caswell et al. (1989) and is associated with both OH and methanol masers, with peak water maser velocity comparable to the systemic velocity of the region as traced by the coincident methanol maser with a mid-range velocity of  $-8 \text{ km s}^{-1}$ .  $313.457+0.193$  has an emission peak near  $-1 \text{ km s}^{-1}$  at both epochs, suggesting that its systemic velocity (and distance) is similar to that of its companion. We regard the slightly stronger emission at  $45 \text{ km s}^{-1}$  seen only in 2004 as a strongly varying high-velocity feature.

$316.360-0.361$  and  $316.361-0.363$ . Near these water masers lie an isolated methanol site ( $316.381-0.379$ ) and a ‘methanol with OH’ site ( $316.359-0.362$ ). The water maser  $316.360-0.361$  is offset from the methanol in the latter pair by 3.2 arcsec and slightly further from the OH. Thus the water maser is formally rejected as

part of an intimate association, but this remains somewhat uncertain. The second water maser source is further offset from these sources than the first and is thus very clearly a distinct, isolated site.

$318.044-1.404$ . The OH and methanol maser counterparts show that the systemic velocity is indeed near  $+45 \text{ km s}^{-1}$  and indicate a distant location outside the solar circle. The large latitude offset from the Galactic plane is consistent with the Galactic warp known to be present in this outer region of the Galaxy.

$318.948-0.196a$  and  $318.948-0.196b$ . This pair of sources is essentially one extended source. Using the 2004 data, we were able to distinguish two main sites (with an angular separation of just over 2 arcsec) which conveniently reveal the association with nearby OH and methanol masers that otherwise would have fallen outside our 3-arcsec coincidence threshold.

$320.221-0.281$ ,  $320.232-0.284$ ,  $320.233-0.284$ ,  $320.255-0.305$  and  $320.285-0.308$ . We suggest that all five sites are at a similar distance in a cluster with systemic velocity near  $-65 \text{ km s}^{-1}$ .  $320.232-0.284$  has associated methanol and OH maser emission and  $320.233-0.284$ , offset by nearly 5 arcsec, seems to be a separate site.  $320.255-0.305$  shows strong emission only near  $-126 \text{ km s}^{-1}$ , highly blueshifted from our suggested systemic velocity near  $-65 \text{ km s}^{-1}$ , and apparently in a small class of water masers where blueshifted emission dominates (Caswell & Phillips 2008). Interestingly, like  $291.284-0.716$ ,  $320.255-0.305$  is not associated with either OH or methanol maser emission. Emission from this region was reported, with lower position precision, by Caswell et al. (1989).

$321.028-0.484$  and  $321.033-0.483$ . Both water masers are offset from the target OH and methanol maser  $321.030-0.485$  by more than 7 arcsec; the second water maser is associated with the methanol maser  $321.033-0.483$ .

$321.148-0.529$ . The spectrum of this maser is shown at both epochs as an example of extreme variability with no common features seen in spectra observed less than 1 yr apart.

$323.459-0.079$ . A water maser was discovered (but without a precise position) by Caswell et al. (1989) towards this OH and methanol site, but was below our detection threshold of 0.2 Jy in both 2003 and 2004.

$324.716+0.342$ . This source was detected by Caswell et al. (1989) at a peak flux density of 138 Jy, coincident with both OH and methanol maser emission. The water maser shows marked variability with peaks of 10 and 26 Jy during 2003 and 2004, respectively.

$326.662+0.521$ ,  $326.665+0.553$  and  $326.670+0.554$ . This group of three sources is spread over 2 arcmin.  $326.670+0.554$  coincides with an OH maser; the water maser peak flared in 2004 relative to 2003. This maser is probably the same as the one reported, with a peak of 780 Jy, but with poor position, by Batchelor et al. (1980). In 2004 no targeted observation was made of the first source and although recognized at the beam edge in another observation, it was confused by a strong flare from  $326.670+0.554$ . Measurement for the second source ( $326.665+0.553$ ) is reported only from the 2004 measurements since the 2003 observations were confused by  $326.662+0.521$ , preventing a useful upper limit estimate.

$326.780-0.241$ . This is a new water maser coincident with an OH maser listed by C98 with approximate coordinates  $326.77-0.26$ ; subsequent (previously unpublished) ATCA measurements of the OH show it to be coincident with the water maser.

$326.859-0.676$ . This weak new water maser coincides spatially with the methanol maser  $326.859-0.667$  (offset by 3.4 arcsec), whose systemic velocity is  $-58.0 \text{ km s}^{-1}$ . It seems likely to be an association in which only a heavily blueshifted water maser feature, at  $-103 \text{ km s}^{-1}$ , is seen.

**327.291–0.578.** This strong water maser with a peak of several hundred janskys is associated with OH and methanol masers. Spectra are shown for 2003 and 2004 revealing great variability of the water maser and can be compared with a spectrum shown by Batchelor et al. (1980) when its peak was over 1000 Jy.

**327.402+0.445.** In contrast to the previous source, this water maser has greatly increased intensity compared to measurements by Batchelor et al. (1980). The water maser is associated with a strong methanol maser. An OH maser is close to the methanol. We therefore treat the OH as an association also, although its separation from water is just outside our formal association criterion.

**328.306+0.432.** This water maser is associated with 22-GHz radio continuum but appears to be truly offset from the target OH maser 328.307+0.430 (which has no accompanying methanol) by more than 5 arcsec.

**328.808+0.633.** This maser is detected towards the OH maser site 328.809+0.633. Also associated are many transitions of methanol and OH, including 6.6-, 12.2-, 19.9-, 85.5- and 107-GHz methanol masers (Caswell 2009; Caswell et al. 1995a; Ellingsen et al. 2004, 2003; Val'tts et al. 1999) as well as 1720-, 4765-, 6030-, 6035-MHz and 13.4-GHz transitions of OH (Dodson & Ellingsen 2002; Caswell 2003, 2004b, 2004c). This source is also associated with strong 22-GHz radio continuum.

**329.021–0.186, 329.029–0.199, 329.030–0.205 and 329.031–0.198.** This cluster of four sources is spread over about 1 arcmin. The first source is solitary (no OH or methanol), the second (which varied below the detection limit in 2004) has OH, and the third and fourth are associated with both OH and methanol, respectively. Ellingsen (2006) showed that these OH, methanol and previously known water masers are associated with a filamentary infrared (IR) dark cloud as well as Class I methanol masers.

**329.342+0.130.** This water maser is clearly offset by almost 1 arcmin from the target OH maser 329.339+0.148, and no other water emission was detectable in the field. The water maser velocity is similar to that of its OH neighbour and they presumably reside in the same star formation cluster, discussed in detail by Caswell (2001, 2004a, 2004c). Note that the OH target is an addition to the C98 list.

**329.404–0.459, 329.405–0.459 and 329.407–0.459.** The second source is at an OH and methanol maser site and its velocity is similar, presumably representative of the systemic velocity. The first source is offset by only 3 arcsec from the second site, whereas its velocity is close to that of the previously discussed, more distant, cluster around 329.339+0.148. None the less, we suggest that it most likely represents high-velocity emission related to 329.405–0.459. The water maser 329.407–0.459, associated with a methanol maser, has shown extreme variability with a peak flux density of 80 Jy in 2003 but not detected above our detection limit of 0.2 Jy in 2004.

**329.421–0.167, 329.424–0.164 and 329.426–0.161.** The only other maser species nearby, both spatially and in velocity, is a 1720-MHz maser 329.426–0.158 (Caswell 2004a). We conclude that all four masers lie in the same star-forming cluster but are not closely associated.

**330.879–0.367.** The water maser has been known for many years (Batchelor et al. 1980) and our precise position confirms that it coincides with one of the strongest known OH masers, accompanied by very weak methanol emission (Caswell 2009).

**330.954–0.182.** The water maser has remained very strong for many years (see Batchelor et al. 1980) and has prominent high-velocity emission (a feature at  $-191 \text{ km s}^{-1}$  has a peak flux density of 0.3 Jy but is too weak to be seen on the spectra displayed here).

OH and methanol emission is present nearby but spread over several arcseconds, and the most detailed maps (Caswell et al. 2010) show the water to be associated with OH emission only, with the methanol emission clearly at another site offset to the south-west by more than 3 arcsec. We measure the flux density of an associated strong UCH<sub>II</sub> region at 22 GHz as 3.2 Jy.

**331.418+0.252.** This 0.6-Jy water maser was detected almost 50 arcsec from the targeted methanol maser 331.425+0.264. The water maser emission is observed towards a UCH<sub>II</sub> region that we detect at 22 GHz.

**331.512–0.103.** Batchelor et al. (1980) observed this source with a peak flux density of 4300 Jy. Observations of this source in 2003 and 2004 showed a decrease in the flux density to 700 and 534 Jy in 2003 and 2004, respectively. The water maser is coincident with an OH maser (but no methanol) and a UCH<sub>II</sub> region that we detect. The strongest water emission is near the systemic velocity, and almost symmetric about this there are multiple high-velocity features extending for  $70 \text{ km s}^{-1}$ .

**332.826–0.549.** This is a strong new water maser coinciding with methanol and a 6035-MHz OH maser but offset by 7 arcsec from a 1665-MHz OH maser.

**333.219–0.062 and G 333.234–0.060.** 333.234–0.060 was detected in both 2003 and 2004 and has been previously observed by Batchelor et al. (1980). At all epochs the peak has been more than 100 Jy at a velocity near  $-88 \text{ km s}^{-1}$ , which is the mid-range velocity of an associated OH maser and the likely systemic velocity. In our 2004 water observations, an extreme high-velocity feature was observed with a peak flux density of 0.3 Jy at  $+81 \text{ km s}^{-1}$ , more than  $160 \text{ km s}^{-1}$  from the systemic velocity. 333.219–0.062 is offset from 333.234–0.060 by almost an arcminute and is solitary. This source was observed with a peak flux density of 0.5 Jy in 2004 and was not detected in 2003 above 0.3 Jy. In the absence of an association with OH or methanol, its systemic velocity is unknown.

**333.387+0.032.** This weak water maser is located at the site of both OH and methanol maser emission. It was detected with a peak flux density of 0.4 Jy in 2003 and had decreased to 0.14 Jy in 2004. Spectra from both epochs are presented in Fig. 1.

**333.608–0.215.** This was one of the earliest observed water masers, discovered by Johnston et al. (1972) and was later observed by Batchelor et al. (1980) in 1976 with a peak flux density of 100 Jy. Breen et al. (2007) carried out interferometric observations of this source in 2006, deriving a precise position for the source that is within 0.4 arcsec of the independent position quoted in Table 1. Both the Breen spectrum of 2006 and that found in the present observations of 2003 differ markedly from the 2004 spectrum shown here, revealing strong variability of high-velocity emission. This source is associated with an OH maser and is offset by 15 arcsec from a bright UCH<sub>II</sub> region which was erroneously reported by Breen et al. (2007) as having an integrated flux density of 631 mJy at 22 GHz. The present observations find that the UCH<sub>II</sub> region has an integrated flux density of more than 16 Jy at 22 GHz.

**333.930–0.134.** This very weak water maser was observed at the 2004 epoch only. While the peak of the detected emission is a mere 0.18 Jy, the source position is in remarkably good correspondence with the targeted methanol maser, the separation being less than 1.5 arcsec.

**335.059–0.428, 335.060–0.427 and 335.070–0.423.** The first two of these sources are separated by 3.3 arcsec and therefore may be essentially a single source spread over a few arcseconds. The second source, 335.060–0.427, with measurements in both 2003 and 2004, shows best positional agreement with an associated OH and methanol maser site. 335.059–0.428 was not recognizable as

a distinct source in the 2003 data owing to confusion from the stronger companion 335.060–0.427.

335.070–0.423 is offset from the previous two sources by 43 arcsec and is solitary.

335.585–0.285, 335.586–0.290 and 335.588–0.264. These three sources are spread over almost 80 arcsec. The first two sources were detected at both epochs and are coincident with both methanol and OH masers. The third source, 335.588–0.264, was detected with a peak flux density of 16 Jy in 2003 but not detectable above 0.2 Jy in 2004. It is isolated from other maser species and is devoid of detectable 22-GHz radio continuum emission.

335.787+0.177, 335.789+0.174 and 335.789+0.183. 335.789+0.174 was detected by Batchelor et al. (1980) as a 25-Jy source towards an OH maser with the same Galactic coordinates. Our observations detect a water maser of 3 Jy in 2003 and detect no emission above 0.2 Jy in 2004. 335.787+0.177, detected in both 2003 and 2004, is a solitary maser and has no detectable radio continuum at 22 GHz. The third source, 335.789+0.183, is also isolated from other maser species as well as 22-GHz radio continuum emission. It was detected with a peak flux density of 4.2 Jy at a velocity of  $-91 \text{ km s}^{-1}$  in 2003 and was not detectable above 0.2 Jy in 2004. If this velocity represents the systemic velocity, then its distance is likely to differ greatly from its apparent companions. Alternatively, it may be a companion at similar distance but showing no significant emission near the systemic velocity, and only blueshifted emission. Such high-velocity features are notoriously variable.

336.864+0.005, 336.864–0.002 and 336.870–0.003. These three sources are located within 40 arcsec of each other and were all detected in both the 2003 and 2004 observations. The first source is associated with both OH and methanol maser emission and the other two sources are solitary.

336.983–0.183. Fig. 1 shows both the 2003 and 2004 spectra for this weak source. The only significant feature in 2003 is a peak at  $-76 \text{ km s}^{-1}$ . In 2004, emission near this velocity is weaker and a high-velocity feature near  $+45 \text{ km s}^{-1}$  is marginally stronger. The source is associated with a methanol maser as well as a UCH $\alpha$  region that we list in Table 7. The methanol maser is strong, with a well-measured position and velocity near  $-81 \text{ km s}^{-1}$ . Nearby is a weak OH maser just outside our criterion for an association with the water position, but slightly closer to the methanol. Furthermore, the position of 6035-MHz OH emission (Caswell 2001) is acceptably within our coincidence criterion, so we add this as an OH maser association with both methanol and water.

336.991–0.024, 336.994–0.027 and 336.995–0.024. These three sources appear clustered within  $\sim 15$  arcsec. 336.994–0.027 is the strongest of the three (160 Jy), detected in 2003, 2004 and by Batchelor et al. (1980), and is associated with both OH and methanol maser emission, with systemic velocity near  $-120 \text{ km s}^{-1}$ . The two weaker water sites have quite different radial velocities, near  $-50 \text{ km s}^{-1}$ , and might be at a distance quite different from the strongest one. 336.991–0.024 was detected in both 2003 and 2004, with a peak flux density of 4 and 1 Jy at the respective epochs, and is associated with a UCH $\alpha$  region that we detect. 336.995–0.024 was detected only in 2004 and had a peak flux density of 1.1 Jy.

337.994+0.133 and 337.998+0.137. Batchelor et al. (1980) detected 337.998+0.137 with a peak flux density of 200 Jy and we detected a decreased flux density of 30 and 27 Jy in 2003 and 2004, respectively. This source is coincident with both OH and methanol maser emission. 337.994+0.133 is a solitary maser, offset from the previous source by 19 arcsec.

338.069+0.011, 338.075+0.012, 338.075+0.010 and 338.077+0.019. Water maser emission from 338.069+0.011

is the strongest in this cluster at both epochs and has no other maser counterpart. 338.075+0.012 detected only in 2003, and the weakest of the group, coincides with OH and methanol maser emission. 338.075+0.010 is associated with a methanol maser with systemic velocity near  $-38 \text{ km s}^{-1}$ ; the water maser emission in 2003 was strongest at a highly blueshifted velocity, but by 2004 this had faded below detectability, leaving only features closely straddling the systemic velocity. 338.077+0.019 was detected in both 2003 and 2004, the spectrum remaining unchanged; it has no apparent association with other masers.

338.920+0.550 and 338.925+0.556. The stronger site, 338.925+0.556, coincides with OH and methanol masers. The weaker site, 338.920+0.550, is associated with a methanol maser with systemic velocity near  $-60 \text{ km s}^{-1}$ , similar to the other site, and the water spectrum in 2003 was dominated by highly blueshifted emission.

343.126–0.065 and 343.127–0.063. These two sources are separated by 9.3 arcsec. The second source is strong and associated with an OH maser, but not methanol. The first source is much weaker but clearly distinct and is solitary.

345.004–0.224. In 2003 the only water emission was near the systemic velocity, as defined by the associated methanol and OH masers. In 2004, high-velocity features dominated. Spectra from both epochs are shown to demonstrate this interesting variability.

345.010+1.793, 345.010+1.802 and 345.012+1.797. In this small cluster, the first water maser coincides with an OH and methanol site, the second has no other maser counterpart and the third, the strongest, has a methanol counterpart.

345.397–0.950, 345.402–0.948, 345.405–0.947, 345.406–0.942, 345.408–0.953, 345.412–0.955 and 345.425–0.951. One of these sites, 345.425–0.951, is coincident with a methanol maser site. We also accept a coincidence between 345.408–0.953 and an OH and methanol maser site, despite an offset of 4.6 arcsec, formally just outside our criterion for a single epoch water measurement; there is evidence (from the comparison of features common to 2003 and 2004 and a feature common to 2004 and FC89) that the 2004 observation of this field yields positions slightly too far south and at too large a right ascension, a correction that would improve the coincidence. The systemic velocity of the two associated, methanol sites is near  $-15 \text{ km s}^{-1}$ . In view of the large offset of the cluster from the Galactic plane in Galactic latitude, all water sites are likely to be clustered at a similar distance, irrespective of the water maser velocity. Their separation from each other is sufficiently large to suggest that each site has its own exciting star, and thus it seems likely to be a remarkable physical cluster of massive stars. Radhakrishnan et al. (1972) suggest that the distance to the complex is half the distance to the Galactic Centre.

345.487+0.314. As seen in the notes tabulating associations, there is a coincident methanol maser and no nearby ground-state OH maser. There is, however, a 6035-MHz excited state OH maser offset by just over 3 arcsec to the north (Caswell 2001).

345.493+1.469, 345.494+1.470 and 345.495+1.473. The first site coincides with an OH maser that has no accompanying methanol maser. Another nearby OH maser site shows no methanol or water emission. All four sites are likely to lie in a nearby cluster, as evident from the large Galactic latitude, and the systemic velocity probably lies between  $-15$  and  $0 \text{ km s}^{-1}$ , based on the OH velocities.

347.623+0.148 and 347.628+0.149. The first water maser, detected in both 2003 and 2004, has no coincident maser of OH or methanol. The second water maser, at similar velocity, was detected only in 2003 and coincides with OH and methanol, with systemic velocity near  $-95 \text{ km s}^{-1}$ .

$348.533-0.974$ ,  $348.534-0.983$  and  $348.551-0.979$ . The third water site is close to the original OH target but is more precisely coincident with the methanol site  $348.550-0.979$  (Caswell 2009). The original ‘OH with methanol’ target,  $348.550-0.979$ , is regarded by Caswell (2009) as a nearby but distinct site and, on this interpretation, it is a site without detected water maser emission. The water masers  $348.533-0.974$  and  $348.534-0.983$  are new, chance, detections in the vicinity.

$348.726-1.038$ . This water maser is offset from the target OH (with methanol) by more than 4 arcsec and is not formally an association. However, the large spread over several arcseconds in the positions of individual water maser spots reveals a larger than usual maser site and the possibility of an association will require further investigation.

$350.105+0.084$   $350.112+0.089$  and  $350.113+0.095$ . The first of these is associated with a methanol site and the second with an OH site. In a cluster of six water maser sites showing peak emission at velocities between  $-72$  and  $-44\text{ km s}^{-1}$ , they are the only two accompanied by maser emission of another species. Spatially in this same cluster, the water maser  $350.112+0.089$  displays a quite different velocity range, from  $-175$  to  $-106\text{ km s}^{-1}$  suggesting that it might be at a quite different location, perhaps in the near side of the 3-kpc arm, whose characteristic velocity at this longitude extends to approximately  $-110\text{ km s}^{-1}$  (Green et al. 2009); see also the note for  $351.582-0.353$ .

$350.299+0.122$ . This is the weakest single epoch water maser that we list, with a peak flux density of 0.17 Jy. The position of the water maser is only 0.7 arcsec from the targeted methanol maser and its emission peak velocity of  $-68\text{ km s}^{-1}$  is within  $6\text{ km s}^{-1}$  of the associated methanol maser peak emission. Furthermore, there are no nearby water maser sources that could confuse the region and be detected as a sidelobe here; there is therefore little doubt that this is a genuine weak water maser.

$351.240+0.668$ ,  $351.243+0.671$  and  $351.246+0.668$ . The first two sites were listed by Caswell & Phillips (2008), with special discussion of a blueshifted outflow that dominates the emission from  $351.243+0.671$ , and remarks that the water maser spots in the outflow are distributed over several arcseconds. All three sites appear to be distinct, with large separations of more than 15 arcsec, yet close enough to suggest that they all lie in the same star-forming cluster, with a systemic velocity of  $+2.5\text{ km s}^{-1}$  as defined by the methanol maser counterpart to  $351.243+0.671$  (Caswell & Phillips 2008), and all lying in the large NGC 6334 complex, at a commonly accepted distance of 1.7 kpc.

$351.417+0.645$ . This maser coincides with an H II region NGC 6334F, a very strong methanol maser, and an OH maser (C97) and its water maser emission was mapped by FC99, showing a scatter of spot positions over several arcseconds, including an apparent jet-like feature.

$351.582-0.353$ . This strong water maser is coincident with an OH and methanol maser site which is located in the near side of the expanding 3-kpc arm (Green et al. 2009; Caswell et al. 2010).

$352.623-1.076$  and  $352.630-1.067$ . The second water maser coincides with an OH and methanol site. It flared from a peak of 35 Jy in 2003 to 700 Jy in 2004. It appears to be the same maser that was first reported by Sakellis et al. (1984) with a peak flux density of 346 Jy. The first source is solitary with no other maser counterpart and offset by more than 40 arcsec.

$353.273+0.641$ . This site is the prime example of a class of water masers dominated by a blueshifted outflow (Caswell & Phillips 2008); its systemic velocity is estimated from a coincident methanol maser.

$353.408-0.350$  to  $353.414-0.363$  inclusive. This is a cluster of six solitary water maser sites. The target OH and methanol maser site  $353.410-0.360$  (C97) lies in this cluster, but none of the water maser sites coincides with it.

$354.703+0.297$ ,  $354.712+0.293$  and  $354.722+0.302$ . The velocity of all three solitary water sites is near  $+100\text{ km s}^{-1}$ , similar to that of the nearby OH with methanol site  $354.724+0.300$ . The velocity of the latter has been interpreted as evidence of a location in the Galactic bar (C97), which we suggest is an appropriate interpretation for all four sites.

$357.965-0.164$  and  $357.967-0.163$ . The two water sites are separated by 9 arcsec. The first site has a weak methanol counterpart but no OH; the second has stronger methanol and also OH. The methanol and OH emission is confined to a small range between  $-9$  and  $+3\text{ km s}^{-1}$ , and thus the systemic velocity for both sites probably lies in this range. Water emission at the first site was strong in 2003 but weak in 2004 and confined to within about  $15\text{ km s}^{-1}$  of the systemic velocity. Water emission at the second site is seen not only near the systemic velocity but also at many blueshifted and redshifted high velocities; in 2004, the high-velocity features were stronger than emission near the systemic velocity.

$359.436-0.102$  to  $359.443-0.104$  inclusive. The six water maser sites in this cluster all have similar velocities. Confusion prevented a useful upper limit estimate for emission from two of them not detected in 2003. One site has an OH with methanol counterpart and another a methanol counterpart. The methanol sites appear to be located in the near side of the 3-kpc arm (Green et al. 2009), and this interpretation can be applied to all six water sites in the cluster.

$0.655-0.045$  to  $0.677-0.028$ . These five sites lie within the Sgr B2 complex and are clearly distinguishable with our spatial resolution. Two of them have associated OH maser emission but none has associated methanol masers.

$5.886-0.392$ . This site has OH and water masers spread over more than 5 arcsec, associated with a compact H II region that is likely to be approaching the end of its maser phase (Caswell 2001) and with various distance estimates, of which 2 kpc is currently favoured (Stark et al. 2007). It was observed by FC89 and FC99, and our 2003 water maser observations were made to assess the changes over a decade. We cite the position of the strongest feature during our observations and note that there are many components at offset positions. Our water reference position and the OH reference position from C98 are 6 arcsec apart, but we list it as an association with OH on the basis of the intermingled features mapped by FC99.

$9.620+0.194$  and  $9.622+0.196$ . These coincide, respectively, with an OH maser site with no reported methanol and the strongest known methanol site which also has a coincident OH maser. A third methanol maser site in this cluster,  $9.619+0.193$ , shows no detectable water maser emission.

$10.473+0.027$  and  $10.480+0.034$ . The first source was detected in both 2003 and 2004, and the spectrum shown is from 2004 when a strong flare occurred. The spectrum shown for  $10.480+0.034$  is from 2003 when  $10.473+0.027$  was not flaring, and confusion from  $10.473+0.027$  was much less.

$10.623-0.383$ . Note a small correction to the C98 OH position, for which the RA should be  $18^{\text{h}}10^{\text{m}}28.67$  (not 28.61). Our water measurement in 2003 is in good agreement with the revised OH position and the measurement of FC89.

$11.903-0.141$ . We detect a weak water maser at this site which is probably the same source that was first reported by Caswell et al. (1983) with a peak flux density of 7.9 Jy (but with position uncertainty exceeding 10 arcsec). Note a small transcription error in the target OH position from FC89, FC99 and C98, for which the

RA should be  $18^{\text{h}}12^{\text{m}}11\overset{\text{s}}{.}46$  (not 11.56). Our water maser position is in satisfactory agreement with the corrected OH position. The corrected OH position also agrees better with the 6035-MHz maser position (C97) and with its associated UCH $\alpha$  region (C97) for which improved measurements by Forster & Caswell (2000) at 8.7 GHz give a flux density of 33.9 mJy.

*15.016–0.679 to 15.034–0.667 inclusive.* These all reside in the well-known nearby star-forming complex M17. All seven masers were recognizable and spatially distinct in the 2004 observations but only three were distinct in the 2003 observations, partly due to the stronger confusing emission from 15.028–0.673 at the earlier epoch. Spectra for the two strongest sources from the 2003 epoch are shown in Fig. 1 and are in addition to the 2004 spectra.

## 5 DISCUSSION

### 5.1 Water maser variability

Water masers have been noted on many occasions for their often extreme variability over relatively short time-scales, and some studies have extended over several decades (e.g. Felli et al. 2007). As our data are confined to only two epochs, and limited to coarse spectral resolution, we do not attempt a detailed study of the variability of our sources. However, we are able to highlight some interesting examples of variability, and the large size of our sample allows us to derive several interesting statistics.

For the 207 sources observed and detected at both epochs, we see variability ranging from sources showing no measurable variability to occasional extreme levels, and many intensities varying by factors of more than 2. High-velocity features can be particularly variable, with many spectral features of sources not being common to both epochs.

As noted in Section 3, Fig. 1 includes the spectra of eight sources from both epochs (284.350–0.418, 321.148–0.529, 327.291–0.578, 333.387+0.032, 336.983–0.183, 345.004–0.224, 15.026–0.654 and 15.028–0.673). They illustrate changes seen over the 10-month time-scale and highlight the fact that, for four of the examples, the feature with the strongest peak at the two epochs is at a different velocity.

A qualitative impression from the full set of spectra at both epochs (including our unpublished material for the 2003 epoch) is that the spectra of many sources show little resemblance at the two epochs. Quantitatively, we use the data of Table 1 to derive the plot of Fig. 2 which compares the velocity of the water maser peak emission in 2003 and 2004. An interesting statistic for the sources measured at two epochs shows that the strongest peak is at a significantly different velocity (offset by more than  $2 \text{ km s}^{-1}$ ) for 38 per cent (78 of 207) of the sites. However, from Fig. 2 we see that a much smaller fraction of velocity differences exceed  $10 \text{ km s}^{-1}$ . These large velocity differences generally represent the truly high-velocity features which, in a few sources, can dominate the spectrum at some epochs since they have highly variable intensities. For example, the source 357.967–0.163 has the 2003 peak intensity at  $0 \text{ km s}^{-1}$  (near systemic) but the 2004 peak at  $-65 \text{ km s}^{-1}$  (a high-velocity feature), and the source 336.983–0.183 has the 2003 peak intensity at  $-76 \text{ km s}^{-1}$  (near systemic) but the 2004 peak at  $+45 \text{ km s}^{-1}$  (a high-velocity feature).

We have observations available in both 2003 and 2004 for 253 water masers; 46 of them (17 per cent) were detected at only one epoch. Only 16 (one-third) of these sources that varied below our detection limit at one of the epochs were stronger than 2 Jy when

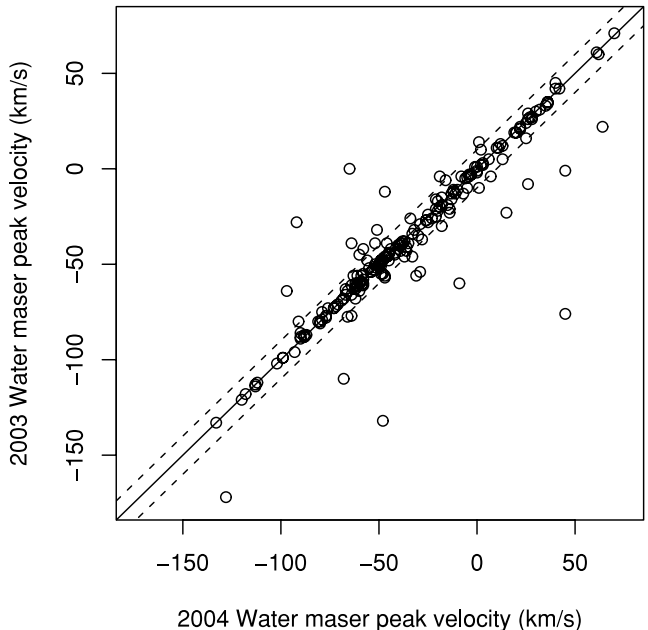


**Figure 2.** 2004 peak water maser velocity versus 2003 peak water maser velocity. Overlaid is a solid line with a slope of 1 and two dashed lines showing a deviation of  $10 \text{ km s}^{-1}$  either side of the solid line.

detectable, with the strongest source being 80 Jy. Half of the sources detected only at one epoch show a single feature and the majority of the others exhibited three or fewer features. In comparison, the vast majority of water maser sources that are associated with OH or methanol masers exhibit five or more spectral features. We have investigated the associations with other maser species for these 46 sources to search for other possible properties in common. Of the 46 sources, 12 are associated with both OH and methanol masers, two are associated with OH masers only, three are associated with methanol masers only and 28 are solitary (no association with another maser species). A  $\chi^2$  test was carried out on the percentage of sources in each of these groups compared to what would be expected if these sources were distributed in the same way as our entire sample. We find that a statistically significant higher percentage of the sources detected at only one epoch are solitary ( $p$ -value 0.02), compared to the distribution of associations in our full sample. The numbers of sources that varied below the detection limit at one epoch and are associated with combinations of OH and/or methanol masers are as expected from the distribution of the entire sample.

Claussen et al. (1996) suggested that water masers associated with low-mass stars were in general both weaker and more variable than those associated with high-mass stars. As we find that the sources only detectable at one epoch are biased towards solitary sources and are in general relatively weak, it is possible that a number of these water masers are in fact associated with lower mass stars perhaps residing in the same stellar clusters as the high-mass SFRs towards which the observations were targeted (see also the end of Sections 5.6 and 5.7).

The potential of water masers for mapping the distribution of massive SFRs throughout the Galaxy has been demonstrated for a few sources by astrometry sufficiently precise to achieve parallax measurements and precise distances (e.g. Sato et al. 2008). Water masers appear to provide the largest population to make these investigations, but with several caveats. First, a site must have individual

maser spots persisting for more than a year. Despite the extreme variability shown by all spots at some sites, and some spots at most sites, our data reassuringly demonstrate that there still remain an enormous number of suitable sites. A second reservation concerns the ability to associate a systemic velocity with the precise distance, enabling mapping of the Galactic velocity field. As we shall see in Sections 5.3 and 5.4, the estimate of the systemic velocity for an isolated water maser is uncertain, but an excellent estimate can be obtained from the OH or methanol masers accompanying many water masers. Note that the spatial correspondence between maser species is usually sufficient to yield very high confidence associations, whereas associations with more diffusely distributed thermal emission in molecular clouds are less reliable. So, associated OH or methanol masers are the key to establishing the systemic velocity of a water maser. We note that for sites with OH but no methanol, parallax determinations are beyond present capabilities except through the use of associated water masers. And even for some methanol sites, it may turn out that an associated water maser provides the best parallax measurement. Thus, the important role of water masers in these Galactic studies is assured.

## 5.2 Spatial distributions of maser spots

The VLA study of water masers by FC89 and FC99 examined the distributions of maser spots, both in velocity and spatially, for the masers that were quite strong and/or displayed many spectral features. It was shown that, where many maser spots were present, they lay either within a diameter rarely exceeding 30 mpc or in a few clusters of this size separated by distances at least several times larger. The quite large beamsize used in the present observations precludes a detailed study of the spot distributions, but allows recognition of clusters with several distinct members, of which there are many. We do, however, find a substantial number of water maser sources that show distinguishable angular separations between clusters of maser spots emitting near the systemic velocity and those emitting at high velocities. The separations are generally of the order of 2 or 3 arcsec and are plausibly attributed to associated outflowing material. Occasionally, separations between systemic and high-velocity components exceed 4 arcsec, and even in these cases it seems credible that these are associated outflows.

## 5.3 Detection statistics and relationship to ground-state OH and methanol masers

The position measurements and new detections of water masers reported in Table 1 mostly arose from a search at all the positions of southern SFR maser sites with ground-state OH main-line (1665- and 1667-MHz) masers that had not previously been searched. The target list corresponded to table 1 of C98, plus a few modifications which we briefly summarize here. Small position corrections were needed for 10.623–0.383 and 11.904–0.141, and an improved (previously unpublished) position has been determined for 326.780–0.241, listed by C98 at the approximate position 326.77–0.26. The list was augmented by 291.274–0.709, 308.754+0.549 and 329.339+0.148 (see notes for these sources in Section 4 and Caswell 2001). The OH source 311.94+0.14 still has no precise position measurement and, although searched for water, has been omitted from the statistics, as discussed under the note on 311.947+0.142.

Because the observations were targeted towards OH masers detected in a blind search, the detection statistics can be meaningfully computed. The new search has established sensitive upper limits

for water masers towards 42 main-line OH maser sources and a net detection rate for water masers towards OH masers of 79 per cent. Additional observations were made towards a selection of 104 methanol masers with no reported OH counterpart (chiefly from Caswell 2009).

As noted in Section 3, of the 379 detected water maser sources, 128 are associated with both OH and methanol masers, 33 are associated with OH masers only, 70 are associated with methanol masers only and 148 are solitary (i.e. not associated with either OH or methanol maser emission). The water maser detection rate towards sources exhibiting both OH and methanol maser emission is 77 per cent (128 of 166). In contrast, the water maser detection rate towards OH maser sites (with no methanol) is 89 per cent (33 of 37). In order to determine if water masers were preferentially detected towards OH masers without associated methanol masers, we carried out a  $\chi^2$  test. The resultant  $p$ -value of 0.6 means that the higher detection rate of water masers towards OH maser sources without associated methanol is not statistically significant.

Because the sample of methanol masers targeted in 2004 was not homogeneous, it is difficult to draw strong conclusions concerning methanol/water associations from the detection statistics. However, the fact that we find 70 associations of water towards methanol masers without OH (from a total sample of 104), and 33 associations of water towards OH masers with no methanol (from a total sample of 37), along with a detection rate of 77 per cent towards sources exhibiting both OH and methanol masers, indicates that the overlap between the lifetimes of water, OH and methanol masers is large. A possible interpretation is that during the evolution of the star, the methanol masers are not only the first maser species to appear but also the first species to turn off whereas both OH and water persist for longer.

Table 5 presents both the average and median flux densities of the water masers that we detect, broken up into categories according to their association with OH and methanol masers as well as 22-GHz radio continuum. Where a source was detected in both 2003 and 2004, we have used the two recorded values of flux density as separate entries. In Column 1, the types of association are listed. Here ‘all sources’ incorporates all water maser peak flux densities detected at either epoch; ‘with’ OH, methanol or continuum refers to water masers that are associated with the afore-mentioned source but not limited to associations with only these sources; ‘only’ OH or methanol incorporates only those water maser sources exclusively associated with either OH or methanol masers, but places no restrictions on their association with 22-GHz radio continuum; and ‘solitary’ refers to water sources that are not associated with either OH or methanol masers. We find that there is a trend of increasing water maser flux density from solitary sources to sources associated with methanol masers to sources associated with OH masers and

**Table 5.** The average and median water maser flux densities for all the sources we detect.

Water classification	Average flux density (Jy)	Median flux density (Jy)
All sources	57.1	5
With OH	96.1	15
With methanol	68.3	9
With continuum	74.9	18
Only OH	138.2	25
Only methanol	26.1	3.5
Solitary	18.9	2.8

22-GHz radio continuum. This may indicate that the water masers increase in flux density as the sources evolve, similar to that found by Breen et al. (2010) for 6.6-GHz methanol masers. We note, however, that the average and median flux density of the solitary water masers is likely to be at least partly due to some of these sources being associated with low-mass stars.

The recent completion of the Southern hemisphere component of the Methanol Multibeam (MMB) survey (Green et al. 2009; Caswell et al. 2010) for 6.6-GHz methanol masers will soon provide an even more extensive catalogue of SFRs than the OH catalogue of C98 to search for associated water maser emission. The MMB survey is the most sensitive survey yet undertaken for young high-mass stars in the Galaxy and is complete within  $2^\circ$  of the Galactic plane. Water maser observations towards this unbiased catalogue of methanol masers will enable meaningful detection statistics for methanol and water maser associations to be derived and allow comparison with our statistics derived from the comparison of OH and water maser associations. Due to this, coupled with the fact that our methanol-targeted sample is not homogeneous, we do not attempt to draw further conclusions from this methanol sample. We anticipate that comparisons between the sources detected in the MMB survey and IR data, in conjunction with follow-up observations for 22-GHz water masers, 12.2-GHz methanol masers and other non-masing molecular species, will uncover unique insights into the differing physical conditions responsible for the presence/absence of the different methanol maser transitions.

Beuther et al. (2002) conducted a high-resolution study of the water and methanol masers in 29 massive SFRs and found that 10 methanol masers coincide spatially with water masers to within their uncertainty of about 1.5 arcsec. They remarked that no spatial correlations exist between the two maser species, which is clearly not an inference from their results and refers presumably to the common expectation that detailed correlations of maser spots are unlikely.

Our finding is that occurrence of a water maser at nearly 80 per cent of the OH maser targets is comparable to the occurrence of methanol at OH targets. This might seem surprising in view of the difference in favoured pumping schemes, where both OH and methanol depend on far-IR radiation, whereas the favoured pumping scheme for water masers is collisional (Elitzur, Hollenbach & McKee 1989). However, it is consistent with the expectation that in most locations where methanol and OH masers occur there are coincident, or nearby, shocked regions with high densities suitable for the excitation of water masers. Pursuing this further, the apparently larger number of water masers than other maser species is consistent with the extremely common occurrence of such shocked regions, not only in the envelope of a high-mass star, but also in outflows and in lower mass stars with less IR flux.

Interestingly, pumping of the formaldehyde masers (which are uncommon, but also trace SFRs) is unclear, since the Boland & de Jong (1981) radiative pump seems deficient and may need shocks and collisions, according to Hoffman et al. (2003).

#### 5.4 Velocity distributions of maser features

The velocity distributions for the water masers have intrinsic interest but are most fruitfully studied in comparison with OH and methanol counterparts where available. The velocity range of water maser emission at many sites is larger than for OH or methanol, with the velocity range of water masers measured in 2003 having an average of  $27 \text{ km s}^{-1}$  and a median of  $15 \text{ km s}^{-1}$  and those measured in 2004 showing an average velocity range of  $30 \text{ km s}^{-1}$  and a median

of  $15 \text{ km s}^{-1}$ . In contrast, methanol masers rarely show emission that exceeds a velocity range of  $16 \text{ km s}^{-1}$  (Caswell 2009), and C98 found the median velocity range of 100 OH masers with flux densities greater than  $2.7 \text{ Jy}$  to be  $9 \text{ km s}^{-1}$ .

Sometimes the water emission is remarkably symmetric about the systemic velocity but, more often, is asymmetric. The strongest water maser emission is generally confined to the velocity ranges of the associated OH and methanol masers. The velocity of methanol maser emission is regarded as a reliable indication of the systemic velocity for the regions that these masers are tracing (e.g. Caswell 2009; Pandian, Menten & Goldsmith 2009), allowing kinematic distances for the sources to be computed. OH masers are slightly less reliable tracers of systemic velocities because small changes to the apparent radial velocity are caused by the Zeeman effect. Water masers, however, are generally regarded as unreliable tracers of systemic velocities, as they commonly trace high-velocity outflows and have large velocity ranges.

We first compare the peak velocities of methanol and OH masers in Fig. 3 (using the population of 165 sources studied in this paper, including sources both with and without associated water maser emission). This clearly demonstrates the close similarity in the velocities of their peaks. The average difference between the peak velocities of the OH and methanol masers is  $3.4 \text{ km s}^{-1}$ , with a median difference of  $2.2 \text{ km s}^{-1}$ .

We now compare the velocity of the peak emission of our large sample of water masers with the peak of associated OH and methanol masers (Figs 4 and 5, respectively). The 2004 peak velocities were used where possible and 2003 peak velocities were used otherwise. In the case of 160 OH–water maser associations, we find that the average difference in the peak velocities is  $7.8 \text{ km s}^{-1}$  and the median difference is  $4 \text{ km s}^{-1}$ . In the case of 197 methanol–water maser associations, we find that the average difference in the peak velocities is  $8.8 \text{ km s}^{-1}$  and the median difference is  $4.2 \text{ km s}^{-1}$ . Thus for the majority of sources there is quite good correspondence between the velocity of the peaks of water masers and that of the

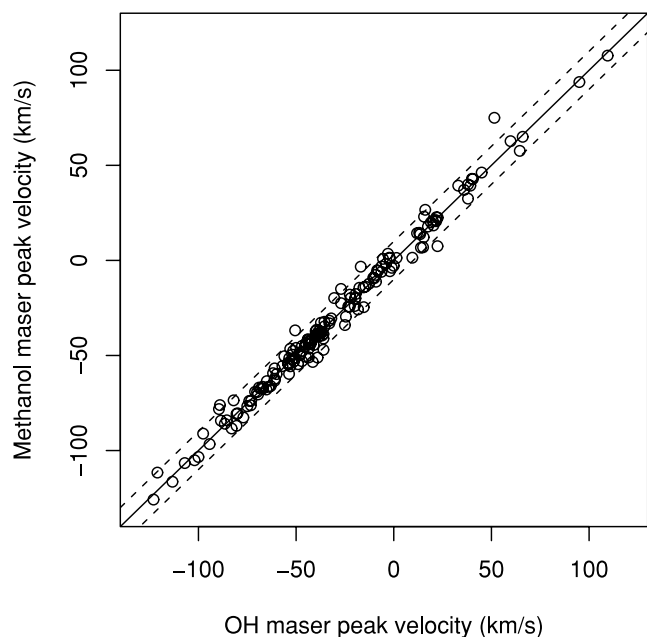


**Figure 3.** OH maser peak velocity versus methanol maser peak velocity. Overlaid is a solid line with a slope of 1 and two dashed lines showing a deviation of  $10 \text{ km s}^{-1}$  either side of the solid line.

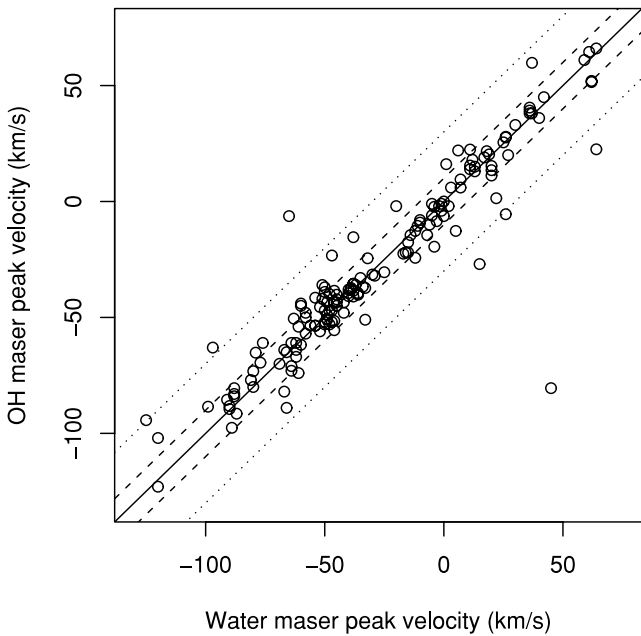


**Figure 4.** Water maser peak velocity versus OH maser peak velocity. Overlaid is a solid line with a slope of 1 and two dashed lines showing a deviation of  $10 \text{ km s}^{-1}$  either side of the solid line. An additional pair of lines (dotted) shows a deviation of  $30 \text{ km s}^{-1}$ .

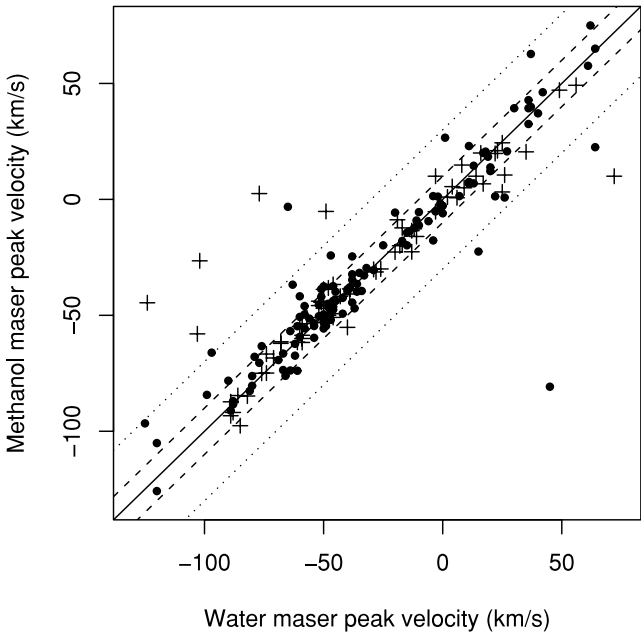


**Figure 5.** Water maser peak velocity versus methanol maser peak velocity. Overlaid is a solid line with a slope of 1 and two dashed lines showing a deviation of  $10 \text{ km s}^{-1}$  either side of the solid line. An additional pair of lines (dotted) shows a deviation of  $30 \text{ km s}^{-1}$ . We distinguish sources with only methanol (cross) from those with OH as well as methanol (dot).

associated OH or methanol maser peak emission, but there are some striking outliers.

Comparison of Fig. 3 with Figs 4 and 5 highlights the closer correspondence between the peak velocities of the OH and methanol masers than either of these species compared to the associated water maser peak velocity. 93 per cent of the OH and methanol maser peak velocities are in agreement to within  $10 \text{ km s}^{-1}$ , whereas for

the water–methanol and water–OH peak velocities this number falls to 78 and 79 per cent.

We now look in more detail at the outlying sources in Figs 4 and 5. The isolated source at the lower right of the plots is 336.983–0.183 and, as remarked in the note of Section 4, the high-velocity water feature is accompanied by emission at the systemic velocity (methanol and OH peak velocities) which is of comparable intensity (or stronger at the 2003 epoch). Disregarding this source, Fig. 4 shows only a small number of dominant high-velocity features (offset by more than  $30 \text{ km s}^{-1}$ ) with no preference for red or blue shifts. In Fig. 5, we distinguish the sources with only methanol from those with OH as well as methanol. We note that there is a striking group of six highly blueshifted features of which five have no OH emission. These are some of the distinct population of dominant blueshifted outflows discussed by Caswell & Phillips (2008).

### 5.5 Clustering of maser sites and association with other masers of OH

In addition to the water maser sources that we find to be intimately associated with the OH and methanol masers that were targeted, we frequently detect water masers separated from the target OH and methanol masers by  $\sim 10$  arcsec or more. Furthermore, we find the occurrence of multiple water maser sites within the HPBW of the ATCA primary beam to be common, with the number of sources often exceeding two and reaching as high as seven. Fig. 6 shows a histogram of the number of water masers in the targeted ATCA fields that are solitary (i.e. in addition to the water masers detected at the targets of OH and methanol). There are 90 cases where there is one or more solitary maser within the HPBW of a target OH or methanol maser. This means that observations targeted towards OH and methanol masers have a 29 per cent chance of detecting at least one unrelated water maser within  $\sim 2$  arcmin of the target source.

Clusters comprising combinations of water, OH and methanol masers spread over  $\sim 20$  arcsec are common. Comparative studies of sites within these clusters, where we can infer that near-contemporaneous formation of several massive stars has occurred, hold promise for unravelling the preferred environments and stellar evolutionary stages for different maser species; future studies of water masers and associated IR sources will play a major role in this investigation.

Six sites of 1720-MHz maser emission, believed to be of the SFR variety but with no other maser species, were listed by Caswell

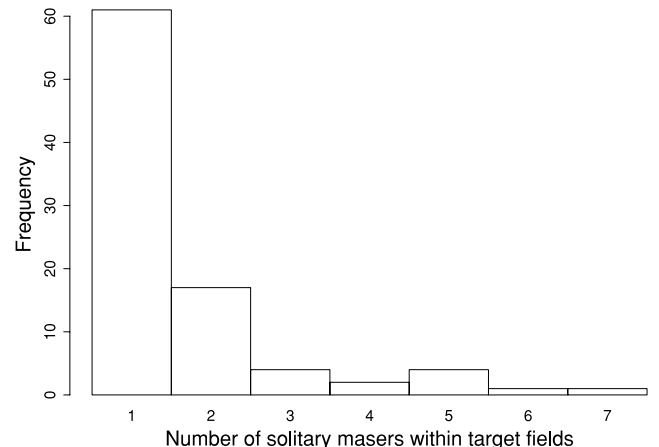


**Figure 6.** Histogram of the number of solitary water masers detected in single ATCA fields.

(2004a), and these have also been searched for water masers. A new water maser was detected towards one of them, 310.146+0.760, as well as towards its cluster companion the 1665-MHz OH and methanol maser 310.144+0.760, offset by nearly 10 arcsec. The 1720-MHz maser 329.426–0.158 was previously the only maser detected in a putative SFR (with an H II region nearby both spatially and in velocity). Although no water was found at the 1720-MHz site, two new water maser sites were discovered, with offsets of only 20 arcsec, and therefore credibly within this SFR and therefore now increasing its known maser population to a cluster of three masers.

Two sites that are currently known as masers only at the 6035-MHz excited state of OH were also searched for water. No water detection was made towards either 311.596–0.398 or 345.487+0.314.

## 5.6 Association with continuum UCHII regions

The present observations, although focused on spectral line emission, also allowed a search at each maser site for an associated UCHII region, to a limit of  $\sim 30$  mJy if the region is not too confused. Although this is two orders of magnitude less sensitive than can be achieved with a targeted wide bandwidth survey (Forster & Caswell 2000), it is at higher frequency and provides in many cases a useful first estimate.

The sensitivity to radio continuum is not uniform for all sources and is especially poor for observations with maser emission over an extensive velocity range, leaving little of the bandpass free from line emission. Due to this and our short integration times, we are sensitive only to relatively strong UCHII regions.

We have not used the continuum data collected at the 2003 epoch since the *uv* coverage (with an EW array) was significantly poorer than achieved with the H168 array in 2004. The 29 water maser sources observed only during the 2003 observations have therefore been removed from the subsequent statistics. Table 6 presents the number of water maser sources observed in 2004, broken up into the categories of solitary, associated with an OH maser, associated with both OH and methanol masers, and associated with a methanol maser (numbers shown in Column 2). Column 3 shows the number of water maser sources in each category that are also associated with 22-GHz radio continuum from UCHII regions that we detect, while Column 4 shows the percentage of sources with detectable 22-GHz radio continuum in each category. We find associations with UCHII regions, indicative of an embedded massive early type star, for 42 of the water maser sources that we detect.

Due to the targeted nature of this search, with the OH sample being complete but the methanol sample incomplete, percentages are presented in Table 5 to reveal more clearly the correlations.

**Table 6.** Comparison between water maser associations and the presence of associated 22-GHz radio continuum.

Water association	No of sources total (2004)	No of sources with continuum	Per cent with continuum
OH and methanol	112	24	21.4
OH	28	6	21.4
methanol	67	5	7.5
solitary	143	7	4.8

*Note.* Column 1 describes the water maser associations, Column 2 shows the number of water maser sources observed in 2004 that fall under the given association. Column 3 gives the number of sources within each category that are associated with 22-GHz radio continuum and Column 4 shows this number as a percentage of the water maser sources in each category.

The percentages of water maser sources with an associated UCHII region in Table 6 show that UCHII regions are preferentially detected towards water maser sources with associated OH masers.

We find that our overall detection rate for UCHII regions towards water maser sources with associated OH masers (with or without associated methanol) is 21.4 per cent while our detection rate towards water maser sources without associated OH masers (solitary or with methanol) is 5.0 per cent. Forster & Caswell (2000) conducted a sensitive search at 8.7 GHz for UCHII regions towards OH and water masers which showed that 52 per cent of the OH masers they targeted had an associated UCHII region. While our observations are almost two orders of magnitude less sensitive than was achieved by Forster & Caswell (2000), they are at a higher frequency allowing us to potentially detect emission from hyper-compact (HC) H II regions which are typically optically thick at centimetre wavelengths. Comparison with the detection rate of Forster & Caswell (2000) suggests that a more sensitive search at 8.7 GHz for UCHII regions towards our OH-maser-associated water maser sources would more than double our detections from 30 sources to  $\sim 71$ .

Our results support arguments (Caswell 2001; Beuther et al. 2002; Breen et al. 2010) that methanol maser emission is often seen prior to any OH maser emission, but is sensitive to the onset of emission from UCHII regions, and less able to survive the later stages of the evolution of the UCHII region. Carrying on these arguments to include water masers we find that the water masers are also present at the early stages of formation, like the methanol masers, prior to the onset of OH maser emission. These statistics for solitary water sites naively suggest that these water masers precede the onset of strong UCHII regions. However, as mentioned in Section 5.1, it is possible that a significant population of the solitary water masers are associated with low-mass stars and this provides an alternative explanation.

## 5.7 Comparison with GLIMPSE objects

### 5.7.1 Association with GLIMPSE point sources

We have compared the positions of the 379 water maser sources with the positions of sources in the GLIMPSE point source catalogue. We find that 343 of our water maser sources are within the Galactic longitude and latitude ranges observed by GLIMPSE and that 165 of these are within 3 arcsec of a GLIMPSE point source (48 per cent). This number increases to 211 if sources from the GLIMPSE archive are included (62 per cent). The fraction of the water maser sources associated with point sources contained in either the GLIMPSE point source catalogue or the supplementary archive catalogue is similar to that found by Ellingsen (2006) when comparing the positions of 56 methanol masers with GLIMPSE sources (68 per cent).

We have further investigated the associations between water maser and GLIMPSE sources by comparing the GLIMPSE source association rates of water masers in their association categories (i.e. associated with both OH and methanol masers, associated with OH masers, associated with methanol masers, etc.). Association rates are as follows.

(i) 76 of the 165 GLIMPSE detections have both OH and methanol (i.e. 46 per cent of the GLIMPSE sources are associated with OH, methanol and water and 60 per cent of the OH methanol and water sources have an associated GLIMPSE source).

(ii) 91 of 165 GLIMPSE detections have OH detections (i.e. 55 per cent of the GLIMPSE sources have an associated OH maser

and 57 per cent of OH maser sources have an associated GLIMPSE source).

(iii) 109 of 165 GLIMPSE detections have methanol detections (i.e. 66 per cent of the GLIMPSE sources have an associated methanol maser and 56 per cent of methanol maser sources have an associated GLIMPSE source).

(iv) 18 of 165 GLIMPSE detections have associated radio continuum (i.e. 11 per cent of the GLIMPSE sources have an associated H II region and 43 per cent of H II regions have an associated GLIMPSE source).

(v) 41 of 165 GLIMPSE detections only have an associated water maser (i.e. 25 per cent of the GLIMPSE sources are only associated with a water maser and 29 per cent of the water-only sources have an associated GLIMPSE source).

The GLIMPSE point source association rates are similar in all categories except for solitary water masers and water masers associated with radio continuum where the association rates are significantly lower. In the case of the radio continuum, it is likely that a large number of sources exhibiting strong radio continuum would no longer be point sources at mid-IR frequencies (because sources exhibiting strong radio continuum are likely to be more evolved) and this would therefore account for the lower association rate. The lower association rate between GLIMPSE point sources and solitary water masers could be explained by a tendency for these water sources to be associated with more extended objects or, alternatively, that the solitary water masers are commonly associated with lower luminosity sources.

Fig. 7 shows a plot of the [3.6]–[4.5]  $\mu\text{m}$  versus [5.8]–[8.0]  $\mu\text{m}$  colours of the GLIMPSE point sources associated with the water masers. Flux density measurements for all four of the Infrared Array Camera (IRAC) bands had to be available for the inclusion in this plot, thus limiting the plotted sample to 14 solitary water masers (i.e. with no methanol or OH maser counterpart) and 58 water masers with either a methanol or an OH counterpart. We find, similarly to previous comparisons (e.g. Ellingsen 2006; Breen et al. 2010), that the GLIMPSE sources associated with the masers are located above the majority of the comparison sources in the colour–colour plot.

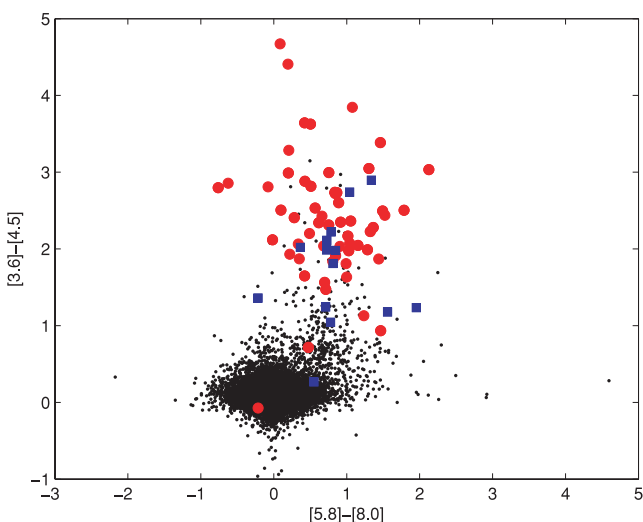


**Figure 7.** Colour–colour plot of GLIMPSE point source data. Water maser sources with associated OH and/or methanol maser emission are represented by red circles and solitary water maser sources are represented by blue squares. The black dots represent all of the GLIMPSE point sources within  $l = 326^\circ.5$ ,  $b = 0^\circ.0$ .

This figure also reveals an apparent difference in the ranges of the [3.6]–[4.5]  $\mu\text{m}$  colours for solitary water masers compared with water masers that are associated with methanol, OH or continuum (or a combination of these).

We have carried out a *t*-test (testing the hypothesis that there is no difference between the means) on both the [3.6]–[4.5] and [5.8]–[8.0]  $\mu\text{m}$  colours of those GLIMPSE sources associated with solitary water masers compared to those associated with water masers as well as OH, methanol or radio continuum. In the case of the [5.8]–[8.0]  $\mu\text{m}$  colours, we find that there is no statistically significant difference between the values associated with the two groups of water maser sources. For the [3.6]–[4.5]  $\mu\text{m}$  colours, we find that there is a statistically significant difference ( $p$ -value of 0.007) between the GLIMPSE sources associated with solitary water masers and those water masers with associated methanol, OH or radio continuum sources.

As can be seen in Fig. 7, the [3.6]–[4.5]  $\mu\text{m}$  colour tends towards smaller values in the case of the solitary water masers. Since there is no difference in the [5.8]–[8.0]  $\mu\text{m}$  colours between the two groups of sources, this means that the solitary water-maser-associated GLIMPSE sources have a much less steep spectrum at wavelengths of  $<5 \mu\text{m}$  than at wavelengths greater than this. This indicates that these sources may be colder in general. Another explanation may be that the GLIMPSE sources associated with the solitary water masers have a relative excess of 4.5  $\mu\text{m}$  flux density, similar to extended green objects (EGOs; Cyganowski et al. 2008).

In Section 5.1, we suggested that some fraction of the solitary water masers are likely to be associated with low-mass stars rather than the high-mass SFRs where these observations were targeted. According to Cyganowski et al. (2008), GLIMPSE is too shallow to detect emission from outflows associated with low-mass stars (except perhaps for the closest low-mass SFRs). Furthermore, if GLIMPSE detected IR emission associated with low-mass stars it certainly would not detect it as a point source because the space density would be much too high. We therefore conclude that none of the sources included in Fig. 7 is associated with low-mass stars and therefore cannot be responsible for the difference. However, it is possible that the lower association rate for solitary water maser sources with GLIMPSE point sources is partially because some fraction of the solitary water maser sources are associated with low-mass stars.

### 5.7.2 Association with extended green objects

We have compared the locations of the EGOs presented in Cyganowski et al. (2008) with our 379 water masers. In order to avoid large numbers of chance associations between EGOs and water masers, we consider an EGO to be associated with a nearby water maser when the angular separation is less than 10 arcsec. Cyganowski et al. (2008) compared the locations of 6.6-GHz methanol masers with the images of their EGOs and showed that this separation captures most of the associations while minimizing the chance coincidences that would result from a larger threshold. We find that 63 of the water masers are coincident with an EGO identified by Cyganowski et al. (2008).

Table 7 shows in the second column the percentage of the full sample of 379 water masers that fall within the four categories: associated with both OH and methanol masers, associated with only OH masers, associated with only methanol masers and solitary, and in the third column it shows the number of water sources in each category that are also associated with EGOs as a percentage of

**Table 7.** Comparison between water maser associations in our full sample with water maser associations for sources associated with EGOs.

Water association	Per cent of full sample	Per cent of sources with EGOs
OH and methanol	33.8	55.6
OH	8.7	7.9
Methanol	18.5	20.6
Solitary	39.0	15.9
Total	100	100

*Note.* Column 1 describes the water maser associations, Column 2 shows the percentage of water maser sources in each category (from the full sample) and Column 3 gives the percentage of sources in each category that are also associated with an EGO (Cyanowski et al. 2008).

the total number of EGO-associated sources. This table shows that those water maser sources coincident with EGOs and associated with only methanol or OH masers are distributed in similar fashion to our complete sample of water masers, with little difference between the percentage of water sources presented in Columns 2 and 3. However, in the case of the solitary water sources, the association rate with EGOs is much lower than would be expected (similar to solitary water masers associated with GLIMPSE point sources). The absence of EGO associations with a large number of the water-maser-only sources may suggest that solitary water masers are associated with lower luminosity sources. Alternatively, considering that the water-maser-only sources tend to be associated with GLIMPSE point sources with dominant 4.5- $\mu\text{m}$  emission, a characteristic shared by EGOs, the water-maser-only sources may represent a class of younger sources, the majority of which have not yet produced an extended outflow. Perhaps this indicates that these solitary water masers are associated with outflow-related sources: compact green objects, pre-cursors to EGOs.

We find that there is a higher association rate with EGOs for those water maser sources accompanied by both methanol and OH masers. This indicates that EGOs persist into the stage of star formation that is evolved enough to have produced an OH maser but not so evolved that the production of an associated strong UCHII region has caused the methanol maser emission to cease. 89 of the water maser sources we detect that are associated with both OH and methanol masers are within the regions covered by GLIMPSE and have been inspected for the presence of EGOs (Cyanowski et al. 2008). We find that 35 of these 89 sources are associated with an EGO, a rate of 39 per cent. This lends further credence to the idea that EGOs are not exclusively tracing the earliest stages of massive star formation but persist well into the stage where OH masers are present. Furthermore, as there is a large number of these objects, they must have a significant lifetime.

## 6 CONCLUSIONS

From a large sample of water masers measured with precise positions at two epochs, we conclude that spectra are highly variable but positions are generally persistent.

The occurrence of a water maser at nearly 80 per cent of the OH maser targets is comparable to that of methanol at OH sites. This is despite the difference in favoured pumping schemes, where both OH and methanol depend on far-IR radiation, whereas the favoured pumping scheme for water masers is collisional.

Our study of water masers at methanol maser sites is preliminary, but the common presence of water at methanol sites is confirmed. We argue that there is indeed an important role for water masers in mapping the Galaxy and its velocity field. The present contribution of a large number of water masers with accurate positions in the southern Galaxy has been an important step in advancing such a project and reveals the value of conducting even larger future surveys with complete Galactic plane coverage.

## ACKNOWLEDGMENTS

The ATCA is part of the Australia Telescope which is funded by the Commonwealth of Australia for operation as a National Facility managed by CSIRO. This research has made use of NASA's Astrophysics Data System Abstract Service, the NASA/IPAC Infrared Science Archive (which is operated by the Jet Propulsion Laboratory, California Institute of Technology, under contract with the National Aeronautics and Space Administration) and data products from the GLIMPSE survey, which is a legacy science programme of the *Spitzer Space Telescope*, funded by the National Aeronautics and Space Administration.

## REFERENCES

- Batchelor R. A., Caswell J. L., Haynes R. F., Wellington K. J., Goss W. M., Knowles S. H., 1980, Australian J. Phys., 33, 139
- Beuther H., Walsh A., Schilke P., Sridharan T. K., Menten K. M., Wyrowski F., 2002, A&A, 390, 289
- Boland W., de Jong T., 1981, A&A, 98, 149
- Braz M. A., Epchtein E., 1983, A&AS, 54, 167
- Braz M. A., Scalise E., 1982, A&A, 107, 272
- Breen S. L. et al., 2007, MNRAS, 337, 491
- Breen S. L., Ellingsen S. P., Caswell J. L., Lewis B. E., 2010, MNRAS, 401, 221
- Caswell J. L., 1997, MNRAS, 289, 79 (C97)
- Caswell J. L., 1998, MNRAS, 297, 215 (C98)
- Caswell J. L., 2001, MNRAS, 326, 805
- Caswell J. L., 2003, MNRAS, 341, 551
- Caswell J. L., 2004a, MNRAS, 349, 99
- Caswell J. L., 2004b, MNRAS, 351, 279
- Caswell J. L., 2004c, MNRAS, 352, 101
- Caswell J. L., 2009, PASA, 26, 454
- Caswell J. L., Phillips C. J., 2008, MNRAS, 386, 1521
- Caswell J. L., Batchelor R. A., Haynes R. F., Huchtmeier W. K., 1974, Australian J. Phys., 27, 417
- Caswell J. L., Batchelor R. A., Forster J. R., Wellington K. J., 1983, Australian J. Phys., 36, 443
- Caswell J. L., Batchelor R. A., Forster J. R., Wellington K. J., 1989, Australian J. Phys., 42, 331
- Caswell J. L., Vaile R. A., Ellingsen S. P., Norris R. P., 1995a, MNRAS, 274, 1126
- Caswell J. L., Vaile R. A., Forster J. R., 1995b, MNRAS, 277, 210 (CVF95)
- Caswell J. L. et al., 2010, MNRAS, 404, 1029
- Claussen M. J., Wilking B. A., Benson P. J., Wootten A., Myers P. C., Terebey S., 1996, ApJS, 106, 111
- Cyanowski C. J. et al., 2008, AJ, 136, 2391
- Dodson R. G., Ellingsen S. P., 2002, MNRAS, 333, 307
- Ellingsen S. P., 2006, ApJ, 638, 241
- Ellingsen S. P., Cragg D. M., Minier V., Muller E., Godfrey P. D., 2003, MNRAS, 344, 73
- Ellingsen S. P., Cragg D. M., Lovell J. E. J., Sobolev A. M., Ramsdale P. D., Godfrey P. D., 2004, MNRAS, 354, 401
- Ellingsen S. P., Voronkov M. A., Cragg D. M., Sobolev A. M., Breen S. L., Godfrey P. D., 2007, in Goss W. M., Murray J. D., Brooks J. W., eds,

- Proc. IAU Symp. 242, Astrophysical Masers and their Environments. Cambridge Univ. Press, Cambridge, p. 213
- Elitzur M., Hollenbach D. J., McKee C. F., 1989, *ApJ*, 346, 983
- Felli M. et al., 2007, *A&A*, 476, 373
- Forster J. R., Caswell J. L., 1989, *A&A*, 213, 339 (FC89)
- Forster J. R., Caswell J. L., 1999, *A&AS*, 137, 43 (FC99)
- Forster J. R., Caswell J. L., 2000, *ApJ*, 530, 371
- Genzel R., Downes D., 1977, *A&AS*, 30, 145
- Green J. A. et al., 2009, *MNRAS*, 392, 783
- Hoffman I. M., Goss W. M., Palmer P., Richards A. M. S., 2003, *ApJ*, 598, 1061
- Hofner P., Churchwell E., 1996, *A&AS*, 120, 283
- Johnston K. L., Robinson B. J., Caswell J. L., Batchelor R. A., 1972, *Astrophys. Lett.*, 10, 93
- Kaufmann P. et al., 1976, *Nat*, 260, 360
- Pandian J. D., Menten K. M., Goldsmith P. F., 2009, *ApJ*, 706, 1609
- Radhakrishnan V., Goss W. M., Murray J. D., Brooks J. W., 1972, *ApJS*, 24, 49
- Reid M. J., Schneps M. H., Moran J. M., Gwinn C. R., Genzel R., Downes D., Roennaeng B., 1988, *ApJ*, 330, 809
- Sakellis S., Taylor M. I., Taylor K. N. R., Vaile K. A., Han T. D., 1984, *PASP*, 96, 543
- Sato M. et al., 2008, *PASJ*, 60, 975
- Sault R. J., Teuben P. J., Wright M. H., 1995, in Shaw R. A., Payne H. E., Hayes J. J. E., eds, *ASP Conf. Ser. Vol. 77, Astronomical Data Analysis Software and Systems IV*. Astron. Soc. Pac., San Francisco, p. 433
- Stark D. P., Goss W. M., Churchwell E., Fish V. L., Hoffman I. M., 2007, *ApJ*, 656, 943
- Val'tts I. E., Ellingsen S. P., Slysh V. I., Kalenskii S. V., Otrupcek R., Voronkov M. A., 1999, *MNRAS*, 310, 1077

This paper has been typeset from a  $\text{\TeX}/\text{\LaTeX}$  file prepared by the author.